CHALMERS

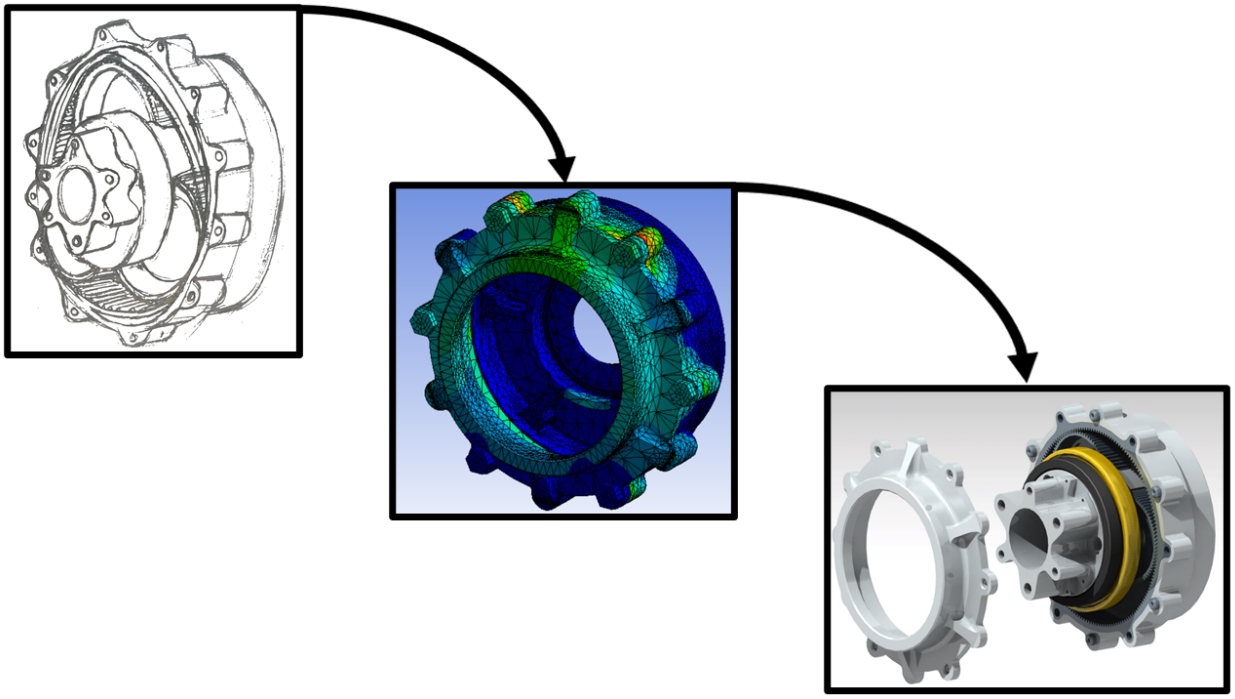

# Design of a Weight-Optimized Gearbox for a Formula Student Car

Bachelor's Thesis in Mechanics and Maritime Sciences

EMIL ALEXSSON
ERIK HENRIKSON
CARL LUND
CHRISTIAN TSOBANOGLOU

Department of Mechanics and Maritime Sciences (M2)
CHALMERS UNIVERSITY OF TECHNOLOGY
Gothenburg, Sweden 2021
www.chalmers.se

Bachelor's thesis 2021
REPORT NO 2021:05

# Design of a Weight-Optimized Gearbox for a Formula Student Car

EMIL ALEXSSON
ERIK HENRIKSON
CARL LUND
CHRISTIAN TSOBANOGLOU


CHALMERS

Department of Mechanics and Maritime Sciences (M2)
Chalmers University of Technology
Gothenburg, Sweden 2021

Design of a Weight-Optimized Gearbox for a Formula Student Car
EMIL ALEXSSON
ERIK HENRIKSON
CARL LUND
CHRISTIAN TSOBANOGLOU



Supervisor: BJÖRN PÅLSSON, Senior Lecturer at Mechanics and Maritime Sciences, Division of Dynamics
Examiner: HÅKAN JOHANSSON, Associate Professor at Mechanics and Maritime Sciences, Division of Dynamics

Bachelor's thesis 2021:05
Department of Mechanics and Maritime Sciences (M2)
Division of Dynamics
Chalmers University of Technology
SE-412 96 Gothenburg
Telephone +46 31 772 1000

Cover: Visualization of gearbox development, from sketch to structurally analyzed.
Typeset in LaTeX
Printed by Chalmers Reproservice
Gothenburg, Sweden 2021

Design of a Weight-Optimized Gearbox for a Formula Student Car
EMIL ALEXSSON
ERIK HENRIKSON
CARL LUND
CHRISTIAN TSOBANOGLOU
Department of Mechanics and Maritime Sciences (M2)
Chalmers University of Technology

# Abstract

Chalmers Formula Student is a team consisting of student engineers that design and build race cars to compete against other universities' teams. Since 2019, Chalmers Formula Student has been designing electric powered four-wheel drive cars. In 2020, Chalmers Formula Student began utilizing electric machines and gearboxes powering all wheels at the wheel hub. This design has many advantages in terms of mechanical packaging and lowering the center of gravity, but the design also means higher mass for the shock absorbers to handle, also called unsprung mass. Higher unsprung mass has a negative effect on the vehicle dynamics. The project purpose is therefore to design a lighter gearbox than the most recently manufactured Chalmers Formula Student gearbox to reduce the unsprung mass.

This report covers the process of developing a gearbox for the Formula Student car with the purpose previously mentioned. The project starts with investigating different gearbox configurations via a concept generation, resulting in that a single stage planetary gearbox is the most suitable concept. Then a method for deriving the dimensioning load cases for the gears, bearings and gearbox housing is developed by translating sensor data from competition to resulting forces.

The load cases are then used for dimensioning the gears with the gear dimensioning software KISSsoft and for stress and deformation analysis on the gearbox housing and bearings with the FEM software ANSYS and 3D-modelling software CATIA V5.

The result is a single stage planetary gearbox with a gear ratio of 11.5:1 that is 2.4% lighter than the most recent manufactured Chalmers Formula Student gearbox. However, if only the shared components are compared the final design is 12.3% heavier. The high gear ratio resulted in problematic gear design resulting in heavy gears in order to achieve acceptable safety factors.

The conclusion is that even though the developed gearbox became marginally lighter, a single stage planetary gearbox is not a suitable gearbox layout for the application. However, the methods for developing the dimensioning load cases are considered accurate and suitable for dimensioning future gearboxes.

Keywords: Gearbox, Formula Student, Gears, Planetary gearbox, Unsprung mass, Design, Dynamics .

# Acknowledgements

The project has had great assistance of the main supervisor Björn Pålsson and the examiner Håkan Johansson. Per Forsberg at Atlas Copco has offered support and advise in the gear design. Peter Wittke and Tommie Hall at Volvo Cars have assessed the project in an early stage and given guidance concerning the safety factors. Finally, it is noteworthy to thank the Chalmers Formula Student alumnus Erik Lund assisting with converting and managing the logged data for the gearbox housing and bearing load case.

Emil Alexsson
Erik Henrikson
Carl Lund
Christian Tsobanoglou
Gothenburg, May 2021

# Acronyms

| **Acronym** | Description |
|---|---|
| ADC | Analog to Digital Converter |
| CAD | Computer Aided Design |
| CANBUS | Controller Area Network |
| CFS | Chalmers Formula Student |
| CFS19 | The Chalmers Formula Student 2019 Team |
| CFS20 | The Chalmers Formula Student 2020 Team |
| CFS21 | The Chalmers Formula Student 2021 Team |
| COG | Center Of Gravity |
| DIN | Deutsches Institut für Normung |
| FEM | Finite Element Method |
| FL | Front Left |
| FR | Front Right |
| FS | Formula Student |
| FSA | Formula Student Austria |
| FSN | Formula Student Netherlands |
| GPS | Global Positioning System |
| MPT | Mechanical Power Train |
| RPM | Revolutions Per Minute |
| RL | Rear Left |
| RR | Rear Right |
| SKF | Svenska Kullagerfabriken |
| OEM | Original Equipment Manufacturer |

# Symbols

| Symbol | Description | Unit |
|---|---|---|
| $a$ | Acceleration | $^{m}/_{s^2}$ |
| $A$ | The area between the ground and rear tire | - |
| $A_D$ | Frontal Area | $m^2$ |
| $a_1$ | Life adjustment factor for reliability | - |
| $a_{SKF}$ | SKF modification factor | - |
| $B$ | Bearing width | mm |
| $C$ | Basic dynamic load rating | kN |
| $C_0$ | Basic static load rating | kN |
| $C_D$ | Drag coefficient | - |
| $d$ | Bearing inner diameter | mm |
| $D$ | Bearing outer diameter | mm |
| $d_m$ | Average diameter | mm |
| $e$ | Limit for the load ratio | - |
| $f_0$ | Calculation factor | - |
| $F_a$ | Axial force on bearings | kN |
| $F_D$ | Drag force | N |
| $F_L$ | Lateral force | N |
| $F_{L,FL}$ | Lateral force on front left tier | N |
| $F_{L,FR}$ | Lateral force on front right tier | N |
| $F_{L,RL}$ | Lateral force on rear left tier | N |
| $F_{L,RR}$ | Lateral force on rear right tier | N |
| $F_N$ | Normal force | N |
| $F_{NF}$ | Normal force front wheel axis | N |
| $F_{NR}$ | Normal force rear wheel axis | N |
| $F_r$ | Radial force on bearings | kN |
| $F_T$ | Tangential force | N |
| $g$ | Gravitational constant | $^{m}/_{s^2}$ |
| $i$ | Gear ratio | - |
| $i_{\text{gearbox}}$ | Gear ratio for gearbox | - |
| $i_{tot}$ | Total gear ratio from motor to ground | - |
| $i_{totnewlow}$ | New lower limit for gear ratio | - |
| $i_{\text{wheel}}$ | Gear ratio that the wheel contributes with | - |
| $K_a$ | Application factor for gears | - |
| $\kappa$ | Viscosity ratio | - |
| $L_1$ | Distance | m |
| $L_{10}$ | Basic rating life (90% reliability) | Million rev |
| $L_{10m}$ | Basic rating life | Million rev |
| $L_2$ | Distance | m |
| $L_3$ | Distance | m |
| $m$ | Mass of the car | kg |
| $m_{\text{wheel}}$ | Mass of the wheel | kg |
| $M$ | Bearing mass | kg |
| $n$ | Rotational speed | $^{r}/_{min}$ |
| $\eta_c$ | Contamination factor | - |

| Symbol | Description | Unit |
|---|---|---|
| $N_{lim}$ | Limiting speed | $^{r}/_{min}$ |
| $N_{ref}$ | Reference speed | $^{r}/_{min}$ |
| $N_{\text{speed bins}}$ | Number of bins of speed bins | # |
| $N_{\text{torque bins}}$ | Number of bins of torque bins | # |
| $\nu$ | Actual viscosity of the lubricant | $^{mm^2}/_{s}$ |
| $\nu_1$ | Required viscosity of the lubricant | $^{mm^2}/_{s}$ |
| $O_{xy}$ | Point, Outer bearing in the xy-plane | - |
| $O_{yz}$ | Point, Outer bearing in the yz-plane | - |
| $OW$ | Offset wheel center | m |
| $P$ | Equivalent dynamic bearing load | kN |
| $p$ | Exponent of life equation | - |
| $P_U$ | Fatigue load limit | kN |
| $R$ | Wheel radius | m |
| $R_{ao}$ | Reaction force axially outer bearing | N |
| $R_{rix}$ | Reaction force radially inner bearing x | N |
| $R_{riz}$ | Reaction force radially inner bearing z | N |
| $R_{rox}$ | Reaction force radial outer bearing x | N |
| $R_{roz}$ | Reaction force radial inner bearing x | N |
| $R_{roz}$ | Reaction force radial outer bearing z | N |
| $\rho$ | Density | $^{kg}/_{m^3}$ |
| $T$ | Applied torque | NM |
| $T_{19}$ | Torque from CFS19 | NM |
| $T_{new}$ | New Torque | NM |
| $T_{tot}$ | Total Torque | NM |
| $U$ | Life cycle fraction | % |
| $v$ | Velocity | $^{m}/_{s}$ |
| $\omega_{19}$ | Rotational speed from CFS19 | $^{rad}/_{s}$ |
| $\omega_{new}$ | New rotational speed | $^{rad}/_{s}$ |
| $X$ | Calculation factor for the radial load | - |
| $Y$ | Calculation factors for the axial load | - |
| $z_1$ | Number of teeth on the input gear | # |
| $z_2$ | Number of teeth on the output gear | # |
| $z_r$ | Number of teeth of the ring gear | # |
| $z_s$ | Number of teeth of the sun gear | # |

# Contents

**List of Figures** **xv**

**List of Tables** **xvii**

**1 Introduction** **1**
1.1 Background . . . 2
1.1.1 Unsprung Mass . . . 2
1.1.2 Formula Student . . . 2
1.1.3 Transmissions for Electric Machines . . . 3
1.1.4 Previous CFS-Transmissions . . . 3
1.1.5 Gear Ratio . . . 4
1.2 Purpose . . . 5
1.3 Methodology . . . 5
1.4 Limitations . . . 5

**2 Theory** **7**
2.1 Gear Geometry and Gearbox Kinematics . . . 7
2.2 Load Cases . . . 9

**3 Concept Generation** **11**
3.1 Method . . . 11
3.1.1 Boundaries . . . 11
3.1.2 Requirements . . . 11
3.1.3 Sub-Functions . . . 12
3.1.4 Concept Matrices . . . 12
3.2 Results . . . 13
3.2.1 Boundaries . . . 13
3.2.2 Requirements . . . 13
3.2.3 Sub-Functions . . . 14
3.2.4 Concept Matrices . . . 15
3.2.5 Final Concept . . . 18
3.3 Discussion . . . 18

**4 Transmission Load Cases** **19**
4.1 Method . . . 19
4.2 Results . . . 20
4.2.1 Data Sourcing . . . 20

4.2.2 Load Spectrum . . . 20
4.2.3 Expected Service Life . . . 22
4.3 Discussion . . . 23

**5 Gear Design 25**
5.1 Method . . . 25
5.2 Results . . . 26
5.2.1 Configurating Fundamental Geometry . . . 26
5.2.2 Defining parameters . . . 27
5.2.3 Contact, Stress and Load Analysis . . . 29
5.2.4 Planetary Bearings . . . 31
5.2.5 Gear Modelling . . . 33
5.3 Discussion . . . 34

**6 Bearings & Housing Load Cases 37**
6.1 Theory . . . 37
6.2 Method . . . 39
6.2.1 Data Sourcing . . . 39
6.2.2 Deriving Load Cases from Data . . . 40
6.3 Results . . . 44
6.3.1 Data Interpretation . . . 44
6.3.2 Deriving Loads From Data . . . 46
6.3.3 Final Load Cases . . . 49
6.4 Discussion . . . 49

**7 Housing Design & Bearing Selection 51**
7.1 Method . . . 51
7.1.1 Housing & Carrier Design . . . 51
7.1.2 Bearing Selection . . . 51
7.2 Results . . . 52
7.2.1 Housing & Carrier Design . . . 52
7.2.2 Bearing Selection . . . 55
7.3 Discussion . . . 59
7.3.1 Housing Design . . . 59
7.3.2 Bearing Selection . . . 60

**8 Final Design 61**

**9 Discussion 65**

**10 Conclusion 67**

**Bibliography 68**

**11 Appendices 71**

# List of Figures


1.1 Madeleine, CFS20's Car - Photographer: Eric Gustafsson . . . . . 1
1.2 Exploded view of the current powertrain assembly for the CFS car . . 3
1.3 Lap time simulation - Created by: Daniel Persson Ilonen, CFS19 [12] 4

2.1 Three examples of geared transmissions . . . . . 8
2.2 Geometry of a gear tooth . . . . . 8

3.1 Morphological matrix for transmission, Excerpt from Appendix B . . 15
3.2 Showing the differences between different transmission layouts from Figure 3.1 . . . . . 15
3.3 Showing the differences between torque transfer output via shaft and torque transfer output via housing from Figure 3.1 . . . . . 16
3.4 Kesselring matrix for transmission concepts, excerpt from Appendix E 16
3.5 Pugh matrix for transmission concepts, simplification of Appendix G 17
3.6 Final concept sketched . . . . . 18

4.1 Bi-variate histogram of torque and speed . . . . . 21

5.1 Gearbox model in KISSsys . . . . . 27
5.2 Definition of stationary components as well as input and output in KISSsoft . . . . . 30
5.3 Normal load distribution on the sun gear in KISSsoft . . . . . 30
5.4 3D-models of the gear designs . . . . . 33
5.5 3D-models of final gears, rendered in CATIA V5 . . . . . 34

6.1 Illustration of normal forces at standstill for the CFS19 Car . . . . . 37
6.2 Illustration of tangential forces on one wheel at the moment of acceleration from standstill, denoted as $F_T$. $F_N$ denotes normal force and T the applied torque. . . . . 38
6.3 Illustration of lateral forces during cornering and deceleration from top view . . . . . 38
6.4 Angle sensor logging the angle of the rear pushrod pivot shaft . . . . 39
6.5 Victoria, developed by CFS19 . . . . . 40
6.6 Free body diagram from side view for hand calculations of normal forces on the front axle . . . . . 41
6.7 Free body diagram for hand calculations of the tangential force, denoted $F_T$, on one wheel . . . . . 42

6.8 Illustration of the position of the three forces $F_N$, $F_T$ and $F_L$ on the wheel used for dimensioning the gearbox housing and bearings . . . . 43
6.9 Imported ADC-values from the front pushrod pivot shaft angle sensors 44
6.10 Transfer function between ADC-signal and angle for both front wheels 45
6.11 All ADC-data points converted into angles on the pushrod pivot shaft 45
6.12 Graph showing the approximated normal forces for FL and FR wheel 47
6.13 Graph showing the approximated tangential forces for one wheel . . . 48
6.14 Graph showing the approximated lateral forces for both front wheels . 48
6.15 Overview of front suspension . . . . . 49

7.1 Rendering and deformation analysis of carrier . . . . . 52
7.2 Reference points for calculating the skewing of the planet gears in carrier . . . . . 53
7.3 3D-modelling and deformation analysis of housing . . . . . 54
7.4 3D-modelling and deformation analysis of final housing . . . . . 55
7.5 Free body diagram of the bearing assembly in the YZ-plane . . . . . 56
7.6 Free body diagram of the bearing assembly in the XY-plane . . . . . 56

8.1 Front and section view of the gearbox . . . . . 61
8.2 Exploded view of the carrier and its associated components . . . . . 62
8.3 Exploded view of the housing and the ring gear, with the rotating assembly in between . . . . . 62
8.4 3D-model of the final gearbox in CATIA V5 . . . . . 63

# List of Tables


3.1 Requirements specification without load cases . . . . . 14
3.2 Overview of sub-functions . . . . . 15

5.1 Input parameters in KISSsoft . . . . . 27
5.2 Materials and oil choice for gears . . . . . 28
5.3 Input parameters in KISSsoft step 2 . . . . . 28
5.4 Manufacturing process and tooth thickness tolerances for gear . . . . 28
5.5 Fine sizing in KISSsoft . . . . . 29
5.6 Axis alignment . . . . . 30
5.7 Operating backlash in KISSsoft . . . . . 31
5.8 Planetary and carrier bearings in KISSsys . . . . . 32
5.9 Final safety factors for gears . . . . . 32
5.10 Micropitting and scuffing for gears . . . . . 32

7.1 Specifications of the final selected bearings for the wheel axis . . . . . 59
7.2 Calculations on final selected bearings . . . . . 59

8.1 Weight comparison between CFS19 and the new gearbox . . . . . 63

# 1
# Introduction

Formula Student (FS) is one of the world's largest engineering competitions for students. Teams from around the world design, build and make a business plan for a small formula style race car. Chalmers Formula Student (CFS) has participated in the competition since 2002. Initially CFS built combustion engine cars but has since 2015 built electric cars. Additionally, they have been implementing a four wheel drive system on the car since 2019. The system consists of four motors mounted on each wheel assembly, each with their respective gearbox. Since it is a racing car, it is greatly advantageous that the gearboxes are light, particularly since the gearboxes are mounted directly on the wheel which should follow the unevenness of the road as smoothly as possible.


**Figure 1.1:** Madeleine, CFS20's Car - Photographer: Eric Gustafsson

In Sweden, there are currently eight Formula Student teams, including the team from Chalmers. The teams build a new race car every year, which they take to various competitions around the world in the summer to compete against other universities.

However, Formula Student is not really about building the fastest car, it is about being able to make the optimal race car based on the conditions that the team has. It is in other words of great concern to be able to create and explain the optimal design.

## 1.1 Background

### 1.1.1 Unsprung Mass

The consequence of mounting the gearboxes in the wheel assembly is that the mechanical powertrain follows the movement of the tyres, resulting in a high unsprung mass compared to an inboard solution [4]. Unsprung mass, in the context of vehicle dynamics, includes all mass that is not supported by a vehicle's suspension. From a performance standpoint, it is important that the unsprung mass is as low as possible since it directly affects the dynamic normal contact force between the road and the tyre's contact patch which is of great significance for the vehicle's handling.

### 1.1.2 Formula Student

Formula Student competitions take place typically during the summer. There are several different competitions around the world, and they usually last for a week. The week begins with the car being inspected to compete, then the competition itself begins. In Formula Student the teams compete in both static and dynamic events.

The dynamic events are:
**Acceleration** 75m straight.
**Skidpad**, race in constant turning, going in a figure 8 circuit, two right hand laps and two left hand laps, fastest time wins.
**Autocross**, one lap on a tight and winding track that is around 1 km long, fastest time wins.
**Endurance**, the same track as autocross but you drive 20 km, one driver change, fastest time wins.
**Efficiency**, the energy consumed during endurance is measured and the time is also taken into account.

And the static events are:
**Engineering Design**, the team presents the car to several judges and questions will be asked about their design and processes. The better the answer, the better the score.
**Cost and Manufacturing**, Like Engineering Design but the judges focus on manufacturing and costs, if the judges are convinced that the work is well done, more points are obtained.
**Business Plan Presentation**, The judges will now be investors and the team will convince the judges that their car can be monetized. How well this is done determines how many points one gets.
A well-developed gearbox and also a well-documented process is obviously favorable for the team, both in the static and dynamic events. A well-developed FS gearbox has two characteristic features. The first one is that it is light, Newton's second law gives the insight that lower mass gives a higher acceleration which is advantageous for a race car. And the second one is that it is reliable and does not fail.

### 1.1.3 Transmissions for Electric Machines

Conventional internal combustional engines can only operate efficiently and deliver the power at a certain RPM interval. This is why transmissions with multiple stages are used, in order to maximize the torque output when accelerating and speed when the vehicle is moving. The difference when it comes to electrical motors is that they are able to offer instant power delivery at a very low RPM while easily being able to rev to 10000 RPM and more. Additionally, electrical motors do not stall, eliminating the need to have a clutch, which increases the simplicity. That is why multi-speed transmissions are not needed and can cause inefficiencies in terms of added weight [15].

### 1.1.4 Previous CFS-Transmissions

Since 2019 CFS has built four wheel drive cars utilizing hub motors for packaging reasons, meaning that there is one driving unit consisting of an electric motor and a transmission powering each wheel mounted directly on the wheel assembly. This assembly is illustrated in Figure 1.2. The CFS21's gearbox solution is a 1.5 step compound planetary gearbox with a 14:1 gear ratio. A compound planetary gearbox has a pair of longitudinally connected planet gears with different radii with one set of gears meshing with the input sun and another meshing with the ring gear [18].

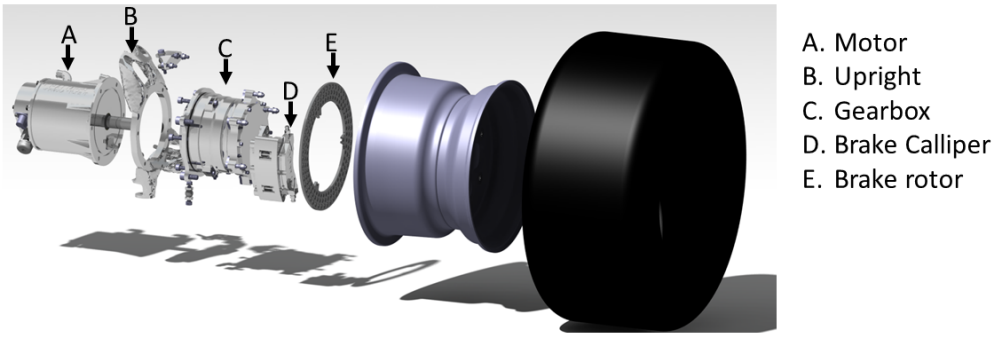


**Figure 1.2:** Exploded view of the current powertrain assembly for the CFS car

In addition, CFS has decided to move towards a lower tyre profile for the 2022 season, which results in a reduced wheel circumference. Therefore, the transmission gear ratio needs to be evaluated which might enable other more effective transmission solutions.

### 1.1.5 Gear Ratio

The gear ratio from the electric machine to the wheel mainly depends on two parameters, the gearbox gear ratio and the roll diameter of the wheel. CFS intends to change from the 18" used in recent years to 16" in wheel diameter. This will affect the total gear ratio, which will be demonstrated in a calculation example below.

CFS wants an equally optimal gear ratio, with a lighter gearbox, which should result in a faster car. To do this, simulations are used, below is a simulation that shows different lap times depending on the gear ratio. It is also known that the gear ratio on the CFS19 car was 14:1 [12].

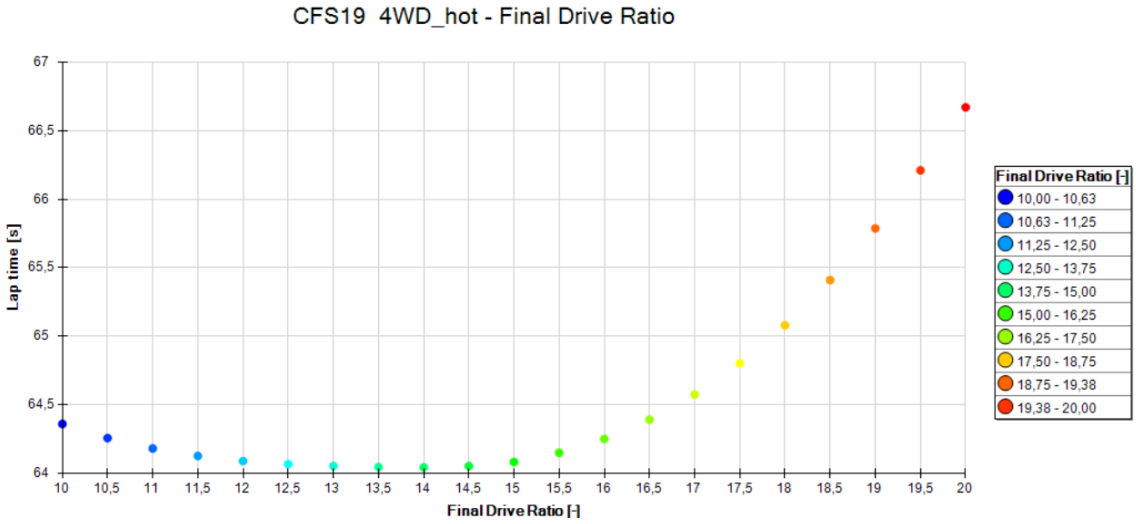


**Figure 1.3:** Lap time simulation - Created by: Daniel Persson Ilonen, CFS19 [12]

The conclusion from Figure 1.3 is that a gear ratio between approximately 13:1 and 14:1 gives the same lap time. An equation for the total gear ratio is generated in Equation 1.1.

$$i_{tot} = i_{\text{gearbox}} \cdot i_{\text{wheel}} \tag{1.1}$$

Where $i_{\text{gearbox}}$ is the gear ratio for the gearbox, which is what this project should determine and design a gearbox that can deliver. $i_{\text{wheel}}$ is the ratio that the wheel diameter change contributes with. If the wheel diameter changes this gives a ratio that needs to be taken into consideration if the same lap time wants to be achieved.

Then the value of the limits that still gives an equally fast car are recalculated with the new smaller wheel (18" $\rightarrow$ 16") is evaluated in equation 1.2 and 1.3.
The lower limit:

$$i_{totNewLow} = 13 \cdot \frac{16}{18} = 11.555... \tag{1.2}$$

The upper limit:

$$i_{totNewLow} = 14 \cdot \frac{16}{18} = 12.444... \tag{1.3}$$

The values are rounded and made to an interval within which the new gearbox must be $[11.5 : 1 - 13 : 1]$.

## 1.2 Purpose

The purpose of this project is to develop a gearbox for the upcoming CFS car that is lighter than the most recent manufactured CFS gearbox. This is done with the overall objective to lower the unsprung mass which should result in a better performing car. The gearbox design should be durable enough to last a full season of running. The secondary purpose is that the outcome of this project should result in a development for a design methodology that can be used by future CFS teams.

## 1.3 Methodology

The structure of this report is presented in a specific way. The report is constituted of different sections beginning with concept generation, transmission load cases, gear design, bearings and housing load cases, housing design and bearing selection and final design. Each section has its own method, results and discussion. This is due to the fact that each section is dependent on the previous section. Before beginning with the gear design for instance, the concept generation and transmission load cases have to be finished, to know what type of gearbox is going to be used and the loads affecting it.

The first step is to generate a concept. This concept is subjected to loads meaning a load case spectrum has to be defined using MATLAB scripts provided by previous CFS teams. A model geometry is then created in KISSsys and the spectrum is uploaded to the software. The loads and stresses are analyzed in KISSsoft and the gears are optimized to get acceptable safety factors. Simultaneously, using MATLAB scripts that compute normal, tangential and lateral forces during the course of a lap, load cases are defined for the housing and bearings in order to dimension them correctly. As a next step, a CAD model is generated in CATIA V5, and finally, the housing is analyzed using a FEM software called ANSYS to study the stresses affecting it.

## 1.4 Limitations

As with many projects, there exists a few delimitations related to this project as well. The budget for all four gearboxes should not exceed a market value of 100 000 Swedish crowns. This will have implications on the design of the gearbox when it comes to the choice of materials, manufacturing processes, how advanced the gearbox can be made and which outsourcing that can be done. It is also important to note that the time for developing the gearbox is limited to the spring of 2021 (2021-01-18 to 2021-05-14).

Moreover, it is worth mentioning that the new design of the gearbox may be bigger than the current one, which implies that the upright (see Figure 1.2) has then to be bigger. Thus it will have a larger volume and consequently a higher mass. However this is not an area which will be studied or analysed in detail in this project but estimating calculations will be done to this matter.

# 2

# Theory

## 2.1 Gear Geometry and Gearbox Kinematics

There exist myriads of different gearbox designs and a multitude of different gear tooth geometries. The ones that are found to be relevant to this project are presented in this chapter to give some background for the reader.

Perhaps the out most simple gear transmission is the *spur gear transmission* (see Figure 2.1 a) which in its most basic form consists of only two cylindrical gears with external teeth on parallel shafts. The gear ratio of a spur gear transmission is calculated as [17]:

$$i = \frac{z_2}{z_1} \tag{2.1}$$

Where $i$ is the transmission ratio defined as the number of turns of the input for every turn of the output[1], $z_1$ is the number of teeth on the driven gear (input gear) and $z_2$ is the number of teeth on the output gear.

Another geared transmission is the *internal gear transmission* (see Figure 2.1 b) this consists of a smaller spur gear (red) enclosed in a larger internally toothed gear (green). The transmission ratio calculation is the same as for the spur gear transmission. The internal gear transmission has a larger *contact ratio* than that of two externally toothed gears working together. This means that more teeth on average are in contact with each other which is beneficial as the load is distributed over more teeth. [17]

A third common gear transmission is the *planetary transmission* (see Figure 2.1 c) (also known as a epicyclic gear train), this is a very compact way to achieve a comparatively high transmission ratio. The input and output may be any of the three: sun gear (yellow), planet carrier (green) or ring gear (red). The transmission ratio of a planetary gearbox is dependant on which parts are made to be input, output and which are stationary.

If the sun gear is the input, the carrier is stationary and the ring gear is the output the ratio will be:

$$i = -\frac{z_r}{z_s} \tag{2.2}$$

Where $i$ again is the transmission ratio as defined under equation 2.1, $z_s$ is the number of teeth of the sun gear and $z_r$ is the number of teeth of the ring gear.

If the sun gear is the input, the ring gear is stationary and the carrier is the

[1]Sometimes defined as the inverse but this is how it is used in this report.

output the ratio will be [17]:

$$i = \frac{z_r}{z_s} + 1 \tag{2.3}$$

This is the highest ratio configuration possible with a this type of planetary gearbox, with one input. Other configurations are possible as well but will not be discussed in this report.

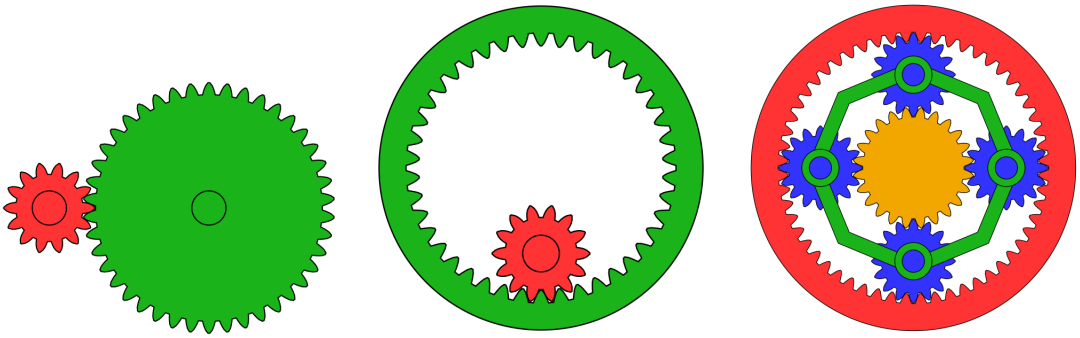

a) Spur gears b) Internal gear c) Planetary gearbox (epicyclic gearing)

**Figure 2.1:** Three examples of geared transmissions

Source: Wikimedia Commons

One of the most used gear geometries is the straight cut involute gear as it has favourable transmission characteristics as well as being relatively easy to produce. This is the type of gear that will be used in all later examples of gearboxes. The *involute* part can be found on the *flank* of the gear tooth which represents the side of the tooth (see Figure 2.2). The gear tooth *root* is the base of the tooth from the flank to the lowest part of the valley. The gear being *straight cut* refers to the teeth being parallel to the shaft on which the gear is mounted, as opposed to helical gears on which the teeth are cut at an angle. [17]

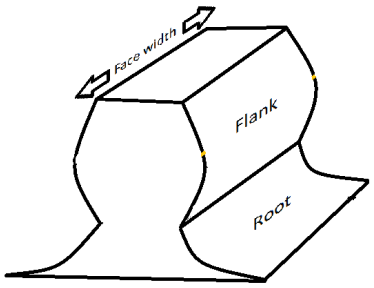


**Figure 2.2:** Geometry of a gear tooth

The gears themselves are defined by a set of parameters which are standardised, a few of these will be very central to the performance of the gearbox, others will be forced by outside influences (not all parameters will be discussed in this part).

One of the first parameters to decide is the number of teeth on each gear to achieve the desired transmission ratio. The kinematics of this looks very different for different types of gearboxes but in the end it is always the number of teeth that in some way decides the gear ratio. Many (theoretically infinite) sets of teeth numbers will yield the desired ratio but only a few will be practical. Here the tooth size needs to be determined, known as the *module*. The module together with the approximate desired size of the gearbox will determine which of the theoretically working sets of number of teeth will be used. Interacting gears, known as *meshing* gears, need to have the same module[2] to be able to mesh correctly. The module may in theory be any value (size) but since for most methods of producing gears a special tool is needed for each module, the sizes are standardised. This means that one should strive to use a standard modulus to save a significant amount of machining cost. A set of gears might have restrictions on the exact distance between the shafts, in this case *profile shifting* might be needed to keep the gears meshing properly. This is a process where the tool is shifted radially from "normal" cutting depth to create teeth with slightly different geometry. [17]

## 2.2 Load Cases

A load case denotes a group of loads, supports or displacements that are applied to a model at a specific time. A model can be subjected to different load cases at different times [2].

[2]Actually, the *base pitch* needs to be the same but in practice this means that the module will have to match.

# 3
# Concept Generation

## 3.1 Method

The process of defining possible concepts to the decision of final concept/concepts to further develop is described in this chapter. First, the fundamental boundaries are defined which sets the rules for the generation of concepts. The requirements needed to ensure the function of the final concept are also defined. The boundaries combined with studies of earlier FS-teams and literature results in a number of possible solutions which are then compared with decision matrices based on the requirements. These methods results in a ranking of most promising concepts, of which the final concept/concepts can be chosen.

### 3.1.1 Boundaries

Since the time frame of the project is narrow the concept generation needs to be very effective. Therefore the method of introducing reasonable boundaries is used to minimize the risk of unnecessary work before the concept generation starts. The boundaries are defined with this purpose in mind and chosen carefully to not exclude any useful and innovative solutions. The literature used to support the boundaries are found at the Chalmers library as well as on web sites on the internet. Members from CFS-teams and experts at Chalmers and from the industry are then contacted to verify that the boundaries are reasonable.

### 3.1.2 Requirements

To eliminate insufficient concepts and to determine which concepts are most suitable for the project, a list of requirements is compiled to a requirements specification. The goal is not to make a heavy product-oriented requirements specification, instead only the most important requirements for function and competition compliance are included to support an effective concept generation. The functions are defined by studying Mechanical Powertrain (MPT) reports from earlier CFS-teams to see what external features (brake disc/caliper, upright mounting etc) are needed to be taken into consideration when developing the transmission housing.

For comparing the concepts, quantifiable *wishes* are also defined, and these can be used as support for those decisions. There are also a few rules regarding the gearbox. These rules are defined by Formula Student Germany which is considered to be the leader in FS.

### 3.1.3 Sub-Functions

A number of sub-functions should be developed by analyzing which functions the gearbox solves, as well as the functions that the gearbox indirectly affects. This is partly done by controlling which requirements the function must maintain [23]. To ensure that the final concept have all these functions, they are called *sub-functions* of the concept and will be the foundation of the concept generation. The idea is that each of the sub-functions will be assigned alternative solutions which then will be combined into multiple complete concepts to compare and choose the final concept from.

### 3.1.4 Concept Matrices

The sub-functions are divided into two separate parts: *transmission* and *accessories*. Transmission includes the sub-functions for the rotating assembly as well as the housing. Accessories includes the sub-functions that will be mounted on the housing, for example the break caliper and upright seen in Figure 1.2. The reason for this division is to simplify the concept generation process since time is limited. The division means that the number of concepts in the first step decreases, this is because the number of concepts is the number of the solution for each sub-function multiplied by each other. By looking at fewer sub-functions at a time, the number of concepts to be compared at the same time is reduced, which eliminates unrealizable and less favorable concepts earlier in the process. There are still theoretically many concepts to be implemented, but the process is narrowed down. The risk with this method is that a "heavy" transmission-concept that is eliminated could be lighter when combined with the Accessories. The risk of this being the case is considered very low.

First, the transmission sub-concept is concept generated with a Morphological matrix [23]. All combinations are evaluated but the physically impossible combinations are ignored. The remaining concepts are evaluated in Pugh [23] and Kesselring matrices. The criteria in both matrices are based on the wishes from the requirement list. In the first iterations of the Pugh matrix for the transmission-concept, the gearbox from CFS21 (explained in Section 1.1.4 and can be seen in Figure 1.2) is used as a reference.

From the last iterations a final ranking from the Pugh matrix method is achieved from which the lowest ranked concepts could be eliminated leaving a fewer number of concepts to continue choosing from.

Before these set of concepts are carried over to the Kesselring matrix, the criteria must be defined and quantified. These criteria are based on the wishes from the requirement list as stated before, but are more specific than in the Pugh matrix. This is because each criteria must be a measurable factor based on which all concepts can be evaluated. Therefore the criteria in the Pugh- and Kesselring matrices might differ. From the Kesselring matrix, a final ranking of the transmission-concepts is achieved. From this ranking, one or two final concepts can be chosen.

Next, the chosen transmission concept/concepts are combined with the accessories in a morphological matrix, which results in a concept of the whole gearbox with accessories. All possible solutions are evaluated in the above mentioned matri-

ces again, resulting in one or two final complete concepts.

## 3.2 Results

### 3.2.1 Boundaries

First different gearbox types are benchmarked to use as basis for the concept selection. To investigate what solutions were suitable a literature study was done. This helped exclude irrelevant solutions.

In the study it was found that a friction gear, a V-belt or flat-belt solution would have a lower efficiency than a gear solution [17]. It was also found that they had a lower precision, which however, does not have a huge significance but is still disadvantageous [17].

When it comes to chains and sprockets, they perform in a similar manner as a gear to gear solution, but with the possibility to move the shafts further apart, which in this case is the opposite of what is wanted to be achieved. FS requires a compact solution that fits inside the rim. The chain also adds mass.

The result of this study is that gear driven transmissions are superior to friction gears, belt and chain drives in terms of packaging, strength and efficiency. Therefore all friction gears, belt and chain drives are excluded from this project since they both are difficult to package in the space given and have low efficiency in terms of friction losses. Therefore only gear-driven transmissions will be evaluated in this project.

Bearings are central components in a transmission and there are many possible types of bearings both in terms of models and locations in the housing. To determine what type of bearing solution is most suitable, the load cases need to be defined in order to know what characteristics are needed (axial movement, etc.). The bearings will not be included as a sub-function in the concept generation. This boundary simplifies the concept generation but also means that the concepts need to be thought through so that there are space for bearings.

Concerning the type of gears to be used, it is concluded that only spur gears would be used. The reason to this choice lies in their simple design, making them easy and cheap to produce. Add to this they produce no axial forces [20].

Moreover, in planetary gearboxes, a different number of planets can be used and each has its own advantages. In this project however, only 3 planets will be used because the axial forces developed between the mesh of the gears cancel each others in a 3 planet-system [3].

### 3.2.2 Requirements

A requirements specification (Table 3.1) was established after both discussions with those who had previously been responsible for MPT within CFS and by analyzing the adaptations required for a new tyre diameter. The requirements specification was made as simple as possible and as quantifiable as possible to simplify the concept generation. It was also affected by a number of rules, Formula Student Germany (FSG) defines the rules regarding FS. There are some specific rules for the gearbox which are available as an extract in the Appendix A. The conclusion drawn from

the rule book was that, primarily, the rotating assembly needs to be protected with 2mm steel or 3mm aluminium alloy 6061-T6, secondly the lubrication needs to be sealed so that no leakage exists when the car is tilted 60°. The details of the load case specific requirements can be found in Chapter 4 and 6.

**Table 3.1:** Requirements specification without load cases

| Chalmers | Document type<br>*Project* | Concept Requirements<br>Gearbox for CFS | | | | |
|---|---|---|---|---|---|---|
| | | *Created:* 2021-02-12<br>*Modified:* | | | | |
| *Criteria* | | *Target Value* | *R/W* | *Value* | *Verification* | *Reference* |
| **Functions** | | | | | | |
| | Torque Transfer Input | | R | | | |
| | Torque Transfer Output | | R | | | |
| | Mounting Electric Machine (Bolt Pattern) | | R | | | |
| | Mounting Brake Disc | | R | | | |
| | Mounting Brake Caliper | | R | | | |
| | Mounting Upright | | R | | | |
| **1. Performance** | | | | | | |
| 1.1 | Gear Ratio | 11.5:1 - 12:.51 | R | | Calculations | |
| **2. Environment** | | | | | | |
| 2.1 | Temperature Intervall | -5 °C to +75°C | R | | Material Analysis | |
| 2.2 | Water Proof | Mildly Rain | R | | 3D-Model | |
| 2.3 | Debris | From Road Surface | R | | 3D-Model | |
| **3. Size** | | | | | | |
| 3.1 | Radial Space | 235 mm Outer Diameter | R | | 3D-Model | |
| 3.2 | Axial Space | As Thin as Possible | W | | 3D-Model | |
| **4. Mass** | | | | | | |
| 4.1 | Total Mass | As Low as Possible | W | | 3D-Model | |
| 4.2 | Rotating Components | As Few as Possible | W | | 3D-Model | |
| **5. Packaging** | | | | | | |
| 5.1 | Brake Disc | Fits Available Space | R | | 3D-Model | |
| 5.2 | Brake Caliper | Fits Available Space | R | | 3D-Model | |
| 5.3 | Upright | Fits Available Space | R | | 3D-Model | |
| 5.4 | Space Efficient Housing | Cylindrical and Concentric Shape | W | | 3D-Model | |
| **6. Rule Complience** | | | | | | |
| 6.1 | Rotating Assembly Protection | 2mm steel/3mm aluminium alloy 6061-T6 | R | | | FSG Rules T7.3.2 |
| 6.2 | Sealed Lubrication | No Leakage (Max Inclination 60 deg) | R | | | FSG Rules T7.2.4 |
| **7. Material** | | | | | | |
| 7.1 | Housing | Steel or Aluminium Alloy | R | | | |
| **8. Cost** | | | | | | |
| 8.1 | Budget | <= 100 000 SEK Market Value | R | | | CFS |
| **9. Maintainance** | | | | | | |
| 9.1 | Service Interval | 50 km | R | | | CFS |
| **10. Manufacturability** | | | | | | |
| 10.1 | Housing | Chalmers Course Lab | W | | | CFS |
| 10.2 | Housing | Outsource | R | | | CFS |
| 10.3 | Gear Set | Outsource | R | | | CFS |

### 3.2.3 Sub-Functions

The requirements from Table 3.1 are used as a base to analyse which sub-functions the concepts need to solve. The main function of the gearbox is of course to transmit torque. This has been divided into two sub-functions, the first is transmission layout and the second is torque transfer output. With transmission layout it is meant the type of planetary gear that is intended and with torque transfer output it is meant how the torque is transmitted to the rim.

The gearbox also has some secondary functions regarding the braking and mounting. Since the brakes must be mounted somewhere between the motor and the wheel, a complete solution must be designed taking this into account. The gearbox must also be mounted together with the wheel suspension, this is usually done with a type of upright solution. The secondary functions are also divided into sub-functions, these are mounting brake disc, mounting brake caliper and upright. These three sub-functions will be called accessories. All functions are compiled in

Table 3.2 to provide a better overview.

**Table 3.2:** Overview of sub-functions

| # | **Sub-functions** |
|---|---|
| | **Transmission Sub-functions** |
| 1 | Transmisson Layout |
| 2 | Torque Transfer Output Solution |
| | |
| | **Accessories Sub-functions** |
| 3 | Mounting Solution Brake Disc |
| 4 | Mounting Solution Brake Caliper |
| 5 | Upright |

The reason for the division between transmission- and accessories sub-functions is discussed in Section 3.1.4.

### 3.2.4 Concept Matrices

The concept generation began with a morphological matrix (see Figure 3.1), based on the transmission sub-functions from Table 3.2, to generate 18 concepts to solve the transmissions part of the gearbox.

| | | Sub function solution | | | | | | | | | |
|---|---|---|---|---|---|---|---|---|---|---|---|
| | **Sub Function** | **A** | **B** | **C** | **D** | **E** | **F** | **G** | **H** | **I** | **J** |
| 1. | Transmisson Layout | 1-Stage Planetary w. Locked Ring | 1-Stage Planetary w. Locked Carrier | 1-Stage Overlap Planetary w. Locked Ring | 1-Stage Overlap Planetary w. Locked Carrier | Compound Planetary w. Locked Inner Ring | Compound Planetary (CFS 19/20) | Compound Planetary w. Locked Carrier | 1 Stage Planetary w. Locked Ring + Conventional Gear Reduction | Excentric Internal Gear Set | Conventional Gear Set |
| 2. | Torque Transfer Output | Shaft | Housing | | | | | | | | |

**Figure 3.1:** Morphological matrix for transmission, Excerpt from Appendix B

In Figure 3.1 different types of solutions for the transmission layout output are stated, some of which are explained in Figure 3.2.

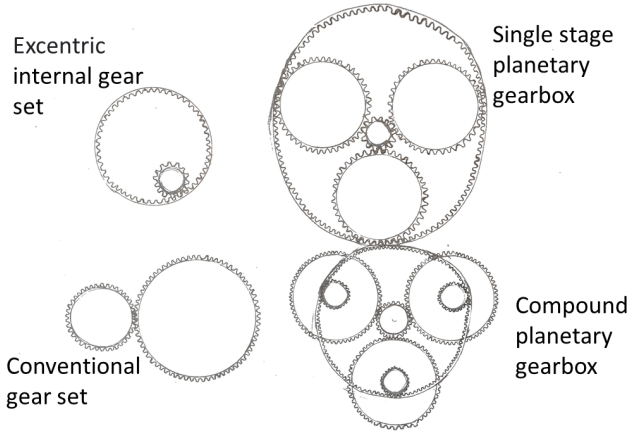


**Figure 3.2:** Showing the differences between different transmission layouts from Figure 3.1

In Figure 3.1 different types of solutions for the torque transfer output are stated, these are explained in Figure 3.3.

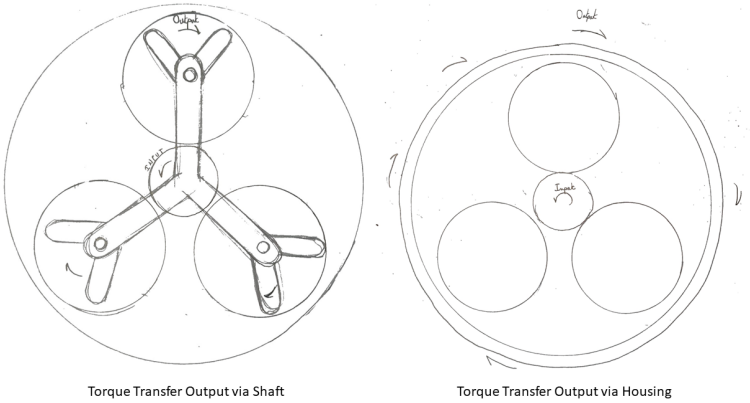


**Figure 3.3:** Showing the differences between torque transfer output via shaft and torque transfer output via housing from Figure 3.1

All combinations are evaluated but the physically impossible combinations are ignored, this was done through evaluating against elimination criteria from the requirements specification (Table 3.1). The evaluation was done using an elimination matrix (Appendix C), this resulted in 15 concepts remaining. The 15 concepts were then evaluated using two iterations of a Pugh Matrix (Appendix D), the criteria for the Pugh matrix are based on the wishes from the requirements specification (Table 3.1).

In the first iteration the CFS21-solution (explained in Section 1.1.4 and can be seen in Figure 1.2) was used as a reference, this was done to ensure that the concepts that have been generated at least have some advantages over the current solution. The second time the highest ranked concept from the first iteration was used as reference, concept-1 (declared in Appendix B). Then the lowest ranked concepts were eliminated leaving eight concepts to choose from.

Before these set of concepts were carried over to the Kesselring matrix (Appendix E), the criteria was defined and quantified. These criteria are based on the wishes from the requirement list as stated before.

| **Chalmers** | | **Kesselring-Matrix** | | | | | | | | | | | | | | | | | |
|---|---|---|---|---|---|---|---|---|---|---|---|---|---|---|---|---|---|---|---|
| | | | | **Created: 2021-02-17** | | | | | | | | | | | | | | | |
| **Criterias** | | **Concepts** | | | | | | | | | | | | | | | | | |
| | | **Ideal** | | **1** | | **2** | | **5** | | **6** | | **7** | | **8** | | **9** | | **12** | |
| | w | v | | v | t | v | t | v | t | v | t | v | t | v | t | v | t | v | t |
| A (Gear Simplicity) | 1,17 | 5,00 | | 4 | 4,67 | 4 | 4,67 | 3 | 3,5 | 3 | 3,5 | 3 | 3,5 | 3 | 3,5 | 3 | 3,5 | 4 | 4,67 |
| B (Housing Simplicity) | 1 | 5 | 5 | 5 | 5 | 3 | 3 | 5 | 5 | 3 | 3 | 2 | 2 | 3 | 3 | 4 | 4 | 4 | 4 |
| C (Housing Axial Thickness) | 0,33 | 5 | 1,67 | 4 | 1,33 | 4 | 1,33 | 4 | 1,33 | 4 | 1,33 | 4 | 1,33 | 4 | 1,33 | 3 | 1 | 3 | 1 |
| D (Space Efficiency) | 0,33 | 5 | 1,67 | 5 | 1,67 | 5 | 1,67 | 5 | 1,67 | 5 | 1,67 | 5 | 1,67 | 5 | 1,67 | 5 | 1,67 | 5 | 1,67 |
| E (Manufacturability at Chalmers CL) | 1 | 5 | 5 | 4 | 4 | 4 | 4 | 4 | 4 | 4 | 4 | 4 | 4 | 4 | 4 | 4 | 4 | 4 | 4 |
| ***T (Total Weighted Value)*** | | 19,17 | | 16,67 | | 14,67 | | 15,50 | | 13,50 | | 12,50 | | 13,50 | | 14,17 | | 15,33 | |
| ***T / T ideal*** | | 1,00 | | 0,87 | | 0,77 | | 0,81 | | 0,70 | | 0,65 | | 0,70 | | 0,74 | | 0,80 | |
| **Rank** | | | | 1 | | 4 | | 2 | | 6 | | 7 | | 6 | | 5 | | 3 | |
| **Decision** | | **Further Development With Concept 1 & 12** | | | | | | | | | | | | | | | | | |

**Figure 3.4:** Kesselring matrix for transmission concepts, excerpt from Appendix E

Two final concepts were then chosen by using a Kesselering Matrix, Figure 3.4. The two final concepts for solving the transmission part were concept number one and twelve. The concepts are described in text form as:

**1:** 1-stage planetary with locked ring in a stationary housing with torque transfer via the output shaft. The brake disc is mounted on the transmission output shaft.

**12:** Compound planetary in a rotating housing with torque transfer via housing. The brake disc is mounted on the housing, same as CFS21 (explained in Section 1.1.4 and can be seen in Figure 1.2).

The concepts were chosen even though they were not the two highest ranked concepts. This was because the group considered it too risky to proceed with two single stage gearboxes in case it turned out that it was not physically possible to construct a single stage gearbox according to the existing requirements. Hence the decision to keep the best single stage and the subsequent best concept that was not single stage.

Next, the chosen transmission concepts were combined with the accessories in a morphological matrix, see Appendix B. Concept 1 and 12 were further developed into eight concepts with accessories, four from each.

An elimination matrix was created (see Appendix F) and used in the same way as before by using the requirements specification from Table 3.1. Two concepts did not reach the requirements of the elimination matrix, thus six concepts remained.

| | Alternatives | | | | | |
|---|---|---|---|---|---|---|
| | 1.1 REFERENS | 1.2 | 1.3 | 1.4 | 12.1 REFERENS | 12.2 |
| Netto | -1 | -1 | 0 | -1 | 1 | 2 |
| Rank | 2 | 2 | 1 | 2 | 1 | 2 |
| **Further Development** | N | N | Y | N | Y | N |

**Figure 3.5:** Pugh matrix for transmission concepts, simplification of Appendix G

Then two pugh matrices were made (next to each other in Appendix G ), the result can be seen in Figure 3.5.

On the left hand side, concepts 1.2, 1.3, 1.4 were evaluated against concept 1.1 and on the right hand side, concept 12.1 was evaluated against concept 12.2. This was done because the group considered that there was a risk in proceeding with only a single stage planetary gearbox if it later turns out that it did not meet the high requirements. So as a backup, it was also analyzed which was the best compound planetary gearbox. The conclusion from the pugh matrices was that 1.3 was the best single stage planetary gearbox concept and 12.1 was the best compound planetary gearbox concept.

### 3.2.5 Final Concept

Primarily, concept 1.3 has been chosen as the main concept to design. The concept can be described with words as:

**1.3:** Single stage planetary gearbox with a locked ring in a stationary housing with torque transfer via the output shaft. The brake disc is mounted on the transmission output shaft and with the brake caliper mounted on the housing. The upright is separate from housing.

The concept has also been sketched for visual understanding in Figure 3.6.

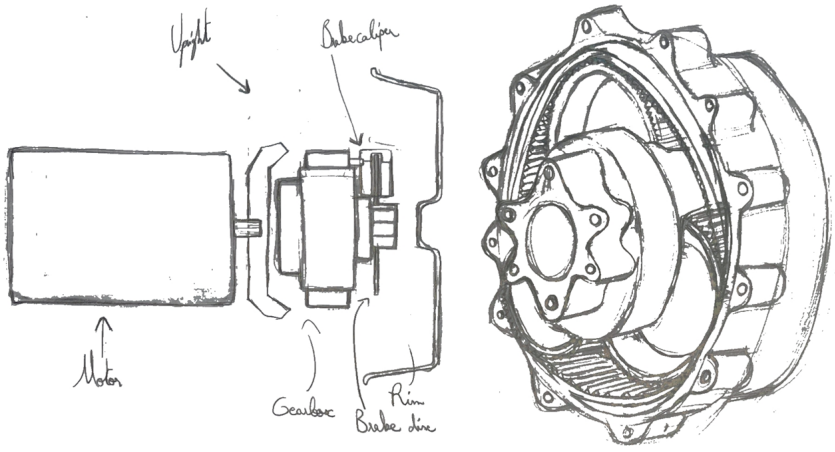


**Figure 3.6:** Final concept sketched

Secondarily, Concept 12.2 has been chosen as a backup concept for design if the primarily concept turns out to not be realizable. Concept 12.2 can be described as:

**12.1:** Compound planetary gearbox in a rotating housing with torque transfer via the housing. The brake disc is mounted on the housing and with the brake caliper mounted on the upright. The upright is separate from the housing.

## 3.3 Discussion

The division of sub-functions that are then concept generated in rounds may have resulted in a heavier total solution. However, the risk that the solution is not the lightest is low. With that said, the final concept in that case should only be slightly heavier than the optimal solution and that is a trade off that needed to be taken since the time is limited and the project is extensive.

Moving forward with two concepts is of great importance because there is a great uncertainty in the best concept. There is a risk when working outside of the normal gear ratio and the conclusion could be that it might not be robust enough.

# 4

# Transmission Load Cases

## 4.1 Method

To create the transmission load cases, data are gathered from the car on the track as this should give a more accurate depiction of the forces acting on the gearbox than computer simulations would. The real world data should contain unpredictable forces that are missed by the computer simulations. Another reason for choosing measured data is that it can easily be applied to future generation of cars, all using data from the previous year without having to update or create new computer models.

Here in this part the *transmission* will refer only to the internal parts of the gearbox e.g. the actual gears. These are assumed to be unaffected by outside forces acting on the gearbox such as those transferred from the wheel hitting bumps on the road. The only forces assumed to act on the transmission are the moments on the input and output shafts.

Even if the torque from the motor is assumed to be the only load acting on the transmission, other data is also important for the analysis. These are: the speed from the motor and GPS data for calculating distance traveled. The speed and torque values are used from all four wheels and the worst value from these four at any given point in time is sorted into one theoretical "worst case" wheel, this "wheel" will include all extraordinary loads experienced by any of the wheels. How this is achieved is discussed in closer detail in the result section.

A bi-variate histogram is created from this "worst case wheel" with a grid of speed and torque intervals respectively and the frequency of these scenarios occurring making up the third dimension. This load spectrum is then used by the gear designing program KISSsoft for an accurate dimensioning goal. The distance traveled during the event can be derived from the GPS data, this in conjunction with the speed of the vehicle determines the expected service life when scaled to the life time distance specified in the requirement specifications (see Table 3.1).

## 4.2 Results

### 4.2.1 Data Sourcing

Five consecutive laps from the *autocross* event of a celebratory unofficial competition at Achen in Germany were used as a basis for all data in the analysis. The race in Achen was used since it is the only one where all four motors were working without issues.

The extracted data was: torque and speed for all four wheels as well as position data from GPS. The torque and speed were sampled at 33.3 Hz and the GPS data was sampled at 10 Hz. The speed was measured directly with a sensor while the torque was (from beforehand) calculated from the current driving the motors.

The data was evaluated in MATLAB. To properly import the data, which was stored in .mdf format in the log it was imported into a MATLAB application (.mlapp) and exported as a MATLAB struct. The MATLAB application was developed by CFS for this purpose.

### 4.2.2 Load Spectrum

A MATLAB program (see Appendix H) was developed to analyse the data from the race and generate a load spectrum to be used in KISSsoft for the dimensioning of the gears.

The torque and speed for all wheels are imported, some sign errors are corrected and the vectors are cut to start at the same time stamp as well as to be the same length. Here the sample rate is also checked so that it is the same for all vectors as some sensors use a different sample rate and it all varies among different races. The data is also put through a low pass filter (using MATLAB's "lowpass" function) to weed out some noise.

To make sure to represent a worst case scenario for dimensioning, the torque and speed from the wheel that is experiencing the most extreme of either of those at any given point in time is sorted into a new vector representing a fictional "worst case" wheel. The most extreme here is defined as the largest, positive or negative. This fictional wheel is the basis for all later calculations in the program.

When the vehicle is stationary the gearbox is not experiencing any significant load, these data point are thus filtered out, with a small margin around zero to cut out any data points close to zero. If they were not filtered out, a majority of the load case exported to KISSsoft would consist of no load which would lower the resolution of the important data points as well as waste computing power.

From these vectors -torque and speed, a bi-variate histogram (see Figure 4.1) is created with a specified number of bins (load levels) in each of the axes. The number of different cases is therefore $N_{\text{torque bins}} \cdot N_{\text{speed bins}}$ ($N$ = number of bins). The number of negative values is very low but might be important for the analysis. If these values were to be removed a potentially critical part of the analysis might be missed but if they were to be left untouched they would just increase the frequency of the lowest bins and therefore artificially make the load spectrum less demanding. A separate bin is therefore created for all negative values and the remaining positive

values are sorted into $N - 1$ number of bins.

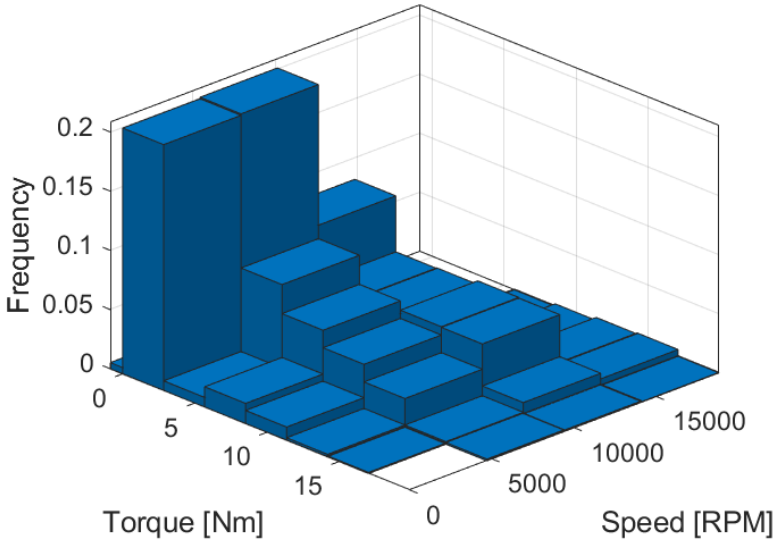


**Figure 4.1:** Bi-variate histogram of torque and speed

Now that the data is broken up into cases comprising the combination of a certain torque and speed, some of such cases never occur e.g. very high speed and no torque. These cases with a frequency equaling zero are removed to not waste computing power and time when the KISSsoft analysis is made.

The histogram data is then restructured such that the $N_{\text{torque bins}} \cdot N_{\text{speed bins}}$ cases are put as a row in a matrix with the columns: frequency, torque and speed. These columns are then normalized such that the highest value in torque equals 1, the highest value in speed equals 1 and the sum of the values in frequency equals 100 (representing 100%). The load case matrix is then written to an Excel spreadsheet (see Appendix I).

Since the data is from a car with another gear ratio some modifications are needed for the implementation in KISSsoft. Assuming the same weight of the new car as the CFS19 car as well as the same overall movement on the track, the speed and torque needs to be adjusted according to the new gear ratio. The load spectrum is normalized as described above, such that the maximum value of the torque and speed is 1, this enables KISSsoft easy control of the load values as the maximum value is simply entered and other values are scaled according to this. The *maximum value* used in KISSsoft is the maximum value of torque and speed bins respectively when scaled to the new gear ratio.
The speed is adjusted as:

$$\omega_{new} = \omega_{19} \frac{{}^{13}/_{1}}{{}^{14}/_{1}} \tag{4.1}$$

Where $\omega_{new}$ is the new speed and $\omega_{19}$ is the old speed (from CFS19). ${}^{13}/_{1}$ is the new "gear ratio" (note that this is not the actual gear ratio of the new gearbox but the gear ratio that would be used if the same tyre is kept, it represents a new value

chosen from Figure 1.3) and $^{14}/_{1}$ is the old gear ratio.

The torque is adjusted as:

$$T_{new} = T_{19}\frac{^{14}/_{1}}{^{13}/_{1}} \tag{4.2}$$

Where $T_{new}$ is the new torque and $T_{19}$ is the old torque (from CFS19). The fractions are the gear ratios as described for the speed above.

When the change in effective gear ratio is accounted for (note again that this is not the actual gear ratio of the transmission but rather only a movement in Figure 1.3) the new and adjusted speed and torque values can be entered in KISSsoft.

### 4.2.3 Expected Service Life

The gearbox must last 1500 km as specified in the requirements specification (see Table 3.1), this distance had to be translated into time for the KISSsoft analysis. Since the Autocross event from Achen was used for the load spectrum this data set was used to calculate the time as well as this ensures that the time is representative of the load case.

The calculation was made in the same MATLAB program (see Appendix H) used to generate the load spectrum as they must match at various attributes.

The GPS data is imported and cleaned since it contains a few errors. First the origin of the data is moved closer to the track as it was found to be placed about 12 km away, this is not strictly necessary but it helps when performing the subsequent processing of the data. A handful of data points were found to be a many hundreds of meters off the track, to the human eye these were an obvious error of the GPS. The faulty data points are removed entirely by the program as no obvious way was found to restore their position short of guessing. This was however not a great loss as the lost data points were few and a straight line drawn between the gaps roughly followed the track (as laid out by other laps where the section in question remained intact).

The distance is found by taking the euclidean norm of two subsequent data points and adding them all together. The time driving is found by taking the time between two subsequent data points, making sure to only add the pairs where the distance between them is non-zero as waiting time would otherwise be included. Thus the time and distance for the autocross event (consisting of five laps) is known. This time is computed with the equation 4.3

$$\text{Expected service life} = \text{time of 5 laps} \cdot \frac{\text{dimensioning distance}}{\text{distance of 5 laps}} = 193 \cdot \frac{1500}{1.76} \approx 164480\,\text{s} \approx 46\,\text{h} \tag{4.3}$$

Note again that “time of 5 laps” is time spent moving. The time it would take to drive 1500 km if the distance is covered in the autocross event was found to be 46 hours.

## 4.3 Discussion

It is far from guaranteed that the autocross event in Achen 2019 represents the toughest of load cases for the gears. The autocross event is generally considered to be the toughest event of the competition, which is why it was chosen for the load case. Yet *this* very race in Achen might not be that demanding compared to another race at a different time and place. If more races would be analysed the load cases could be set with more confidence.

The load level for each case in the load spectrum exported to KISSsoft is the middle value of the bin edges in the bi-variate histogram. This means that the load spectrum do not actually contain the maximum loads (nor the minimum), this might be a risk in the analysis. Experimentation in KISSsoft showed that the actual maximum load did not influence the expected service life significantly as the analysis concerned fatigue failure. It should be noted that by taking the middle value of a bin, not only is the values above the middle lowered to the middle but the values below the middle are raised to the middle, this somewhat cancels out in the fatigue calculation.

# 5
# Gear Design

## 5.1 Method

To be able to determine if the concept will be durable enough and not fail during the season, a model has been created in a commercial software called KISSsys, and then analyzed in KISSsoft. The analysis is done based on the load spectrum created earlier, that is uploaded to KISSsoft's database tool. The model comes included with the shafts, bearings, couplings and all other necessary components. The next step is to add the boundary conditions and define some key parameters. The maximum torque and speed of the motor is then defined and a gear ratio is chosen. When the model is updated, only the size of the gears is changed. Thus, a resizing of all the other elements needs to be done.

Moreover, to be able to effectively develop a gearbox that is dimensioned correctly, a load case report has to be generated. The report analyses the durability, fatigue of all the components in the transmission as well as giving safety factors for the root, flank, micropitting and scuffing. Micropitting is the phenomena where pits (holes) begin to form on the tooth of the gear as a result of excessive stress or the lubrication film not succeeding to protect it well enough [14]. Scuffing describes the phenomena when the lubrication film fails to separate two metal parts, increasing friction and causing material to transfer from one part to the other. This is revealed by scratches on the surface of the metal [19].

When the model is finished and the kinematics are checked to see if the gearbox works properly, the work with KISSsoft begins. The focus in this software is to obtain flank and root safety factors higher than 1 for all gears while not exceeding the maximum allowable outer diameter for the gearbox. The first step is to choose the appropriate materials for the sun gear, planet gears and the ring gear as well as a proper oil for the transmission. The next step is to set the maximum input torque, motor revolutions, service life and the application factor $K_a$ that indicates what type of the shock, the driven and driving machines will be subjected to. The calculation method comes to play afterwards as it needs to be chosen properly so that it suits the type of module designed.

After defining the previous parameters, fine sizing comes to play. Here a combination of teeth for the sun, planets and ring are chosen by defining a range for different parameters. The first one is defining a range for the module. The next parameter is the normal pressure angle as it affects the tooth strength and the contact ratio. A range for the center distance should be decided next while staying within the maximum allowable dimensions of the gearbox. The number of teeth on

the gears can be left for KISSsoft to decide by itself or can be partly decided by the user by having a fix number of teeth on only one gear and letting KISSsoft generate different combinations based on that. The last parameter to adjust is the face width of the gears which has a strong effect on the outcome of the safety factors and face load distribution.

The manufacturing process is determined in the next step to indicate how the gears are going to be machined. A range of different manufacturing and modification processes are available to choose from. The gear reference profile has to be defined as well to determine how the gears are going to be machined and which tool to select for that purpose.

The following step is to do a contact analysis to see the load distribution along the width of the gears and the stresses that the teeth are subjected to. To be able to do that correctly values for the planet carrier tilting relative to the gear axis and the tilting of the planet gears relative to the planet pin axis have to be defined. Furthermore, it is important to define again that the input torque drives the sun gear and the carrier provides the output torque, so that the calculations are done correctly. After the calculation is finished, graphs that show the normal load distribution along the width of the gears, tooth root stress and Hertzian stress should be checked to see how evenly the load is distributed. Hertzian stress denotes a type of stress that is formed when a load is applied between two surfaces with different radii that are in contact [6].

The final step in KISSsoft is to carry out an operating backlash calculation. What it does is that it calculates how much play there exists in between the teeth of the gears in contact as well as the angular play of the sun gear.

Last but not least, a choice for the bearings inside the planet gears and on the carrier shafts has to be done. Different types of bearings can be suitable for the same application so the choice can be made based on the previous years' decisions and on what seems to be reasonable.

## 5.2 Results

### 5.2.1 Configurating Fundamental Geometry

Starting with KISSsys, a template for a single-stage planetary gearbox was chosen (since this was the conclusion from Section 3.2.5).

The input shaft was chosen to drive the sun gear and the carrier was chosen as the output. A value of 19.89 Nm was set for the input torque and 15 282 RPM for the speed of the motor, these values are the highest values in Figure 4.1 scaled with equations 4.1 and 4.2. They are intended to represent scale factors for the load spectrum that is uploaded into the software.

Section 1.1.4 states that the gear ratio should be in the range $[11.5:1-12.5:1]$. Since a single-stage planetary gearbox has a recommended gear ratio between $[1:3-1:10]$ [10] it was therefore chosen to design for a $11.5:1$ gear ratio. It is acceptable to work outside the recommended range as the software will calculate and controls that it lasts. The chosen gear ratio was then used as an input parameter(see Table 5.1).

The output torque and speed obtained were 255.73 Nm and 1328.9 rpm respectively. The shafts, bearings, carrier and planet pins were then resized accordingly. The resulting model is shown in Figure 5.1.

**Table 5.1:** Input parameters in KISSsoft

| | |
|---|---|
| Ratio | 11.5:1 |
| Input torque (Nm) | 19.89 |
| Input motor speed (RPM) | 15282 |
| Output torque (Nm) | 255.73 |
| Output speed (RPM) | 1328.9 |

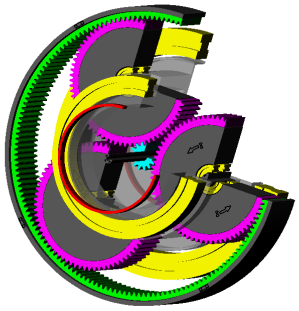

**Figure 5.1:** Gearbox model in KISSsys

### 5.2.2 Defining parameters

Regarding the material choice, by relying partially on the choice of the material done by the CFS team of the previous year and partially on the recommendations from Per Forsberg, an R&D engineer who works at Atlas Copco Industrial Technique, the following choices shown in Table 5.2 were made. A hardened steel means that carbon has been incorporated into the steel to make it harder. Case hardened steel is a steel where just the surface has been hardened to make it more resistant to fractures while retaining a softer core, whereas through hardened steel is a steel where both the surface and the core are hardened, making it very hard but more brittle [24]. Thus, Case hardened steel was chosen for the sun and planet gears as it is commonly used in the automotive industry for powertrain components and offers high tensile strength, impact resistance, fatigue strength and hardenability. For the ring gear nitrided through hardened steel was chosen as this gear has a thin wall section, thus it should be stiff as it can be subjected to distortion [24]. The oil was also chosen to a consistency of 75W-90 since this is a common oil used in transmissions according to Forsberg. Important to note that since the transmission has a very short service life the choice of oil will not strongly affect how the gearbox performs and how long it lasts.

**Table 5.2:** Materials and oil choice for gears

| | Materials choice | Oil choice |
|---|---|---|
| Sun gear | Case hardening steel-18CrNiMo7-6 | Klubersynth GE 4 75 W 90 |
| Planet gears | Case hardening steel-18CrNiMo7-6 | Klubersynth GE 4 75 W 90 |
| Internal gear | Through hardening steel-34CrNiMo 6 | Klubersynth GE 4 75 W 90 |

The lifetime of the transmission was set to 46 hours which corresponds to the amount of time that the vehicle is competing and subjected to the load cases defined. Important to point out that when using a load case spectrum in KISSsoft the application factor should be set to 1, otherwise the software will send a warning. However a factor of 1.25 was chosen to ensure a higher safety margin. This specific number means that the car will be subjected to light shocks which should be more than enough since it will be driven on a slick track. The calculation method was chosen as DIN 3990:1987 Method B, which according to KISSsoft is recommended for planetary stage gearboxes. All of those parameters are shown in Table 5.3.

**Table 5.3:** Input parameters in KISSsoft step 2

| | |
|---|---|
| Service life (h) | 46 |
| Application factor ($K_A$) | 1.25 |
| Calculation method | DIN 3990:1987 Method B |

The choices made in the manufacturing process here did not affect the durability of the gearbox, however they were still important as it had to be checked if the steel maker had the possibility to manufacture the gears as described in KISSsoft. Consequently, hobbing was chosen for the sun and planet gears since it is a relatively fast process as well as being precise. For the ring gear hobbing was not possible because of the shape of the hobbing machine, shaping was thus chosen [8]. For the modifications process the option "not defined" was chosen as the other options only included grinding. According to Forsberg it was not advised to grind the gears considering that the module is so small as the process could eat away from the hardened surface of the teeth, thus making the surface less wear resistant. The optimal solution was consequently to tumble the gears. For that same reason, the tooth thickness tolerances were set to DIN 58405 8e standard for the sun and planet gears and DIN58405 9e for the ring gear as shown in Table 5.4. This meant that the gears did not need to be ground [7].

**Table 5.4:** Manufacturing process and tooth thickness tolerances for gear

| | Sun gear | Planet gears | Ring gear |
|---|---|---|---|
| Manufacturing process | Hobbing | Hobbing | Shaping |
| Tooth thickness tolerance | DIN 58405 8e | DIN 58405 8e | DIN 58405 9e |

For fine sizing a module of 0.6 mm was first chosen however the safety factors were not met as the flank safety for the sun for example was lower than one. By setting a range from 0.4 and to 1, it was found that a module of 0.8 mm met

the requirements for the safety factors. A module of 1 mm rendered the gearbox dimensions too big to fit inside the rim. Normal pressure angle was set to 20°since this is the standard [17].

A range of 20 to 40 mm was chosen for the center distance and the goal here was to remain in the allowable dimensions at the same time as creating a large range for KISSsoft to generate many results and see which ones that fulfill the requirements better. The number of teeth was also noticed to play a big role when it comes to safety factors. The higher the amount on the gears the worse the safety factors as the teeth get smaller. Thus, the number was reduced to obtain the best achievable durability and was the following: 14 teeth for the sun, 74 for each planet gear and 166 for the ring gear. The last parameter to adjust was the facewidth of the gears. It affected the safety factors the most and after starting with small width of 13 mm, it was noticed that the safety factors were not met. Thus, the value was quickly risen to 22 mm for the planet gears and 23 mm for the sun and ring gear. Values bigger than that did not bring a significant improvement and rendered the gearbox rather wide, which also had a negative effect on the load distribution on the teeth as it became uneven. The sun and ring gear were chosen to be 1 mm wider than the planet gears after consulting Per Forsberg in order to reduce the bending stress in the sun gear. Table 5.5 illustrates all of the chosen parameters.

**Table 5.5:** Fine sizing in KISSsoft

| | |
|---|---|
| Module (mm) | 0.8 |
| Normal pressure angle (deg) | 20 |
| Center distance (mm) | 36 |
| Number of teeth for the sun | 14 |
| Number of teeth for the planets | 74 |
| Number of teeth for the ring gear | 166 |
| Face width of the sun (mm) | 23 |
| Face width of the planets (mm) | 22 |
| Face width of the ring gear (mm) | 23 |

### 5.2.3 Contact, Stress and Load Analysis

The tilting values in the axis alignment window were set to 10 and 20 µm consecutively and are shown in Table 5.6. Moreover, these values were obtained by creating a model of the planet carrier in ANSYS and doing a FEM analysis. Additionally, the sun gear had to be chosen to come from I, as shown in Figure 5.2, in other words from the input side. That means that KISSsoft will take into consideration that the sun gear is driven by the motor axis, thus taking into account the torsion of this gear caused by the torque of the motor. That step was done based on the recommendation of Forsberg. Per Forsberg also gave the recommendation to have a floating sun gear, which means that the sun is allowed some radial movement, since this allows more skewing and which greatly improves the safety factors.

**Table 5.6:** Axis alignment

| | |
|---|---|
| Tilting of the planet carrier relative to the gear axis (µm) | 10 |
| Tilting of the planet pin relative to the planet carrier axis (µm) | 20 |

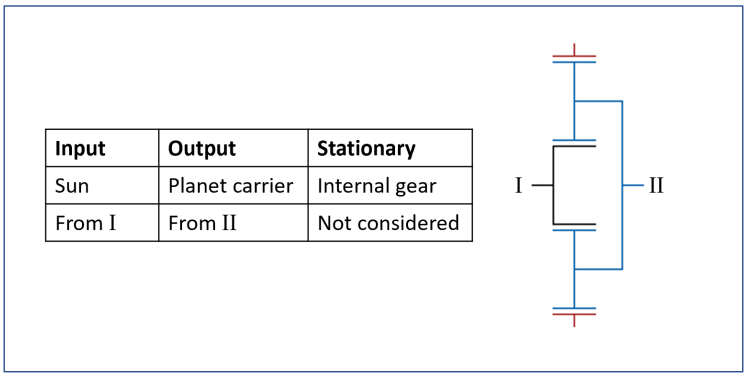


**Figure 5.2:** Definition of stationary components as well as input and output in KISSsoft

After doing the contact analysis, the next step was to analyse the load distribution along the width of the gears. Ideally one would want the distribution to be even, in this case though, the load seem to peak at the edge of the face width of the sun as shown in Figure 5.3. It begins to subside moving along the width with a minimal load in the middle. That has a negative effect on the gear performance as there will be variations, it also increases the bending stresses in the gear and causes micropitting and increased vibrations.

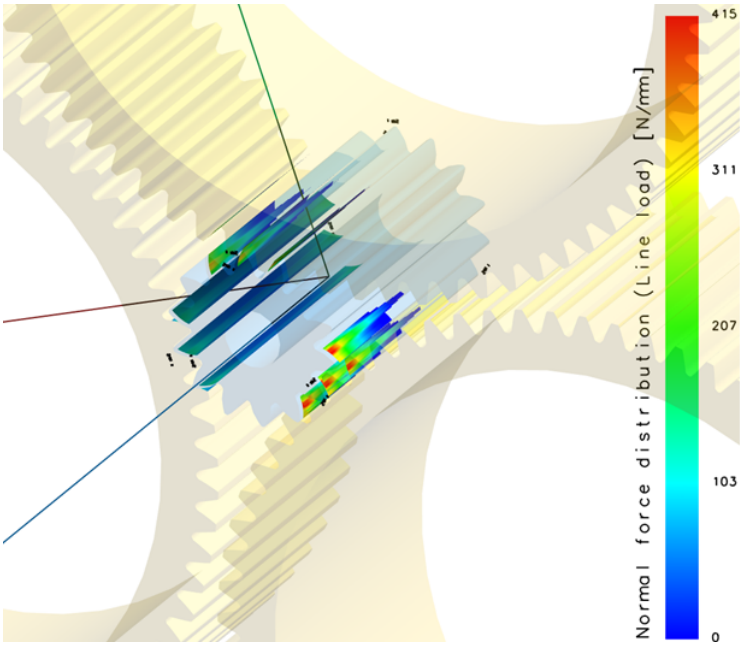


**Figure 5.3:** Normal load distribution on the sun gear in KISSsoft

Taking a look at Appendix J showing the tooth root stress of the sun gear, it can be seen that the stresses are more or less evenly distributed. The hertzian stress between the sun and planets however, is higher at the edges of the tooth as shown in Appendix K.

Moreover, when running the analysis on the gears, a message from KISSsoft kept appearing saying the following: "Mesh gear 2-3: Pitch point C is outside the path of contact. The calculation of scuffing or micropitting can be inaccurate!". With gear 2 representing the planet gear and gear 3 representing the ring gear. After contacting KISSsoft support, it was found that it was a special case and gears having the pitch point outside the path of contact could even have a better performance in scuffing or micropitting and that it was not a cause for concern. This was also confirmed by Forsberg.

For the operating backlash, the material for the planet carrier was chosen to be billet aluminium considering it is lighter than steel and following last year's team's choice. After running the calculation, the results in Table 5.7 showed reasonable values for the play with none of the values being negative meaning that there was no clash occurring in the teeth.

**Table 5.7:** Operating backlash in KISSsoft

Planet Carrier's angel of rotation for a fixed sun/fixed gear rim

| | | |
|---|---|---|
| Without planet carrier pitch deviation(degrees) | 0.092 / 0.340 | |
| With planet carrier pitch deviation(degrees) | 0.030 / 0.277 | |
| | Pair 1 | Pair 2 |
| Min. circumferential backlash (mm) | 0.031 | 0.044 |
| Max. circumferential backlash (mm) | 0.181 | 0.211 |
| Pitch error due to dilatation (µm) | 0.000 | 0.000 |
| Minimum tip clearance (mm) | 0.170 | 0.268 |
| Maximum tip clearance (mm) | 0.393 | 0.617 |
| Min. transverse contact ratio | 1.246 | 1.337 |
| Max. transverse contact ratio | 1.371 | 1.609 |

Comment: The calculation is performed with the working pressure angle

### 5.2.4 Planetary Bearings

Going back to KISSsys, Figure 5.8 a) shows that two bearings were inserted into each planet gear. These were chosen to be needle roller bearings. The bearings for the carrier shaft on the input side was chosen to be a deep groove ball bearing as shown in the cross-sectional view in Figure 5.8 b). For the bearing on the output side the same type of bearing was chosen as the one on the input side, these are shown in Figure 5.8 b). Important to note, however, that the choice for the carrier bearings was done only to have a complete model in KISSsys to be able to generate a load case report later on. The carrier bearings that were actually chosen are shown in Chapter 7.

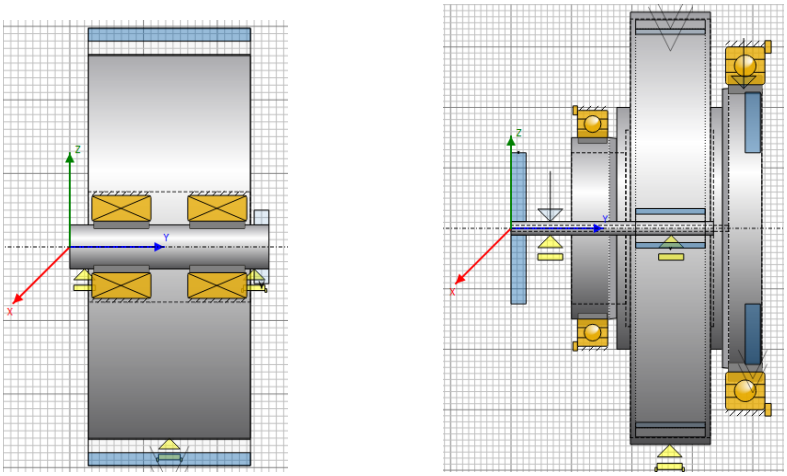

a) Planetary bearings in KISSsys b) Carrier bearings in KISSsys

**Table 5.8:** Planetary and carrier bearings in KISSsys

The final results displayed in Tables 5.9 and 5.10 show all the safety factors for the gears. It is obvious that the ring gear has more than acceptable flank and root safety factors of 1.971 and 1.730, which means that the possibility of a failure occurring is little. For the sun gear the safety factors are 1.261 and 2.119 for the flank and root respectively. Being over 1, the flank should be fine for the loads that they are dimensioned against during the course of the competition. Concerning the planet gears, the obtained flank and root safety factors were 1.374 and 1.891 respectively. In other words, while having an application factor of 1.25 over the load case, all gears still got a minimum flank and root safety factors of over 1. Regarding the safety against micropitting and scuffing, it was noticed that all factors were above 1 except for the micropitting factor between the sun and the planets, which was at 0.539.

**Table 5.9:** Final safety factors for gears

| | Flank safety | Root safety |
|---|---|---|
| Sun | 1.261 | 2.119 |
| Planets | 1.374 | 1.891 |
| Ring gear | 1.971 | 1.730 |

**Table 5.10:** Micropitting and scuffing for gears

| | Safety factors |
|---|---|
| Micropitting between sun and planets | 0.539 |
| Micropitting between planets and ring gear | 1.042 |
| Scuffing between sun and planets | 4.972 |
| Scuffing between planets and ring gear | 7.725 |

### 5.2.5 Gear Modelling

With all parameters defined resulting in a gear geometry with acceptable safety factors, the model generated with KISSsys is exported for the final modelling. The KISSsys model is represented in Figure 5.4 a).

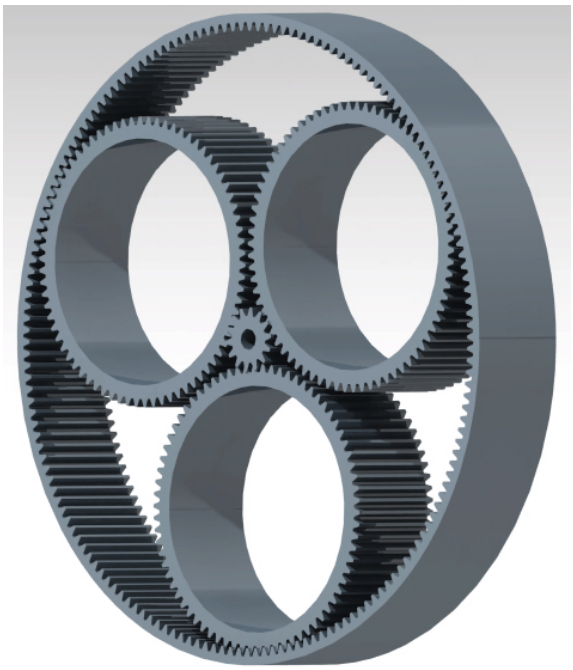

a) The sun, ring and planet gears generated by KISSsys, rendered in CATIA V5

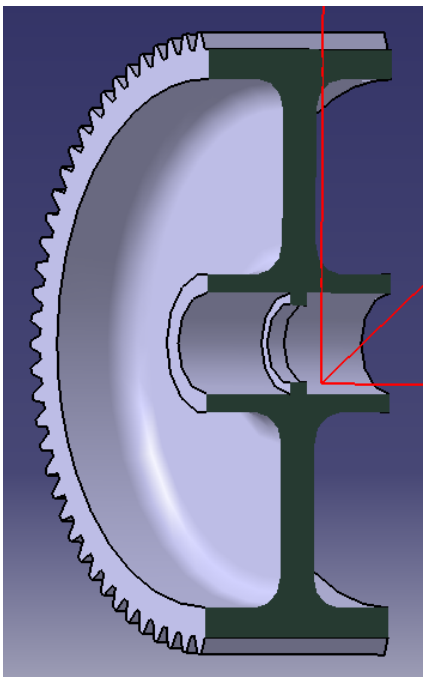

b) Section view of one planet gear in CATIA V5

**Figure 5.4:** 3D-models of the gear designs

As seen in the figure, KISSsys exports a model with the gear geometries as shells. Therefore, the gear walls must be further 3D-modelled in CATIA V5. In order to decide a appropirate wall thickness for the planet gears, CFS19 planet gears are studied. These gears have a wall thickness of 5 mm and since CFS19 used a 1.5 step compound planetary gearbox, the planet wall is subjected to twisting forces from the secondary planet gear which is not present in a 1 stage planetary gearbox. Therefore, a wall thickness of 4 mm is assumed to be adequate for this application. Two bearing seats divided by a lip for the planetary bearings are also designed. See figure 5.4 b).

As described in Section 5.2.2, Per Forsberg recommended a floating sun gear. Therefore, a splined input shaft is added to the sun gear geometry as well as a hole for a M4 bolt for locking sun gears axial movement, see Figure 5.5 a). The ring gear remains the same as the KISSsys model except for the addition of flanges for mounting. See figure 5.5 b) for the gear design including planetary bearings. All wall thicknesses generated from KISSsys have remained unchanged since this have great effect on the gear strength.

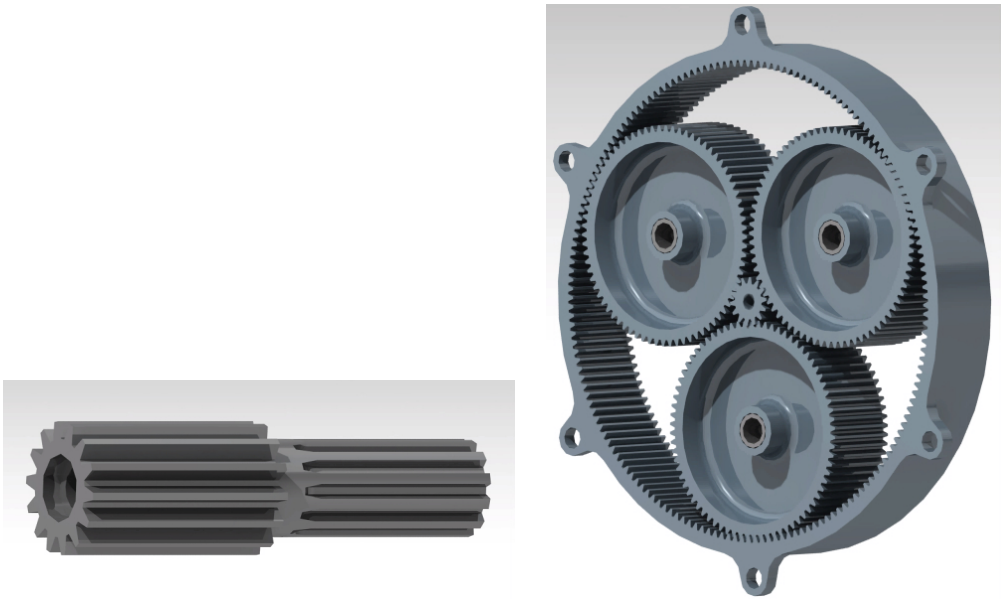

a) Sun gear with splined shaft

b) Final design of the gears including the planetary bearings

**Figure 5.5:** 3D-models of final gears, rendered in CATIA V5

## 5.3 Discussion

As mentioned before, the main goal of the work in KISSsoft was to ensure that the gearbox would last through the whole season by making sure the safety factors were over 1. The question after that would become how much over 1 the factors needed to be; here a delimitation had to be made as the primary goal of the project was to make the gearbox lighter than the years before. With that being said, and taking into consideration that it is a new concept that has not been implemented before, it was deemed to be reasonable to have a bit of a safety margin. That, to ensure that the gears would be more than capable to take the loads, thus reducing the chance of a failure in the middle of the competition as much as possible. Furthermore, it would have been possible to increase the width of the gears in order to obtain a minimum factor of 1.5 for all gears, following Peter Wittke and Tommie Hall's recommendation, two engineers that work with developing transmissions at Volvo Cars. Their point was that this factor would then consider the dynamic loads that can arise if there is not enough traction and the wheels slip for example. However, this would have made it harder to reach the goal of obtaining a lighter gearbox.

Concerning the uneven load distribution that was obtained, it was deemed to not affect the service life of the gearbox, as the flank and root safety factors achieved were obtained taking it into account. In other words if the load distribution was even the safety factors would have been even higher.

As seen in the results, there were no risk of the gears scuffing. Nevertheless, when it came to micropitting between the sun and planet gears the low safety factor obtained meant that pits would probably form on the surface of the teeth during the lifetime of the gearbox. Be that as it may, this did not play as much role in

predicting failure as the flank and root safety factors did. The micropitting safety factor would not bring much concern in terms of a catastrophic failure happening on the short term but would cause a problem on the long term [13]. In other words, the gearbox would still be functional even with micropitting symptoms on the gears. An investigation to see if the gear has been subjected to micropitting would however be interesting to do after the runtime to understand how it has affected the teeth.

The reason to why a double bearing setup was used was that using only one bearing resulted in having to choose a large one. This in its turn meant that the minimal bearing load was not achieved. Using two small bearings meant that the load was equally distributed between these and that they were appropriately loaded. When generating the load case report, it was noticed that the bearings sitting on the carrier shaft were not exposed to the minimal load required. After being in contact with KISSsoft support and Forsberg, it was assured that for the bearings on the carrier it was normal for the minimal load not to be reached when the gravity force is deactivated and with no extra radial forces or moments. There would be no resulting extra force as a result.

When setting the service life to 10000 hours, it was noticed that the safety factors obtained were not much lower than before. The flank safety for the sun went down from 1.261 to 0.880 which came as a surprise. It was expected that the factors would be considerably lower, as they would be subjected to fatigue stress.

# 6

# Bearings & Housing Load Cases

## 6.1 Theory

The gearbox housing and its bearings are components that experience great forces during acceleration, retardation and cornering. To design a light gearbox housing while being able to handle the stresses it is important to properly define the forces that cause the stresses.

At standstill, a static *normal force* is acting on the wheels from the ground as a result of the vehicle's mass. The force is acting radially on the tyre perpendicular to the ground, see Figure 6.1. During acceleration, retardation and cornering the normal forces acting on each wheel vary depending on the acceleration of the mass centre of the vehicle. This is one of two radial forces acting on the centre of the wheel.

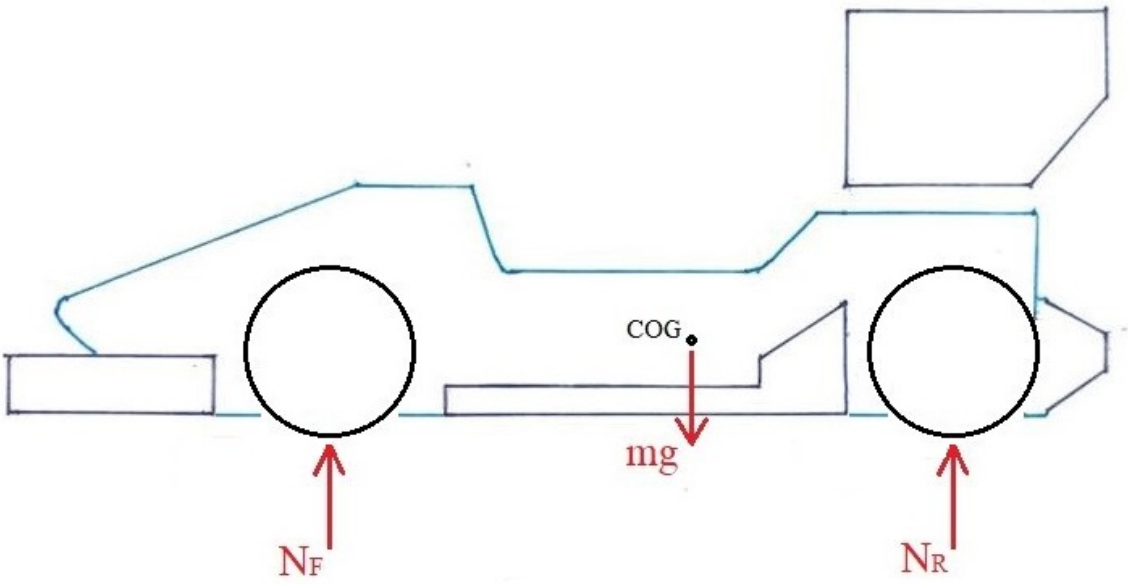


**Figure 6.1:** Illustration of normal forces at standstill for the CFS19 Car

The second radial force is the *tangential force* acting on the gearbox transmission shaft during acceleration and retardation as a result of the torque transmitted from the electric machine and the brakes at each wheel, see Figure 6.2.

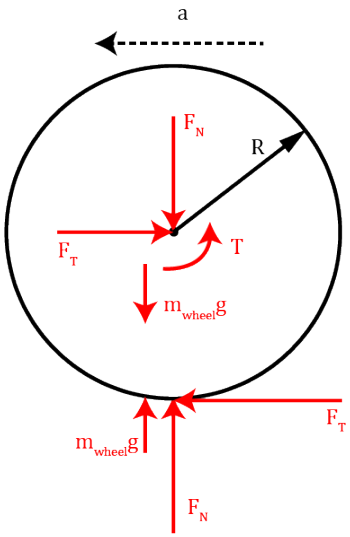


**Figure 6.2:** Illustration of tangential forces on one wheel at the moment of acceleration from standstill, denoted as $F_T$. $F_N$ denotes normal force and T the applied torque.

The third and last force is the *lateral force* acting axially on the wheel centre during cornering. This axial force is pushing the centre of the wheel inwards the vehicle on one side and pulling the centre of the wheel outwards the vehicle one the other side during cornering. This force is the reason the gearbox needs to house a guiding bearing in order to prevent the inner wheel to tear the gearbox apart in a corner, see Figure 6.3.

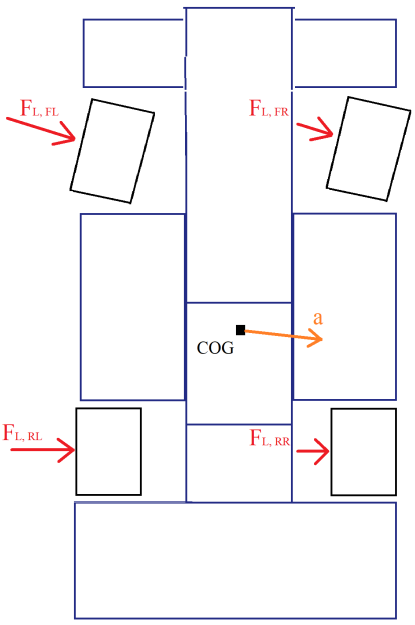


**Figure 6.3:** Illustration of lateral forces during cornering and deceleration from top view

## 6.2 Method

The gearbox housing and its bearings are subjected to the forces defined in Section 6.1 via the wheels. These forces are therefore used for dimensioning of the gearbox housing. The more trustworthy approximation of the forces, the less safety margin is needed during dimensioning, resulting in a lighter design with sufficient strength to handle the stresses.

Therefore, much effort is put into finding reliable data defining the forces corresponding to the maximum loads during competition which can be used to analyse strength and deformation as well as average repetitive forces for fatigue analysis on the carrier and the housing. From the maximum loads, equivalent forces can be computed which is used to dimension the bearings.

### 6.2.1 Data Sourcing

The data needs to contain information that can be translated to how much force the wheels or suspension endures during its most critical use, which in the case of this project is during the competition.

This type of information can be found from multiple types of sources. In order to find the most suitable source for this project, the available information was found by consulting CFS-members and the project supervisor Björn Pålsson.

Historically, the load cases for the gearboxes have been derived from software computations in MATLAB, simulation models in ADAMS and OptimumLap. It is also concluded that the cars have a set of sensors logging various information from the car each time it is tested or competed with. After inspecting the logged sensor data from the competitions it seemed like a promising data source. Acceleration in three dimensions, angles of the pushrod pivot shaft and the torque output from each motor, see Figure 6.4, are logged. This information is considered enough to construct a good estimation of all loads on each wheel during competition which can be translated into forces on the housing and its bearings.

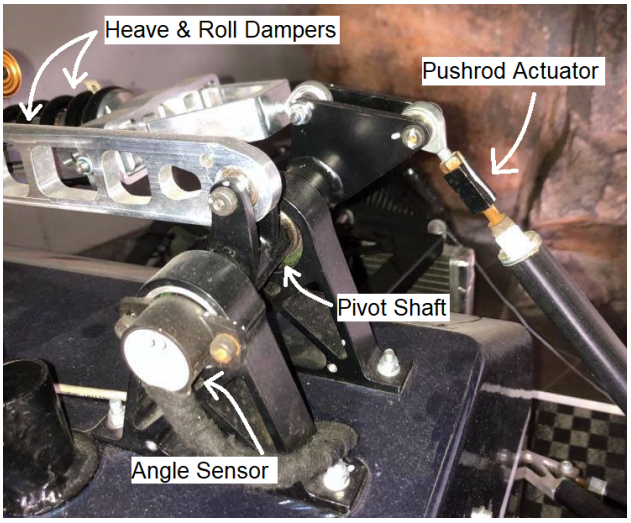


**Figure 6.4:** Angle sensor logging the angle of the rear pushrod pivot shaft

Since the alternative sources are based on software simulations including assumptions and simplifications, the data from physical testing is considered more accurate.

Furthermore, the use of physical sensor data is considered more interesting from a CFS methodology perspective. If this project results in a method for defining accurate load cases for the gearboxes, the logged data can be updated with the data from the most recent competition each year. Because of these reasons, the logged data from the accelerometer and the angle sensor on the pushrod pivot shaft are chosen as the data source of the gearbox housing and bearing load cases. This choice is further motivated by the fact that the hypothesis of the project is that earlier CFS gearboxes have been over dimensioned when designed utilizing these simulations.

CFS19 was the most recent team to compete with their car named *Victoria*, see Figure 6.5. Therefore, the logged data from Victoria is chosen as the data source for developing load cases for the gearbox housing and bearings. More specifically, the data from autocross competition in Achen 2019.


**Figure 6.5:** Victoria, developed by CFS19

### 6.2.2 Deriving Load Cases from Data

All sensor data is loaded into MATLAB with tools from CFS into a new script. Then, the plots of the data are studied and interpreted with the help of former CFS member Erik Lund. Lund was a member of the group responsible for the low voltage-system in CFS19 which installed the sensors on Victoria. Erik Lund provided information about the specifications of the angle sensor and assisted during measurement of the output of the angle sensor in relation to the wheel motion. This data is then loaded into a SIMULINK model that defines the transfer function between the logged data and the angle of the pushrod pivot shaft angle. Because of problematic data logs, this methodology deviated from the project purpose. It was also concluded that only the pushrod pivot shaft angle sensors on the front wheels gave a reliable output. For further reading, see Appendix L.

The logged data is converted to represent the angles of the pushrod pivot shaft with the SIMULINK transfer function. Because of above mentioned uncertainties, the data needs to be calibrated in order to ensure reliable results. The angle data is normalized and scaled with approximated normal forces. These approximations are done with hand calculations supported by the logged accelerations and vehicle

specifications from CFS reports. See Figure 6.6 followed by the equations 6.1 and 6.2.

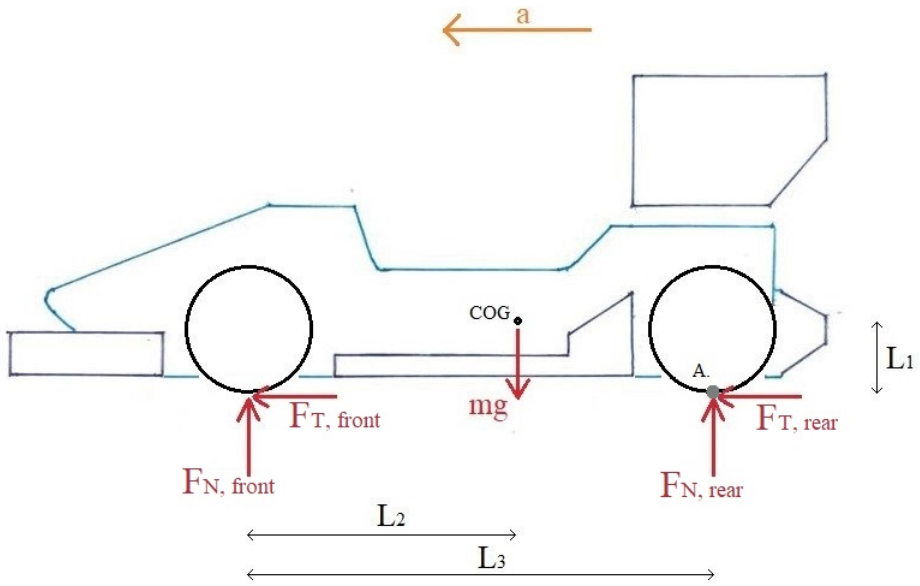


**Figure 6.6:** Free body diagram from side view for hand calculations of normal forces on the front axle

$$\curvearrowright A : F_N \cdot L_3 - m \cdot g \cdot (L_3 - L_2) - m \cdot a \cdot L_1 = 0 \tag{6.1}$$

$$\implies F_N = \frac{m(a \cdot L_1 + g \cdot (L_3 - L_2))}{L_3} \tag{6.2}$$

The accelerometer data log is supplemented by a video recording from the competition and an arbitrary time stamp in the data log is used as a reference. The chosen timestamp is at acceleration from standstill. At standstill, the downforce generated from the aerodynamic features of the vehicle can be neglected which provides a more accurate reading. The longitudinal acceleration at this timestamp is inserted into equation 6.2 which computes the normal force on the front axle. This normal force is evenly distributed between the two front wheels and compared to the angle reading at the same timestamp. All other data points are then calibrated by comparing their angle to the angle of this timestamp. This results in a data log of normal forces suitable to use for dimensioning.

The tangential force, is computed with the logged torque output-data and the radius of the wheel when acceleration see Figure 6.7 followed by the equation 6.3 for computation of tangential forces for one wheel.

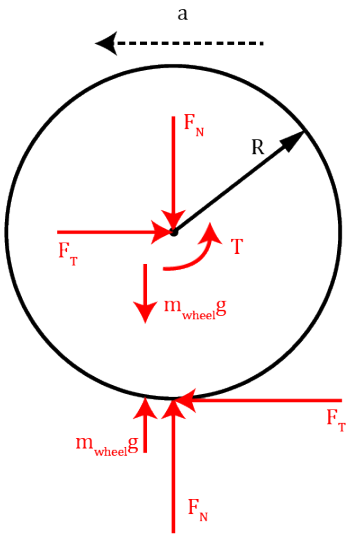


**Figure 6.7:** Free body diagram for hand calculations of the tangential force, denoted $F_T$, on one wheel

$$F_T = \frac{T}{R} \tag{6.3}$$

When the car decelerates the tangential force is derived from Newton's second law using the car's accelerometer data and mass:

$$F_T = m \cdot a \tag{6.4}$$

The reason for using both equation 6.3 and equation 6.4 is that when the car accelerates the motors draws current which is then logged. But when the car decelerates this type of data becomes unreliable since the car uses both generative breaking and traditional disc brakes. Therefore, during deceleration, the car's accelerometer is used instead. The accelerometer could be used for both acceleration and deceleration, however, this is not done because the current data is a more direct source.

With the tangential and normal force defined, the lateral forces are next. These are computed with the lateral acceleration data from the accelerometer and the normal forces. According to CFS report [16], the weight distribution between the front and rear axle is even during cornering. In order to define the weight distribution between the left and right wheels, an assumption that the distribution is directly proportional to the distribution between left and right normal forces is done. See equations 6.5 to 6.7 below for the calculation of the FR wheels lateral forces.

$$F_{L,tot} = m \cdot a \tag{6.5}$$

$$F_{L,front} = \frac{F_{L,tot}}{2} \tag{6.6}$$

$$F_{L,FR} = F_{L,front} \cdot \frac{F_{N,FR}}{F_{N,tot}} = \frac{m \cdot a}{2} \cdot \frac{F_{N,FR}}{F_{N,tot}} \tag{6.7}$$

Now all forces affecting the wheel are defined from which the load cases can be constructed, see Figure 6.8. The maximum values of the forces can be used as a reference for finite analysis and when calculating the service life of the bearings the whole driving cycle can be used.

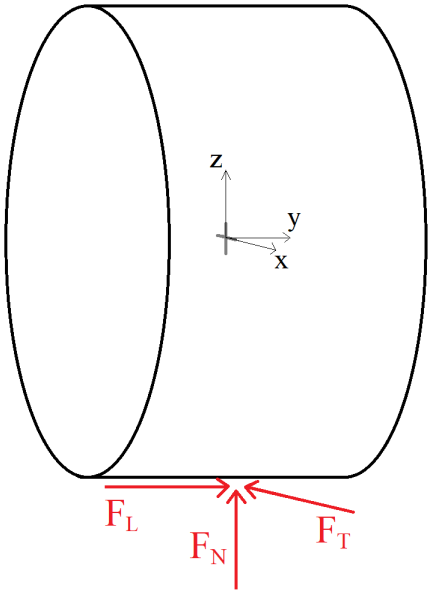


**Figure 6.8:** Illustration of the position of the three forces $F_N$, $F_T$ and $F_L$ on the wheel used for dimensioning the gearbox housing and bearings

## 6.3 Results

### 6.3.1 Data Interpretation

The complete data log from the final autocross lap in Achen 2019 is loaded into MATLAB and plotted. The data log includes five laps with pauses in between. To concentrate the data to relevant data points, only the data from the final lap is chosen. The raw Analog to Digital Converter-values (ADC) from the pushrod pivot shaft angle sensor are presented in Figure 6.9

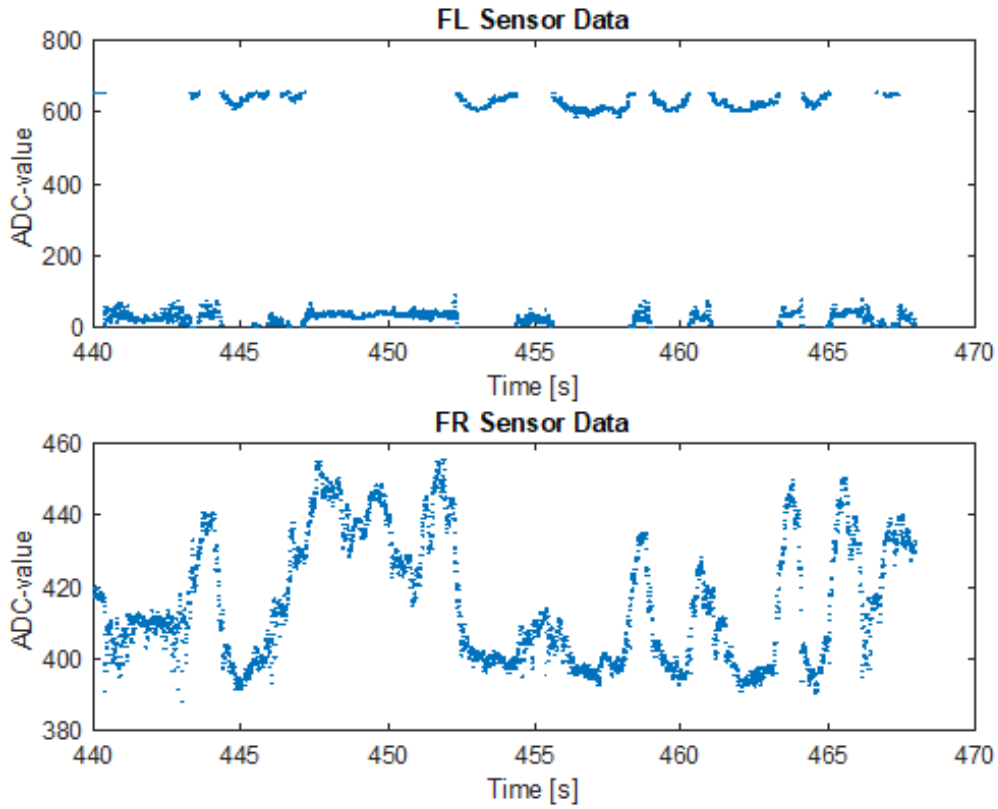


**Figure 6.9:** Imported ADC-values from the front pushrod pivot shaft angle sensors

The SIMULINK-model described in Appendix L generates a transfer function that is used to convert the ADC-values into angles on the pushrod pivot shafts. Figure 6.10 illustrates the transfer function with ADC-values on the y-axis and corresponding angles on the x-axis.

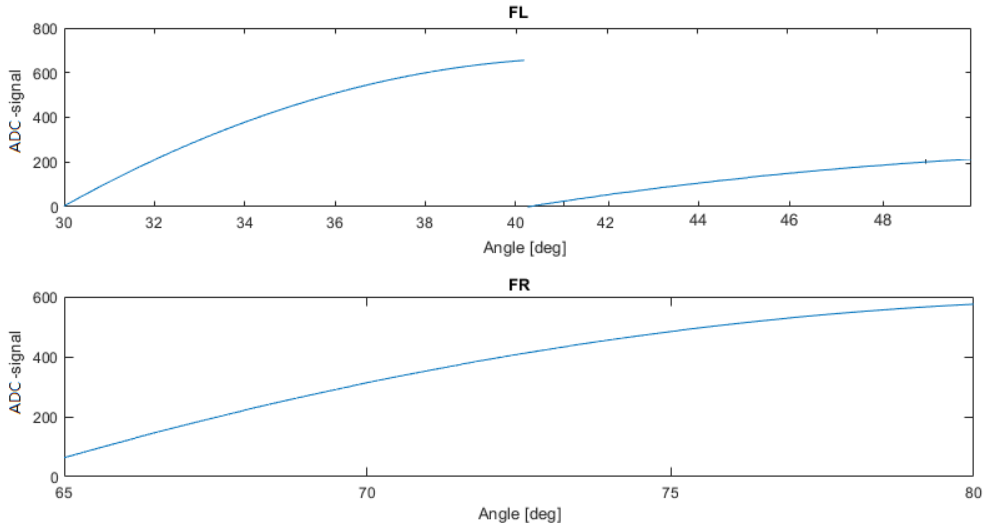


**Figure 6.10:** Transfer function between ADC-signal and angle for both front wheels

As seen in the figure above there are intervals where the transfer function for the front left wheel can output two different angles for one ADC-signal. For example, if the ADC-value is 200 the angle could either be circa 32°or 48°. Since there are non-continuous values in the data log for the front left wheel, the angle sensor must cross the threshold at circa 40.5°. Furthermore, the wheel motion must be continuous. This knowledge enables a limited interval of $[33°, 48°]$ to be assumed. All data points from the Achen 2019 data log are converted into angles with the transfer function. This results in a new data set plotted in Figure 6.11.

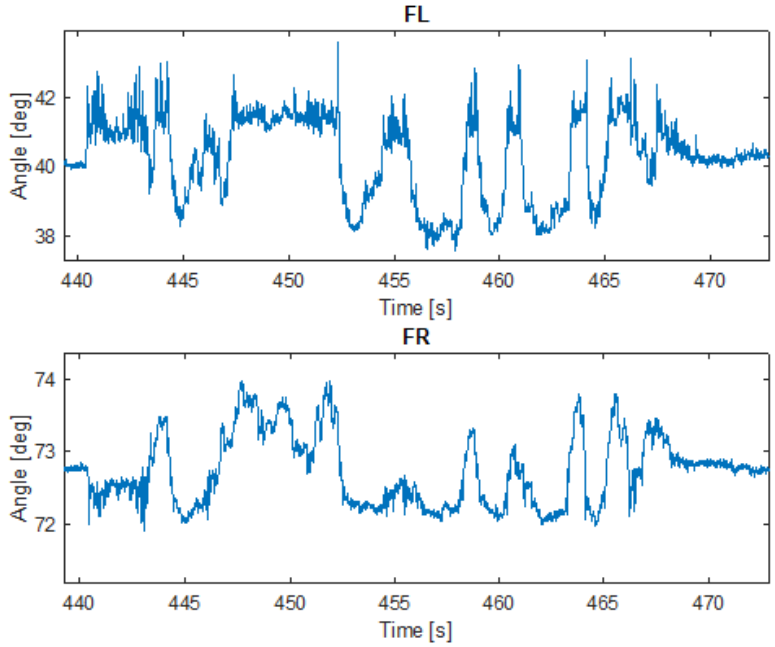


**Figure 6.11:** All ADC-data points converted into angles on the pushrod pivot shaft

### 6.3.2 Deriving Loads From Data

To calibrate the angles to their corresponding normal force, the theoretical stationary normal force is used as a reference. The normal force is calculated with equations 6.8, 6.9 and 6.10 and data from Carl Larsson's CFS-report [16].

$$F_{N,tot} = \frac{m(a \cdot L_1 + g \cdot (L_3 - L_2))}{L_3} = 990.6 \text{ N} \tag{6.8}$$

$$F_{N,FL} = \frac{F_{N,tot}}{2} = 495.3 \text{ N} \tag{6.9}$$

$$F_{N,FR} = \frac{F_{N,tot}}{2} = 495.3 \text{ N} \tag{6.10}$$

The pushrod pivot shaft angle data points are normalized and scaled in such way that the angles at standstill corresponds to above calculated stationary normal forces. In order to scale the amplitude of the angles to corresponding loads, the angles during a specific time stamp in the data log is used as a reference against the theoretical normal force amplitude. The moment when the car accelerates from standstill is used as the reference time stamp since the aerodynamic impact of the angles are considered low during this moment. During the chosen time stamp the longitudinal acceleration is 9.42 $m/s^2$ according to the acceleration data log. The normal force amplitude is calculated according to equations 6.11, 6.12 and 6.13 with the data from Carl Larsson's CFS-report [16]. Acceleration is noted with negative values and retardation is noted with positive values since the front axle is evaluated. This notation simplifies calculation of normal forces since the front axle lifts during acceleration which results in less normal forces.

$$F_{N,tot,amp} = \frac{m(a \cdot L_1)}{L_3} = -169.0 \text{ N} \tag{6.11}$$

$$F_{N,FL,amp} = \frac{F_{N,tot,amp}}{2} = -84.5 \text{ N} \tag{6.12}$$

$$F_{N,FR,amp} = \frac{F_{N,tot,amp}}{2} = -84.5 \text{ N} \tag{6.13}$$

Similarly to the calibration of the stationary normal forces, the normal force amplitudes are computed by scaling the angle amplitude to the corresponding normal force amplitude. All other angle data points are then scaled with the same factor which results in the data set of normal forces in Figure 6.12.

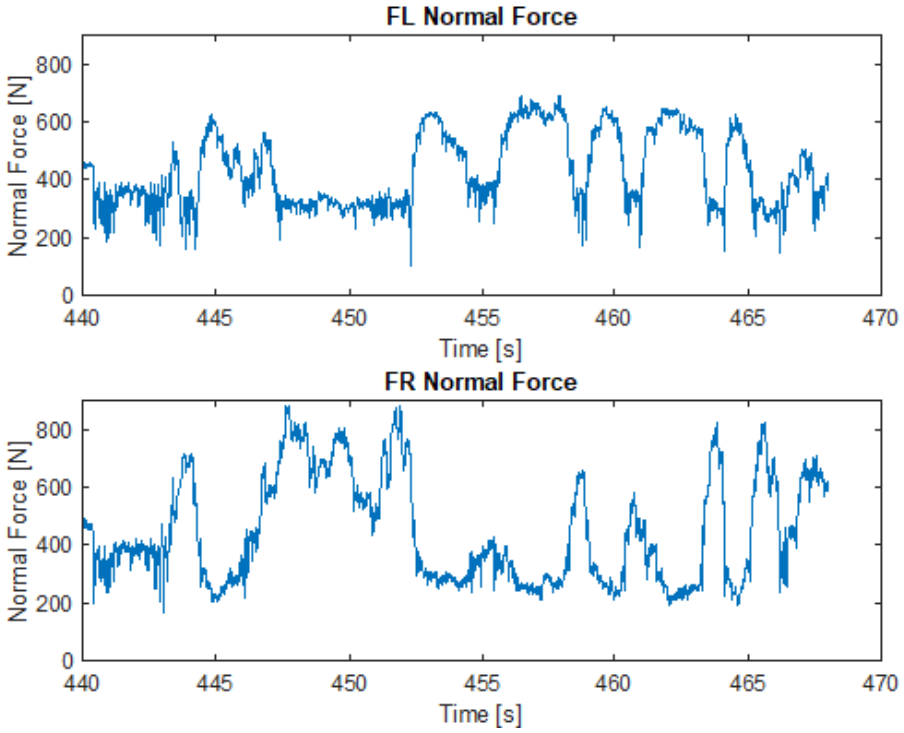


**Figure 6.12:** Graph showing the approximated normal forces for FL and FR wheel

The tangential forces are computed with the resulting forces from the torque output of the electric machines when the car accelerates. When the car decelerates, the accelerometer is used in combination with Newton's second law.

If the car accelerates:

$$F_T = \frac{T_{tot} \cdot i_{gearbox}}{R} \cdot \frac{1}{4} \tag{6.14}$$

In equation 6.14 a factor of $\frac{1}{4}$ is used, this is to divide the forces evenly between all four wheels. $T_{tot}$ is the total torque from all four motors combined. When the car decelerates Newtons second law is used to calculate the tangential forces.

$$F_T = m \cdot a \cdot \frac{1}{4} \tag{6.15}$$

The resulting tangential forces for each data point from all wheels are calculated in MATLAB. To simplify the calculation, all wheels are assumed to have equal tangential forces, see Figure 6.13 for one wheel's tangential force. Negative values means that the car is retarding which gives the forces the opposite direction to the forces during acceleration.

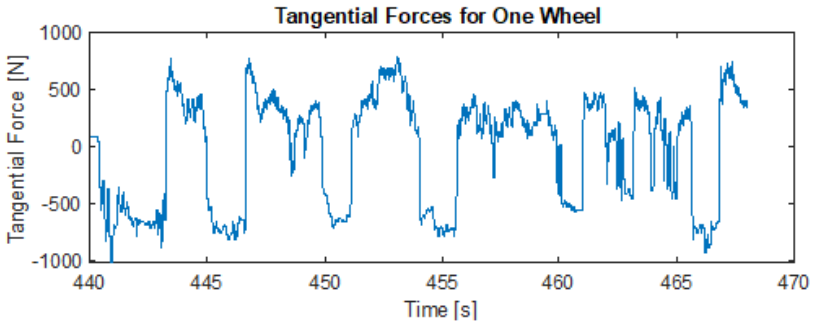


**Figure 6.13:** Graph showing the approximated tangential forces for one wheel

The lateral forces are computed with the data from the lateral accelerometer, the total mass of the vehicle and the normal forces. The total lateral force from the lateral acceleration of the mass centre is distributed evenly between the front and rear axle because of the evenly distributed weight distribution of the vehicle. The left and right lateral force distribution is approximated to correspond to the left and right normal force distribution. Each lateral acceleration data point is computed with its corresponding normal force data into a lateral force according to equation 6.16, 6.17 and 6.18. This results in the lateral force data set plotted in Figure 6.14.

$$F_{L,tot} = m \cdot a_L \tag{6.16}$$

$$F_{L,FL} = F_{L,tot} \cdot \frac{F_{N,FL}}{F_{N,tot}} \tag{6.17}$$

$$F_{L,FR} = F_{L,tot} \cdot \frac{F_{N,FR}}{F_{N,tot}} \tag{6.18}$$

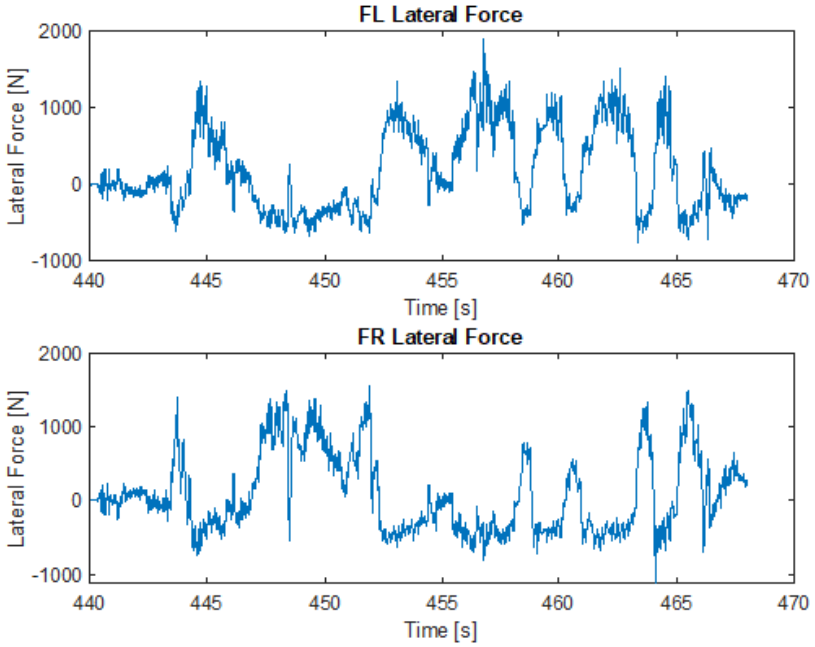


**Figure 6.14:** Graph showing the approximated lateral forces for both front wheels

### 6.3.3 Final Load Cases

The load vectors shown as graphs in Figure 6.12, 6.13 and 6.14 defines the final load cases. The gearbox housing is only stress- and deformation analyzed, therefore the maximum normal-, tangential- and lateral forces defines the gearbox housing load case. For the bearings the complete load vectors combined with the motors' rotational speeds are used as the load case for computing the bearing service life.

## 6.4 Discussion

Initially, the idea was to use the pivot shaft angle sensor data combined with a kinematic model for the springs and dampers to approximate the normal forces. Because of complications described in Appendix L this was not possible, which is the reason that the data was scaled with hand calculations. This method requires the simplification that the shock absorbers are fully linear but since CFS19 utilized a heave-roll suspension system it is highly likely that the suspension system is non-linear, see figure 6.15. This is because the heave-roll system compresses a roll-spring during cornering (lateral acceleration) and a heave-spring during longitudinal acceleration or unevenness in the road surface. Since Victoria have a stiff suspension and low center of gravity, it is assumed that the roll of the vehicle is negligible. CFS did also explain that the damper and spring rates might have been adjusted during competition and can therefore be considered as unknown variables. For the intended kinematic model, this would have meant assumptions which could have affected the final approximated normal force considerably. Therefore, the hand calculation assisted scaling of the angle sensor data is considered a more reliable method.


**Figure 6.15:** Overview of front suspension

As mentioned in the results, the wheels are assumed to have equal tangential forces. This however, is a simplification due to a malfunction of the pushrod pivot shaft angle sensors on the rear wheels. In other words, one or more wheels could be subjected to higher tangential forces than the others which mean that some of the bearings and housings could be subjected to higher loads, thus underestimating the load cases.

Estimates were made as to whether the aerodynamics of the car needed to be taken into account when the car decelerated. This is since formula student cars are equipped with many aerodynamic features. This is relevant to the tangential forces since the aerodynamics helps the car decelerate without affecting the longitudinal

forces acting on the wheel centre. The force that would affect this is $F_D$, which is the drag force.

$$F_D = C_D \frac{\rho v^2}{2} A_D \tag{6.19}$$

This force was calculated for a few data points and was found to be negligible. However, this is conservative and if the drag force is bigger then calculated the gearbox could become a bit over dimensioned.

Another simplification that was made was that the tangential force is equal on all four wheels at any given time. This is reliable when the car is accelerating because the torque used is relatively even. It may change a bit, left and right, when cornering, but there are no major differences. When braking however, the majority of the power should be moved to the front axle. In this case, the load case is being underestimated.

In order to make a more accurate approximation of the distribution of lateral forces on the front wheels, the normal force distribution were used. This however, might not be completely accurate but is considered a reasonable method for distributing the lateral forces on the front wheels.

# 7

# Housing Design & Bearing Selection

## 7.1 Method

### 7.1.1 Housing & Carrier Design

First, the previous gearbox housing and carrier designed by CFS19 are examined. This gearbox has been successfully manufactured and the design has been proven to work which makes for a good starting point. Shared components that are possible to carry over are designed similarly with adjusted dimensions.

The gearbox housing is 3D-modelled in CATIA V5 and analysed for deformation and stress in the finite element (FEM) analysis tool ANSYS. ANSYS will help ensure that the skewing of critical components is within a tolerable level that is set when dimensioning the transmission part of the gearbox in KISSsoft.

From the gear design, the maximum deformation of the carrier is defined since the gears can only take so much skewing. To ensure sufficient stiffness of the carrier for these criteria the carrier is modelled, then analysed and then modified with the gained knowledge in an iterative process.

In addition to the maximum deformation of the carrier itself, the maximum deflection of the carrier's bearing seats is also estimated (this results in a skewing of the whole carrier). This is a factor both affecting the bearing life and the gear strength. Many internal components of the gearbox help stiffen the gearbox which is a factor that is not fully represented in ANSYS. Therefore, this analysis is not taken as a definitive but rather as a reference between housing designs.

After assuring acceptable skewing, the stress on the gearbox housing is controlled. Since very little skewing is accepted, the stresses are typically not the dimensioning factor for the carrier in this case but for the housing they are of greater importance.

Packaging and potential clashing are also evaluated in the model by examining section views and using clash tools. The model is built with nominal dimensions.

### 7.1.2 Bearing Selection

SKFs methodology is used to calculate the service life on the bearings. The methodology is retrieved from the SKF catalog [1]. Since a gearbox has varying loads and speeds it may be good to sort the cases in different operating intervals, this is done with a 3 dimensional histogram.

The SKF method is based on first calculating the equivalent dynamic bearing load, this is done by using the radial and axial forces on the bearing and then comparing them with the normal backlash [1]. The axial and radial forces on the bearings are obtained from the free body diagrams of the wheel axles where the previously calculated forces on the wheels are used. The forces on the wheels are derived in Section 6.3.2.

The second step is to produce $a_{SKF}$ which is done by using diagrams [1]. Then $L_{10m}$ is calculated, which is the nominal service life with 90% reliability. This is done for all the different cases from the histogram.

All these service lives can then be calculated into a common service life based on how long the bearing is expected to be exposed to the different cases [1]. The total service life of the bearing is then compared with the intended life of the gearbox to provide a safety factor.

## 7.2 Results

### 7.2.1 Housing & Carrier Design

A number of features of the housing and carrier design are carried over from CFS19 since this gearbox has been manufactured successfully and the design has been proven to work. First the material, which is aluminum alloy 7075, is carried over to both the housing and the carrier since it is a proven and accessible material. The wheel and brake disk mounting interface are carried over with minor changes. In order to accommodate the planetary gears, the carrier is shortened and the diameter is increased compared to the carrier of CFS19. The method for mounting the planetary gears is also remained the same as CFS19, utilizing separable planetary shafts that are pressed into the carrier from the inside. This is also true for the lubrication passages that are more or less a copy of the CFS19 solution to ensure satisfactory lubrication. See Figure 7.1 a) for the carrier design.

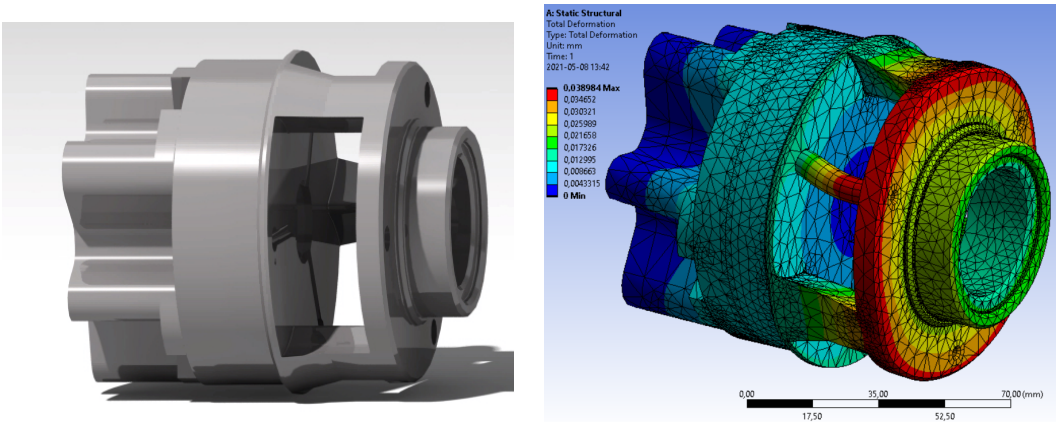


a) 3D-model in CATIA V5 (left side pointing outwards)

b) Deformation analysis in ANSYS (with planetary shafts)

**Figure 7.1:** Rendering and deformation analysis of carrier

A few iterations were made analysing the carrier in ANSYS and making changes to the model accordingly, see Figure 7.1. The planet shafts (visible in Figure 7.1 b) but not in Figure 7.1 a)) were included in the ANSYS analysis as they play a notable role in stiffening the carrier. The part of the carrier that interferes with the wheel was locked with a fixed support in ANSYS and a bearing load was put on the planet shafts. A *bearing load* is meant to more accurately model the affect of a cylindrical body than just a force on the surface. The magnitude of these forces was calculated from the maximum torque in the transmission load case, the magnitude of each was set to 1700 N.

The principal reason for analysing the deformation of the carrier is to determine how much the planet gears skew. This is done by finding the difference in deflection between the two points on a shaft, see Figure 7.2.

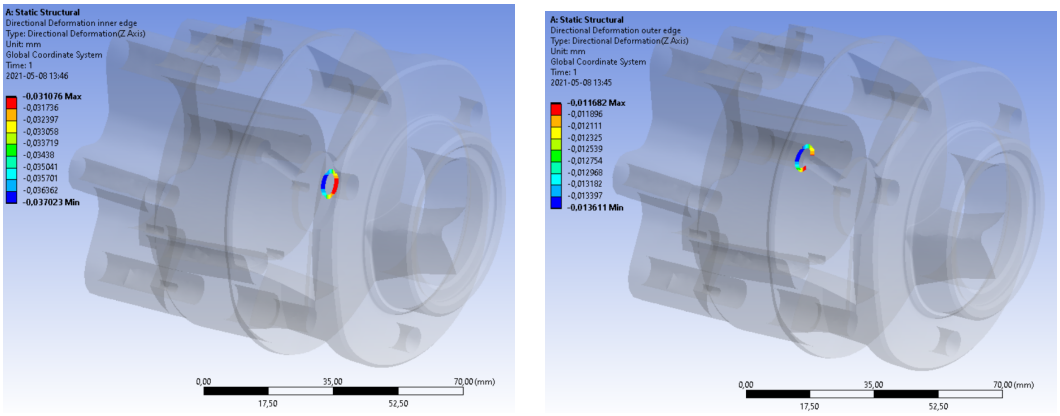


a) Inner b) Outer

**Figure 7.2:** Reference points for calculating the skewing of the planet gears in carrier

The final design yielded a skewing of the gears that was greater than initial results from rough mock ups of the carrier that was analysed in ANSYS. These initial values were meant to be set in the gear designing stage and then drive the dimensions of the carrier, but when it emerged that the initial values could not be replicated with proper packaging taken into consideration the values had to be updated in the gear design. This meant that the safety factor of the transmission part was lowered additionally.

The gearbox housing could not be carried over from the earlier CFS19 gearbox since the upright was integrated in the gearbox housing in that design. Therefore, the gearbox housing is completely designed from scratch, beginning with building a shell around the carrier, planets and bearings. The only design that is inspired from CFS19 is the use of six M6 bolts in threaded steel inserts to hold the inner and outer housings. The housing is also designed to use these bolts for holding the ring gear, see figure 7.3.

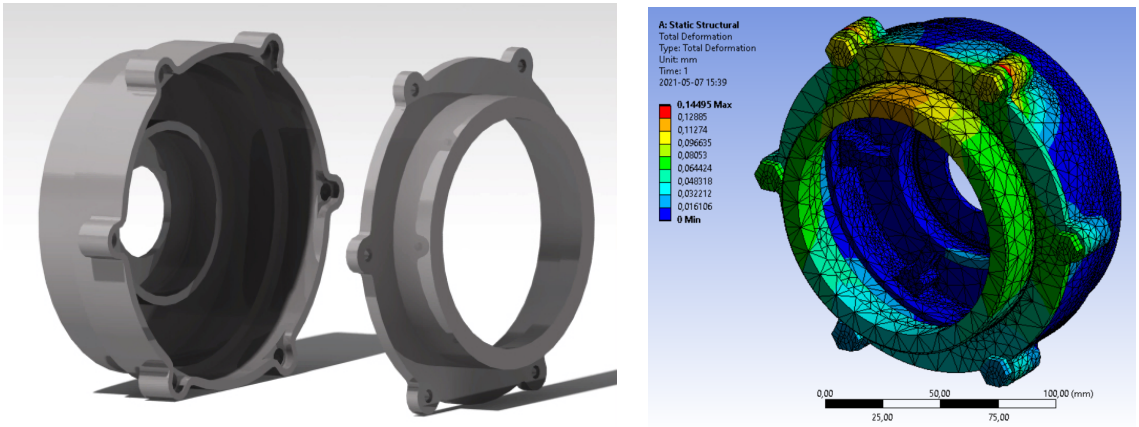


a) 3D-model in CATIA V5 b) Deformation analysis in ANSYS
Left: inner housing Right: outer housing

**Figure 7.3:** 3D-modelling and deformation analysis of housing

The deformation of the housing was also analysed in ANSYS, see Figure 7.3 b). This deformation is harder to determine fully as internal components stiffens the gearbox. Bearings are an example of these components, they would however be hard to model in ANSYS. The housing was therefore modeled without the internal components except for the ring gear which interferes with the housing directly. This assembly is more flexible than the real gearbox would be but it gave a (conservative) approximation of the deformation of the housing. The bolt holes connecting the inner housing (inner housing can be found as the left body in Figure 7.3) to the motor were locked with fixed supports and the bearing seats for the carrier bearings were loaded with a bearing load equal to the maximum of the load case found by the free body analysis in Section 7.2.2.1. The force on the inner bearing seat was set to 3000 N and the force on the outer was set to 3500 N in the opposite direction.

From this deformation the skewing of the planet carrier can be derived. This again is done by calculating the difference in deflection between the relevant parts. Here the skewing is found by taking how much difference there is between the outer bearing seat and ring gear, the inner bearing seat was found to not deflect significantly. Since the sun gear is defined as “floating” only the ring gear is taken into consideration when analysing the skewing of the carrier.

Since the housing is designed as a shell without any structural reinforcements, the housing is redesigned in order to get less skewing of the carrier bearing seats. After a few iterations between CATIA V5 and ANSYS the final gearbox housing design is constructed. The six bolts holding the outer housing are assisted by six steel pins and both the inner and outer carrier bearing seats are reinforced with six braces on the outside. See Figure 7.4 for the final design.

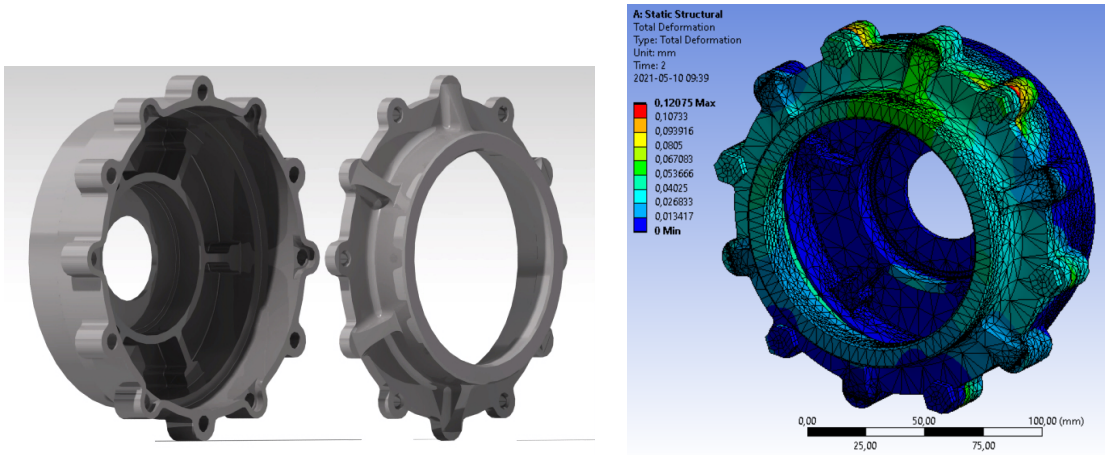


a) 3D-model in CATIA V5 b) Deformation analysis in ANSYS

**Figure 7.4:** 3D-modelling and deformation analysis of final housing

The analysis in ANSYS showed that the steel pins helped significantly in making the housing more rigid, as did the ridges supporting the outer bearing seat. The pins will also help in assembling the gearbox with the required concentricity. The outer bearing moved upwards of 65 µm but since the ring moved about 55 µm in the same direction the net skewing of the carrier was estimated to be 10 µm, bearing in mind that the housing is assumed to be more rigid than modeled here when stiffened by the internal components.

### 7.2.2 Bearing Selection

The calculations on the bearings are done using MATLAB in a script called Bearings.m (Appendix M). The calculations are done both on the left and right wheel axis since one lap from Achen is used, which was running clockwise. Since the toughest load case should be taken into consideration one should not use means of left and right since that should give an smaller value. In the MATLAB program, the user can first select the bearing they want to do the calculations on, if the bearing is not in the list, it is easy to add more bearings. The data that the program needs is: d, D, B, C, $C_0$, $P_U$, $N_{ref}$, $N_{lim}$, M and $f_0$.

#### 7.2.2.1 Free Body Diagram

Two free body diagrams are created so that a number of equilibrium equations can be established. The free body diagrams are set up for the wheel axle(grey in picture).

The coordinate system is defined as :
Y- The horizontal direction of the car
X- The Longitudinally direction of the car
Z- The vertical direction of the car

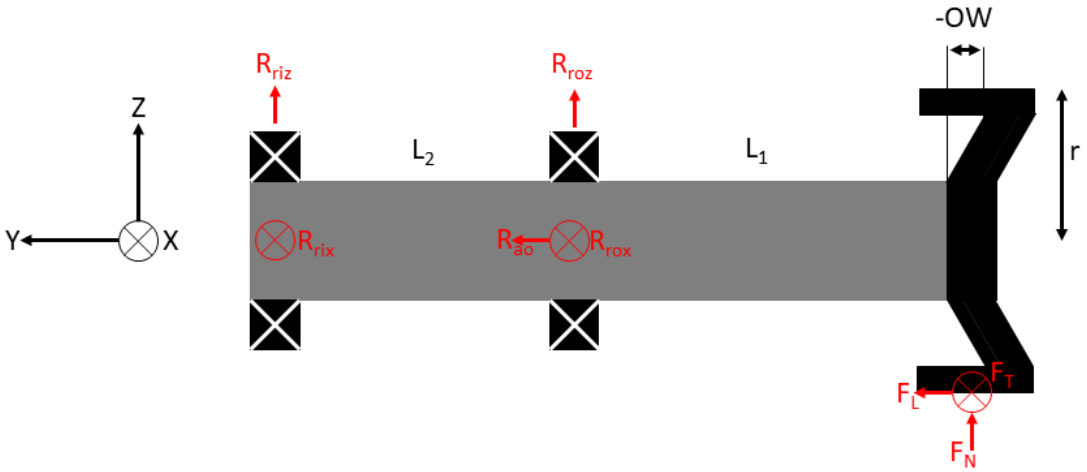


**Figure 7.5:** Free body diagram of the bearing assembly in the YZ-plane

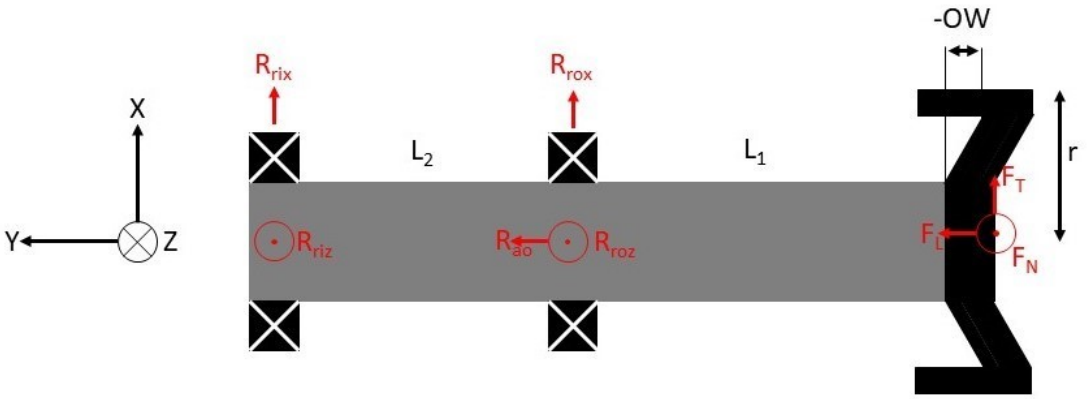


**Figure 7.6:** Free body diagram of the bearing assembly in the XY-plane

Equilibrium equations are set up for the wheel axle. This is done via free body diagrams. The forces that are known and have previously been analyzed (see Section 6.3.2) are $F_L, F_T$ and $F_N$ these are used as input variables in the equilibrium equations. Note that the forces are from one lap in Achen and vary over time.
Equilibrium equations from Figure 7.5:

$$\overset{\curvearrowright}{O}_{YZ} : F_L \cdot r + R_{riz} \cdot L_2 - F_N \cdot (L_1 - OW) = 0 \tag{7.1}$$

$$\uparrow_{YZ}: Priz + Rroz + F_N = 0 \tag{7.2}$$

$$\leftarrow_{YZ} R_{ao} + F_L = 0 \tag{7.3}$$

Equilibrium equations from Figure: 7.6

$$\overset{\curvearrowright}{O}_{XY} : R_{rix} \cdot L_2 - F_T \cdot (L_1 - OW) = 0 \tag{7.4}$$

$$\uparrow_{XY}: R_{rix} + R_{rox} + F_T = 0 \tag{7.5}$$

Some simpler calculations are made to solve the searched variables to get them expressed in known variables.
Equation (7.1) gives:

$$R_{riz} = \frac{F_N(L_1 - OW - F_L) \cdot r}{L_2} \tag{7.6}$$

Equation (7.2) gives:

$$R_{roz} = -F_N - R_{riz} \tag{7.7}$$

Equation (7.4) gives:

$$R_{rix} = F_T \cdot \frac{L_1 - OW}{L_2} \tag{7.8}$$

Equation (7.5) gives:

$$R_{rox} = -F_T - R_{rix} \tag{7.9}$$

Equation (7.3) gives:

$$R_{ao} = -F_L \tag{7.10}$$

The equilibrium equations take the forces on the wheel and give the forces on the bearings. The input forces and number of revolutions should be the forces from one lap i Aachen. Note that one lap implies that the forces and number of revolutions vary with time.

#### 7.2.2.2 Service Life Calculations

The service life expectancy is calculated using a large number of equations that take into account a large number of factors. One of the most important factors are the forces that affect the bearing, these forces are based on the calculations developed in Section 7.2.2.1. They can be converted to equivalent dynamic bearing loads [1], expressed as $P$.

$$\frac{F_a}{F_r} \geq e \rightarrow P = F_r \tag{7.11}$$

$$\frac{F_a}{F_r} \geq e \rightarrow P = X \cdot F_r + Y \cdot F_a \tag{7.12}$$

$$P = \begin{cases} F_r & \text{if} \quad \frac{F_a}{F_r} \leq e \\ X \cdot F_r + Y \cdot F_a & \text{if} \quad \frac{F_a}{F_r} > e \end{cases} \tag{7.13}$$

$X$, $Y$, and $e$ from equation 7.11 and 7.12 are values that depend on the chosen bearing, these can be find on page 315 in the SKF catalogue [1], Table 8.

$F_a$ is directly from equation (7.10) since it is the only axial force on the bearing. In case of $F_r$ both $X$-direction and the $Y$-direction need to be taken into consideration, these are combined using Pythagoras theorem.

The data can then be divided into a three-dimensional histogram with respect to equivalent dynamic bearing loads and speed.

A MATLAB function was created to calculate $a_{SKF}$ called a_SKF_calculation.m (Appendix N). The function needs the input values: $P$, $n$ ,$P_U$, $d_m$, $\eta_c$, $\nu$ and type. What is meant with type is if a ball bearing or a roller bearing is being used. The function first determines the contamination factor $\eta_c$, this is done based on the $d_m$

and the assumption that the oil is "slight contamination" based on Table 4 page 74 in the SKF Catalogue [1].

Then different graphs have been approximated into the MATLAB function, this has been done by taking a number of points from each graph to then approximate the lines as linear. The number of points varies greatly because it is depending on how the curvature looks, straight lines give few points and nonlinear lines gives a larger number of points. The graph that the function has approximated is:

1. Required viscosity of the lubricant at operating temperature, chart 5 page 72 SKF catalogue [1].
2. $a_{SKF}$ for radial ball bearings, chart 1 page 66 SKF catalogue [1]
3. $a_{SKF}$ for radial roller bearings, chart 2 page 67 SKF catalogue [1]

The first graph is used to calculate the required viscosity of the lubricant at operating temperature, $\nu_1$ this is then compared with the actual viscosity of the lubricant at operating temperature, $\nu$. This gives the relationship $\kappa = \frac{\nu}{\nu_1}$ which is the viscosity relationship.

Afterwards the function calculates $a_{SKF}$, the function chooses graph 2 or 3 depending on the type of bearing. The implementation however, is the same. The program interpolates to the most suitable $\kappa$-line and then calculates the value onto the x-axis by calculating $\eta_c \frac{P_u}{P}$ which then gives the value on the y-axis($a_{SKF}$) by interpolation. This is the value that the function then gives as an output. Afterwards the program calculates the nominal service life of the bearing showed in equation (7.14), according to ISO 281 [1].

$$L_{10} = \left(\frac{C}{P}\right)^p \tag{7.14}$$

The nominal service life is then scaled according to SKF nominal service life ($L_{10m}$) with $a_1$ and $a_{SKF}$. $a_1$ is a factor that regulates the operational reliability, since 90% operational reliability is used, which is standard $a_1 = 1$. $a_{SKF}$ is a factor that regulates operating conditions, the calculations for it are made through the previously described MATLAB-function, a_SKF_calculation.m, which can also be seen in the Appendix N.

$$L_{10m} = L_{10} \cdot a_1 \cdot a_{SKF} \tag{7.15}$$

Since $L_{10m}$ is calculated for a number of different cases produced by the previously mentioned 3 dimensional histogram, the cases can be named $L_{10m1}$, $L_{10m2}$, $L_{10m3}$,...,$L_{10mn}$. All these cases generate different $L_{10m}$ which can calculate a common service life that takes into account how large proportion ($U$) of the time the bearing is loaded in different cases.

$$L_{10m} = \frac{1}{\frac{U_1}{L_{10m1}} + \frac{U_2}{L_{10m2}} + \frac{U_3}{L_{10m3}} + ... + \frac{U_n}{L_{10mn}}} \tag{7.16}$$

The safety factor is then calculated by comparing the $L_{10m}$ with the intended number of revolutions which is generated when the car drives 1500km with a wheel of 16 inches. Finally the code prints the number of revolution and the safety factor for each of the bearing at both the left and right wheel axis.

#### 7.2.2.3 Final Selection

The final choice of bearings was made when the house and assembly were designed. A number of bearings were tested and run trough the MATLAB-script.

The bearings chosen were SKF 61910-2RS as the inner bearing and SKF 61817-2RZ as outer bearing. Table 7.1 shows some specifications on the bearings. It is obvious that to get these results, a good lubrication is required. Previous years' lubrication has worked well and due to this a carry over was made and adapted to this new type of gearbox.

**Table 7.1:** Specifications of the final selected bearings for the wheel axis

| | | Inner bearing | Outer bearing |
|---|---|---|---|
| Name | | SKF 61910-2RS | SKF 61817-2RZ |
| Inner diameter | $d$ | 50 mm | 85 mm |
| Outer diameter | $D$ | 72 mm | 110 mm |
| Width | $B$ | 12 mm | 13 mm |
| Mass bearing | $M$ | 0.13 kg | 0.28 kg |
| Basic dynamic load rating | $C$ | 14.6 kN | 19.5 kN |
| Basic static load rating | $C_0$ | 11.8 kN | 16.6 kN |
| Fatigue load limit | $P_u$ | 0.5 kN | 0.88 kN |
| Reference speed | $N_{ref}$ | 19 000 r/min | 12 000 r/min |
| Limiting speed | $N_{lim}$ | 9500 r/min | 6000 r/min |
| Calculation factor | $f_0$ | 16.1 | 13.5 |

The output from running these bearings through the created MATLAB-script (Appendix M) can be seen in Table 7.2.

**Table 7.2:** Calculations on final selected bearings

| | Unit | Outer Left bearing | Outer Right bearing | Inner Left bearing | Inner Right bearing |
|---|---|---|---|---|---|
| $L_{10m}$ | Million revolutions | 8440 | 7320 | 209 | 178 |
| Calculated driving distance | km | 3430187 | 2974664 | 84749 | 72172 |
| Safety factor | | **2287** | **1983** | **57** | **48** |

The safety factors of the bearings are high and should not cause the gearbox to fail.

## 7.3 Discussion

### 7.3.1 Housing Design

The assumption that the internal components stiffen the gearbox might be a source of error. The thought is that the carrier and its bearings stiffens the housing, which is not verified. This deformation analysis is therefore only used as a reference.

As described in Section 5.2.3, the developed gears are very sensitive to skewing. Therefore, the housing needs to be very stiff which requires much material resulting in a heavier gearbox housing than a gearbox less sensitive for skewing.

Another assumption is that the ring moves with the housing resulting in less skewing of the carrier. This seems reasonable in the deformation analysis but might differ in reality when the fitting of components are taken into consideration, as e.g. play between the ring and housing might alter this result.

### 7.3.2 Bearing Selection

Since it is quite easy to state that the bearings will last, it may not be necessary to make such a general and complicated method for calculating them. The time and energy put into this may have given a better return in some other parts of the project, but it was impossible to know that before it was thoroughly researched.

It should be borne in mind that the loadcases could be incorrect, which could have resulted in incorrect safety factors for the bearings. But if that is the case, there is still a large safety factor that should be able to tolerate a relatively large error in the load cases.

The load cases could be completely correct, but the track the data is from is not the toughest track to compete on. If the car is driven on a track that loads the bearings harder, this would shorten the service life of the bearings and reduce the safety factor, but as previously mentioned, the safety factors are relatively large and they should be able to withstand more extreme loads.

It should also be mentioned that the selected bearings have previously been used by CFS. However, they were used in a different type of gearbox and were not calculated as accurately as this report does.

# 8
# Final Design

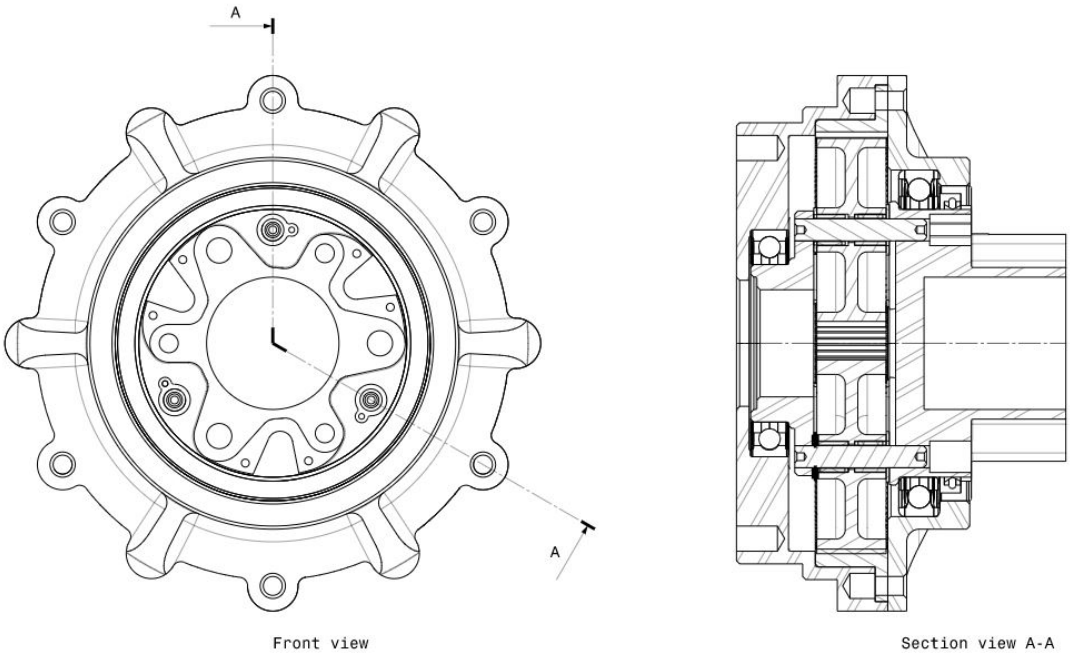


**Figure 8.1:** Front and section view of the gearbox

The final design is a single stage planetary gearbox with a gear ratio of 11.5:1. The benefits of this transmission layout is its simple design, few moving components and short axial length. The gear dimensions are found in Table 5.5 in Chapter 5.2.2. The gears are supported by two SKF 7x10x10 needle bearings and two axial plain bearings.

The carrier is made out of aluminium alloy 7075 and utilizes a similar wheel and brake disk mounting interface as CFS19. The brake disc can be mounted to flanges on the mounting interface. The lubrication passages, planetary shafts and axial bearings are carried over from CFS19 with minor adjustments. See Figure 8.2 for an exploded view of the carrier and its associated components.

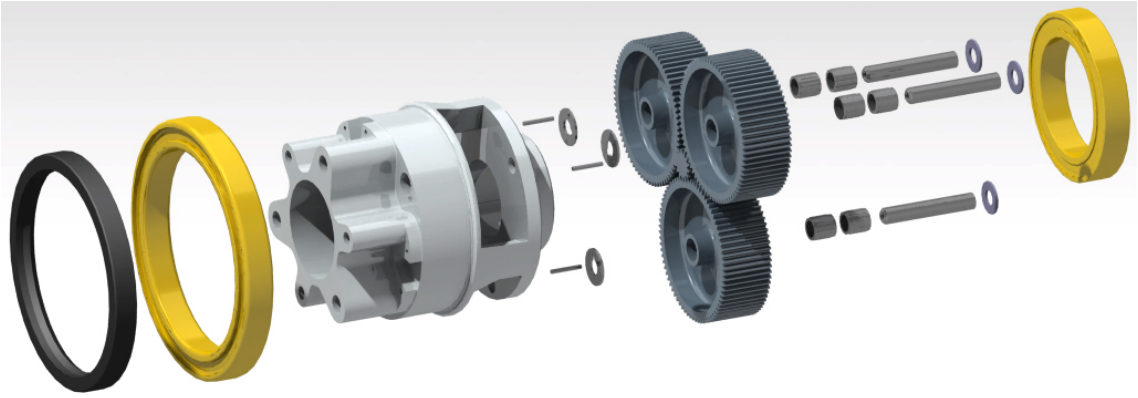

**Figure 8.2:** Exploded view of the carrier and its associated components

The outer bearing holding the carrier is a SKF 61817-2RZ and the inner bearing is a SKF 61910-2RS. The radial shaft seal outside the outer bearing is a SKF HMS5 V. These bearings and the seal are the same model as in CFS19's solution, as described in Section 7.3.2.

The housing consists of an inner- and an outer housing holding the ring gear and the carrier bearings, both of which are made out of aluminium alloy 7075. There are threaded holes for steel inserts for 6 M6x16 bolts in the inner housing to fasten both the ring gear and the outer housing. In addition to the bolts, holes for 6 steel pins are designed in the housings to stiffen the gearbox. See Figure 8.3 for an exploded view of the housing and the ring gear and Figure 8.4 a) for a assembled isometric view of the gearbox from the front.

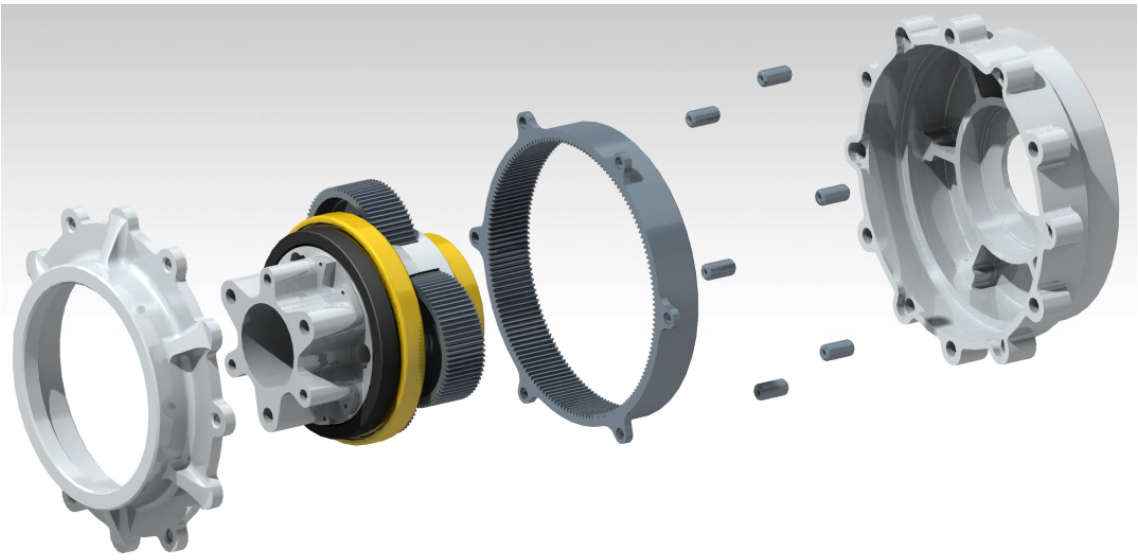

**Figure 8.3:** Exploded view of the housing and the ring gear, with the rotating assembly in between

The interface for mounting the electric machine and upright consists of holes for steel inserts for 6 M6 bolts. To ensure that the electric machine mounts up concentric to the gearbox, there is a hole with an inner diameter of 40 mm to use

as a locating feature for the electric machine. The input shaft is splined with 12 1x1.5x20 mm grooves. See Figure 8.4 b).

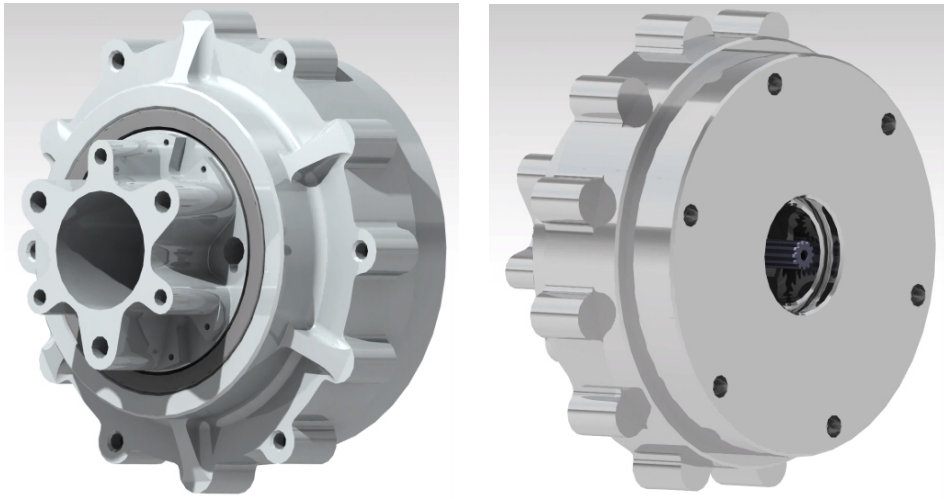

a) Front isometric view b) Rear isometric view

**Figure 8.4:** 3D-model of the final gearbox in CATIA V5

Axially, the gearbox measures 104 mm with a largest outer diameter of 170 mm measured on the bolt flanges. The complete gearbox is weighed in CATIA V5 which estimates that the complete gearbox weighs 2.883 kg. In order to make the weight comparable to the CFS19 solution, the weight of an upright must be included. Since the CFS21 upright is meant to be mounted similarly to the intended mounting on this gearbox, the weight of CFS21 upright is included in the total weight. The upright weighs 0.518 kg which sums up the gearbox total weight to 3.401 kg.

**Table 8.1:** Weight comparison between CFS19 and the new gearbox

| | **CFS19** | **New gearbox** |
|---|---|---|
| Carrier | 629 g | 621 g |
| Planet gears | 384,15 g | 591 g |
| Sun gear | 44 g | 27 g |
| Ring Gear | 333 g | 387 g |
| Inner Housing | 426 g | 494 g |
| Planet Pins | 51 g | 36 g |
| Planet Bearings | 18 g | 18 g |
| Outer planet bushing | 6 g | 4 g |
| Inner planet bushing | 2,22 g | 0,35 g |
| Outer Bearing | 280 g | 280 g |
| Inner Bearing | 130 g | 130 g |
| Outer Housing + Upright | 1179 g | 810 g |
| **Complete gearbox:** | **3482,37 g** | **3398,35 g** |
| **Shared components:** | **2303,37 g** | **2588,35 g** |

# 9
# Discussion

As discussed in Section 3.3, there was a risk that the concept generation did not generate the lightest solution. This is because the process greatly depends on the group members' knowledge about transmission solutions when deciding elimination factors, which is limited since none of the group members has earlier experience with gearbox design. In this project, the single stage planetary gearbox was considered the most suitable transmission layout because of its few components and simple design. During the concept generation, these design benefits were considered very valuable which resulted in it becoming the final concept. However, during gear design it was found that the high gear ratio of 11.5:1 resulted in the sun gear becoming very small. This meant that in order to get acceptable safety factors the gears needed to become wide which resulted in heavy gears. Another negative effect of the high gear ratio is that the diameter of the gearbox needed to become large which resulted in a heavy ring gear and gearbox housing. If more time was available, the focus could have been changed to the secondary final concept from the concept generation, see Section 3.2.5. Unfortunately, it was too late at the time of realization that the single stage planetary gearbox might not be the optimal solution.

Regarding the load cases, the transmission load cases are considered reliable. As described in Section 4.2.2, the wheel experiencing the most torque and speed at any point defines the load case. Furthermore, the service life of 1500 km autocross competition is considered a tough load case since much of the vehicle's mileage is done during testing and endurance competition.

One aspect that might be of more significance than estimated is the added dynamic torque from the wheel slipping and gaining traction during cornering. As described in Section 5.3, these dynamic loads are usually accounted for with an increased safety factor by automotive engineers. In this application however, the road surface that the vehicle will travel on is considered smoother and the tires are considered stickier than the average commuter car. Therefore, the torque on the transmission is considered even, with low dynamic loads. A parameter in KISSsoft made to compensate for these loads is also adjusted to compensate for light shocks, as described in Section 5.2.2.

Another source of error is that the complete gear geometry is computed with the softwares KISSsoft and KISSsys. There is a possibility that mistakes have been made during the choices of parameters and that there are better solutions to be generated from the program. The computation was however done many times during the project which minimized this risk. If the time span of the project would have been longer, it would have been good to compare the results with another similar software or with hand calculations.

Initially, the methodology for developing load cases for the gearbox housing and bearings was to use the pivot shaft angle sensor data and a kinematic model to compute the forces from the shock absorbers. This methodology was considered more desirable than the resulting methodology but because of problematic data described in Appendix L this was unfortunately not possible. However, the resulting methodology using hand calculations is considered reasonably reliable. One source of error is that the normal forces were calibrated during acceleration and not during retardation. Since the car has many aerodynamic features generating normal forces, it was considered more accurate to calibrate the normal forces during acceleration from standstill. If the data was calibrated based on maximum retardation, the maximum resulting normal forces would have been more controllable since the normal forces would have been calibrated with their maximum value instead of their minimum value. With that said, the resulting forces were still considered reasonable.

The final design does not include the mounting for a brake caliper, which was an accessory specified as a sub-function in Section 3.2.3. This is a result of other parts of the project being more time consuming than expected. However, it is considered possible to package a brake caliper in the intended position illustrated in Figure 3.6.

The final weight of the gearbox is described in two different weights depending on what components are included. This is to simplify the comparison to the most recent manufactured CFS gearbox, which is that of CFS19, that has the upright integrated into the gearbox. Therefore, the first comparison is between the gearbox including the weight of CFS21's upright which is 3.398 kg and the CFS19's gearbox weight of 3.482 kg, see Table 8.1. If only the shared components are weighed, the weight of the gearbox is 2.588 kg compared to CFS19's gearbox weight of 2.303 kg. This means that in this case, CFS19's gearbox is 12.3% lighter than the developed gearbox. However, if the complete functional assemblies including the uprights are compared, this new gearbox is 2.4% lighter. This implies that the integrated upright solution of CFS19 is heavy rather than that the developed gearbox as a whole is lighter. If CFS19's gearbox would have utilized a similar upright to CFS21, that gearbox would have been lighter than the gearbox developed in this project.

The most prominent weight difference of the gearboxes lies in the weight of the planetary gears. Even though CFS19 essentially have twice as many planetary gears, the weight of the planetary gears in the developed gearbox is about 35% heavier than those of CFS19, see figure 8.1. This is due to the large diameter needed to reach the desired 11.5:1 gear ratio, which also negatively affects the weight of the housing and ring gear.

One advantage of the developed single stage planetary gearbox worth mentioning is that it is marginally axially thinner. The gearbox itself is 14 mm thinner than CFS19's gearbox but since the upright is to be mounted in between the gearbox and the electric machine the thickness of the upright must be included. CFS21's upright is used again as a reference with a thickness of 10 mm resulting in a total reduction of 4 mm axial thickness.

Finally, it should be noted that this project became more extensive than expected. Due to this, it has not been possible to go into depth as much as desired on certain topics.

# 10
# Conclusion

This project resulted in the development of a single stage planetary gearbox with a 11.5:1 gear ratio. The gearbox has a splined input shaft and transmits the torque via a similar output shaft as CFS19's gearbox to the wheel. The brake disk mounts up to the output shaft, the electric machine and upright mount up to a mounting interface consisting of a locating feature and six M6 bolts which can also be utilized for mounting the brake caliper. Therefore, all functions specified in the requirement specification are considered fulfilled, see Table 3.1.

The environmental requirements consist of a temperature interval as well as protection from water and debris. When the electric machine and upright are mounted to the gearbox, the input shaft is completely closed and a seal is located on the output shaft protecting the gearbox from mild rain and debris. The gearbox is made out of steel and aluminium which handles the temperature interval well. With that said, all environmental requirements are fulfilled. The housing has a minimal wall thickness of 4 mm of aluminium alloy 7075 which is stronger than the required wall thickness and material [5].

The gearbox has a maximum diameter of 170 mm which is less than the specified requirement of maximum 235mm. The brake disc and caliper can be located in the same position as in CFS19's gearbox since the output shaft is very similar. Therefore, the requirements regarding maximum diameter as well as packaging are fulfilled.

The budget for the four gearboxes should not exceed 100 000 SEK in market value according to the requirements specification. Since the developed gearbox do not differ greatly in materials or manufacturing procedures from the gearbox of the previous year, while having planet gears deemed easier to manufacture, this criterion is considered to be met.

The required service interval is set at 50 km. This should not be a problem to handle, as the gearbox's service life is calculated without any oil changes at all. Thus, the requirement is met.

The housing is possible to manufacture with the machines available in the Chalmers facilities which was a wish in the requirements specification. The gear set however, needs to be outsourced and since the selected gears are based on standards, there should be no problems to do so. Thereby, all requirements from the requirement specification are fulfilled, see Table 3.1.

The gearbox concept including the weight of CFS21 upright is 2.4% lighter than CFS19's gearbox including its integrated upright, see Table 8.1. From that perspective the project purpose of developing a lighter gearbox than the most recent manufactured gearbox is fulfilled. However, if only the shared components are

included in the weight of the gearboxes CFS19's gearbox is 12.3% lighter. Therefore the project purpose of devloping a lighter gearbox than the latest manufactured CFS gearbox is per definition fulfilled.

With that said, since the gears and housing are heavier than CFS19's gearbox and the developed gearbox have many flaws in term of reliability described in Chapter 9 it is safe to say that the gearbox is far from optimal. Therefore, the main conclusion withdrawn from this project is that a single stage planetary gearbox is not suitable for this application.

The methodology described in this report for deriving the transmission load cases from competition data is on the other hand strongly recommended. The load cases are considered accurate and very suitable for dimensioning this type of transmission since the method uses real physical data from competition. Because of the problematic data described in Appendix L the load cases for the gearbox housing and bearings are unfortunately not as directly linked to the physical competition as the transmission load cases. If the sensors were calibrated correctly prior to the competition and the transfer function from the sensor data to the suspension movement was properly definable the load case would have been as reliable as the transmission load case.

As stated above, the 11.5:1 gear ratio results in weaknesses in the design that makes a single stage planetary gearbox unsuitable for this application. The further recommendation is instead to continue use a 1.5 stage compound planetary gearbox designed with loadcases derived from the methodology developed in this project.

# Bibliography


[1] SKF-koncernen 2019. *Rullningslager*. SKF-koncernen, 2019.

[2] altair. *Load Cases*. URL: https://www.altair.com/training/inspire_2018/content/material_loads/load_cases.htm. (Accessed: 2021-04-15).

[3] J. Amendola. *Advantages of an Epicyclic Gear*. URL: https://www.artec-machine.com/wp-content/docs/Advantages%5C%20of%5C%20an%5C%20Epicyclic%5C%20Gear.pdf. (Accessed: 2021-04-23).

[4] Martyn Anderson and Damian Harty. *Unsprung Mass with In-Wheel Motors - Myths and Realities*. 2018. URL: https://www.proteanelectric.com/f/2018/04/protean-Services3.pdf.

[5] Sunpreet Singh Chander Prakash Grzegorz Krolczyk and Alokesh Pramanik. *Advances in Metrology and Measurement of Engineering Surfaces*. Studentlitteratur, 2017. ISBN: 978-981-15-5150-5.

[6] DANIELLE COLLINS. *What are Hertz contact stresses and how do they affect linear bearings?* URL: https://www.linearmotiontips.com/what-are-hertz-contact-stresses-how-do-they-affect-linear-bearings/. (Accessed: 2021-04-25).

[7] Federal Gear. *The 5 Advantages of Gear Hobbing*. URL: https://www.federalgear.com/blog/the-5-advantages-of-gear-hobbing. (Accessed: 2021-04-20).

[8] KHK STOCK GEARS. *INTERNAL GEARS*. URL: https://khkgears.net/new/internal_gears.html. (Accessed: 2021-04-18).

[9] Formula Student Germany. *FS-Rules 2020 V1.0*. URL: https://www.formulastudent.de/fileadmin/user_upload/all/2020/rules/FS-Rules_2020_V1.0.pdf. (Accessed: 2021-04-12).

[10] Howard Horn. *Planetary gears — A review of basic design criteria and new options for sizing*. URL: https://www.machinedesign.com/motors-drives/article/21834575/planetary-gears-a-review-of-basic-design-criteria-and-new-options-for-sizing. (Accessed: 2021-03-30).

[11] Dogan Ibrahim. *Arm-Based Microcontroller Multitasking Projects*. URL: https://www.sciencedirect.com/science/article/pii/B9780128212271000013. (Accessed: 2021-04-19).

[12] Daniel Persson Ilonen. *Final Report CFS19*. \\sol.ita.chalmers.se\groups\formula\2019\Reports\Final\MPT
(Accessed: 2021-02-10).

[13] ONYX InSight. *Edge Loading - Gear failure*. URL: https://onyxinsight.com/wind-turbine-failures-encyclopedia/gear-failures/edge-loading. (Accessed: 2021-04-06).

[14] ONYX InSight. *Micropitting – Gear failure*. URL: https://onyxinsight.com/wind-turbine-failures-encyclopedia/gear-failures/micropitting/. (Accessed: 2021-04-23).

[15] KIA. *Do electric cars have transmissions?* URL: https://www.kia.com/dm/discover-kia/ask/do-electric-cars-have-transmissions.html. (Accessed: 2021-05-03).

[16] Carl Larsson. *Individual design report CFS20, Actuation & Linkages*. \\sol.ita.chalmers.se\groups\formula_c\2021\HandOverFromCFS20\FinalReports\Suspension
(Accessed: 2021-02-05).

[17] Kjell Melkersson Mart Mägi and Magnus Evertsson. *MASKINELEMENT*. Springer Nature Singapore Pte Ltd, 2019. ISBN: 978-91-44-10905-3.

[18] Matlab. *Compound Planetary Gear*. URL: https://se.mathworks.com/help/physmod/sdl/ref/compoundplanetarygear.html. (Accessed: 2021-05-03).

[19] Martin McCormick. *Scuffing*. URL: https://gearsolutions.com/departments/materials-matter-scuffing/. (Accessed: 2021-04-23).

[20] Gear Motions. *Helical Gears vs. Spur Gears*. URL: https://gearmotions.com/helical-gears-vs-spur-gears/. (Accessed: 2021-04-23).

[21] Dobrivoje Popovic Nan Liang. *Intelligent Vehicle Technologies*. URL: https://www.sciencedirect.com/science/article/pii/B9780750650939500049. (Accessed: 2021-04-19).

[22] novotechnik. *Sensor Potentiometers Series SP2800*. URL: https://www.elfa.se/Web/Downloads/ta/_e/fxSP2800_data_e.pdf. (Accessed: 2021-04-19).

[23] David G. Ullman. *The Mechanical Design Process, Fourth Edition*. McGraw-Hill, 2010. ISBN: ISBN 978-0-07-297574-1.

[24] Megan Woodland. *Case (Surface) Hardening versus Through Hardening of Steel*. URL: https://axisfab.com/steel-hardening/. (Accessed: 2021-04-23).

# 11

# Appendices

# Contents


A Extract from the FSG-rule book . . . . . II
B Morphological Matrix, Transmission . . . . . III
C Elimination Matrix Accessories . . . . . IV
D Pugh matrix, Transmission . . . . . V
E Kesselring Matrix Transmission . . . . . VI
F Elimination Matrix Total . . . . . VII
G Pugh Matrix Total . . . . . VIII
H Data_analysis_FSAC_Autocross_2021_03_23.m . . . . . IX
I Load spectrum For Transmission . . . . . XVIII
J Tooth root stress for the sun in KISSsoft . . . . . XIX
K Hertzian stress between the sun and planets in KISSsoft . . . . . XX
L Calibration of Angle Sensor Data . . . . . XXI
L.1 Interpretation of Angle Sensor Data . . . . . XXI
L.2 Data Formating . . . . . XXIII
L.3 Translating Sensor Angles to Resulting Forces . . . . . XXVI
M Bearings.m . . . . . XXVIII
N a_SKF_calculation.m . . . . . XXXV

## A. Extract from the FSG-rule book

- T 7.3.3 - “Scatter shields for high-speed rotating final drivetrain parts (such as electric motors, clutches, sprockets, gears etc.) that have an OEM casing that do not comply with T 7.3.2 may be used, if material is added to achieve the minimum required thickness.” [9]
- T 7.3.2 “Exposed rotating final drivetrain parts, chains and belts must be fitted with scatter shields. Scatter shields and their mountings must:
  - Cover chains and belts from the drive sprocket to the driven sprocket/chain wheel/belt or pulley.
  - Start and end parallel to the lowest point of the driven sprocket/chain wheel/belt or pulley.
  - Be constructed of non-perforated 2 mm steel or 3 mm aluminum alloy 6061-T6.” [9]
- T 7.2.4 “Any cooling or lubrication system must be sealed to prevent leakage” [9]. The biggest known tilt is during scrutineering, 60°.

# B. Morphological Matrix, Transmission

## Morphological Matrix

Sub function solution

| | Sub Function | A | B | C | D | E | F | G | H | I | J |
|---|---|---|---|---|---|---|---|---|---|---|---|
| 1. | Transmisson Layout | 1-Stage Planetary w. Locked Ring | 1-Stage Planetary w. Locked Carrier | 1-Stage Overlap Planetary w. Locked Ring | 1-Stage Overlap Planetary w. Locked Carrier | Compound Planetary w. Locked Inner Ring | Compound Planetary (CFS 19/20) | Compound Planetary w. Locked Carrier | 1 Stage Planetary w. Locked Ring + Conventional Gear Reduction | Excentric Internal Gear Set | Conventional Gear Set |
| 2. | Torque Transfer Output | Shaft | Housing | | | | | | | | |
| 3. | Mounting Brake Disc | Output Transmission | Housing | | | | | | | | |
| 4. | Mounting Brake Caliper | Upright | Housing | | | | | | | | |
| 5. | Upright | Separate From | Included in Housing | | | | | | | | |

-AB No need to have rotating housings and conventional rims
-BA Not centerless and brake on conventional output
-AC Contradiction

### Transmission

| Nr | Solutions | Explaination |
|---|---|---|
| 1 | AAA | 1-stage planetary w. locked ring in a stationary housing with torque transfer via output shaft. The brake disc is mounted on the transmission output shaft. |
| 2 | ABB | 1-stage planetary w. locked ring in a rotating housing with torque transfer via housing. The brake disc is mounted on the housing. |
| 3 | BAA | 1-stage planetary w. locked carrier in a stationary housing with torque transfer via output shaft. The brake disc is mounted on the transmission output shaft. |
| 4 | BBB | 1-stage planetary w. locked carrier in a rotating housing with torque transfer via housing. The brake disc is mounted on the housing. |
| 5 | CAA | 1-stage overlap planetary w. locked ring in a stationary housing with torque transfer via output shaft. The brake disc is mounted on the transmission output shaft. |
| 6 | CBB | 1-stage overlap planetary w. locked ring in a rotating housing with torque transfer via housing. The brake disc is mounted on the housing. |
| 7 | DAA | 1-stage overlap planetary w. locked carrier in a stationary housing with torque transfer via output shaft. The brake disc is mounted on the transmission output shaft. |
| 8 | DBB | 1-stage overlap planetary w. locked carrier in a rotating housing with torque transfer via housing. The brake disc is mounted on the housing. |
| 9 | EAA | Compound planetary w. locked inner ring in a stationary housing with torque transfer via output shaft. The brake disc is mounted on the transmission output shaft. |
| 10 | EBB | Compound planetary w. locked inner ring in a rotating housing with torque transfer via housing. The brake disc is mounted on the housing. |
| 11 | FAA | Compound planetary in a stationary housing with torque transfer via output shaft. The brake disc is mounted on the transmission output shaft. |
| 12 | FBB | Compound planetary in a rotating housing with torque transfer via housing. The brake disc is mounted on the housing. (CFS21) |
| 13 | GAA | Compound planetary w. locked carrier in a stationary housing with torque transfer via output shaft. The brake disc is mounted on the transmission output shaft. |
| 14 | GBB | Compound planetary w. locked carrier in a rotating housing with torque transfer via housing. The brake disc is mounted on the housing. |
| 15 | HAA | 1-stage planetary w. locked ring + conventional gear reduction in a stationary housing with torque transfer via output shaft. The brake disc is mounted on the transmission output shaft. |
| 16 | HBB | 1-stage planetary w. locked ring + conventional gear reduction in a rotating housing with torque transfer via housing. The brake disc is mounted on the housing. |
| 17 | IBB | Excentric gear powering an excentric ring gear in a rotating housing with torque transfer via housing. The brake disc is mounted on the housing. |
| 18 | JAA | Conventional gears in a stationary housing with torque transfer via output shaft. The brake disc is mounted on the transmission output shaft. |

### Transmission + Accessories

| Nr | Solutions | Explaination |
|---|---|---|
| 1.1 | AAAAA | AAA + brake caliper mounted on upright. The upright is seperate from housing. |
| 1.2 | AAAAB | AAA + brake caliper mounted on upright. The upright is included in housing. |
| 1.3 | AAABA | AAA + brake caliper mounted on housing. The upright is seperate from housing. |
| 1.4 | AAABB | AAA + brake caliper mounted on housing. The upright is included in housing. |
| 12.1 | FBBAA | FBB + brake caliper mounted on upright. The upright is seperate from housing. (CFS21) |
| 12.2 | FBBAB | FBB + brake caliper mounted on upright. The upright is included in housing. |
| 12.3 | FBBBA | FBB + brake caliper mounted on housing. The upright is seperate from housing. |
| 12.4 | FBBBB | FBB + brake caliper mounted on housing. The upright is included in housing. |

## C. Elimination Matrix Accessories

| Chalmers | Elimination matrix for: Transmission Assembly | | | | | | | | | | | | | | | | | | | | | | | | | | | | | | |
|---|---|---|---|---|---|---|---|---|---|---|---|---|---|---|---|---|---|---|---|---|---|---|---|---|---|---|---|---|---|---|---|
| Made by: | Emil Alexsson & Carl Lund | | | | | | | | | | | | | | | | | | | | | | | | | | | | Created: 21-02-18<br>Modifierad: | | Sid 1 |
| | | | | | | | | | | | | | | | | | | | | | | | | | | | | | + Yes<br>- No | | + Keep Solution<br>- Eliminate solution |
| Concept | Elimination criteria | | | | | | | | | | | | | | | | | | | | | | | | | | | | Comment | | DECISION |
| | Requirement 1.1 Gear Ratio 11:1 - 12:1 | Requirement 2.1 Water Proof | Requirement 2.2 Temperature Intervall | Requirement 2.3 Debris | Requirement 3.1 Radial Space | Requirement 3.2 Axial Space | Requirement 5.1 Brake Disc | Requirement 5.2 Brake Caliper | Requirement 5.3 Upright | Requirement 6.1 Rotating Assembly Protection | Requirement 6.2 Sealed Lubrication | Requirement 7.1 Housing | Requirement 8.1 Budget | Requirement 9.1 Service Interval | Requirement 10.2 Housing | Requirement 10.3 Gear Set | Requirement 10.1 Housing | | | | | | | | | | | | | |
| 1.1 | + | + | + | + | + | + | + | + | + | + | + | + | + | + | + | + | + | | | | | | | | | | | | | + |
| 1.2 | + | + | + | + | + | + | + | + | + | + | + | + | + | + | + | + | + | | | | | | | | | | | | | + |
| 1.3 | + | + | + | + | + | + | + | + | + | + | + | + | + | + | + | + | + | | | | | | | | | | | | | + |
| 1.4 | + | + | + | + | + | + | + | + | + | + | + | + | + | + | + | + | + | | | | | | | | | | | | | + |
| 12.1 | + | + | + | + | + | + | + | + | + | + | + | + | + | + | + | + | + | | | | | | | | | | | | | + |
| 12.2 | + | + | + | + | + | + | + | + | + | + | + | + | + | + | + | + | + | | | | | | | | | | | | | + |
| 12.3 | + | + | + | + | + | + | + | - | | | | | | | | | | | | | | | | | | | | | Caliper on Rotating Housing | | - |
| 12.4 | + | + | + | + | + | + | + | - | | | | | | | | | | | | | | | | | | | | | Caliper on Rotating Housing | | - |

# D. Pugh matrix, Transmission

**Pugh-Matrix First Iteration (Reference: CFS21 solution)**

| Criterias | Alternatives | | | | | | | | | | | | | |
|---|---|---|---|---|---|---|---|---|---|---|---|---|---|---|
| | 1 | 2 | 5 | 6 | 7 | 8 | 9 | 10 | 11 | 12 | 13 | 14 | 16 | 18 |
| Housing Simplicity | + | 0 | + | 0 | - | + | - | - | 0 | REFERENCE | - | - | 0 | 0 |
| Housing Axial Thickness | + | + | + | + | + | + | 0 | 0 | 0 | | 0 | 0 | - | - |
| Cylindrical and Concentric Shape | 0 | 0 | 0 | 0 | 0 | 0 | 0 | 0 | 0 | | 0 | 0 | - | - |
| Manufacturability In Chalmers Course Lab | 0 | 0 | 0 | 0 | 0 | 0 | 0 | 0 | 0 | | 0 | 0 | 0 | 0 |
| ∑ + | 2 | 1 | 2 | 1 | 1 | 2 | 0 | 0 | 0 | 0 | 0 | 0 | 0 | 0 |
| ∑ 0 | 2 | 3 | 2 | 3 | 2 | 2 | 3 | 3 | 4 | 0 | 3 | 3 | 2 | 2 |
| ∑ - | 0 | 0 | 0 | 0 | 1 | 0 | 1 | 1 | 0 | 0 | 1 | 1 | 2 | 2 |
| Netto | 2 | 1 | 2 | 1 | 0 | 2 | -1 | -1 | 0 | 0 | -1 | -1 | -2 | -2 |
| Rank | 1 | 2 | 1 | 2 | 3 | 1 | 4 | 4 | 3 | 3 | 4 | 4 | 5 | 5 |
| **Further Development** | Y | Y | Y | Y | Y | Y | Y | Y | Y | Y | Y | Y | N | N |

More complex bearing solution than reference

Non-concentrical stationary housing with a rotating cylindrical housing

**Motivation:**

| |
|---|
| Housing Simplicity - Easier to optimize the weight of a simple house and that the probability of realizable concept increases with reduced complexity. It is more important that the concept can result in a solution than that it is a light theoretical solution that is not realizable in reality. |
| Gear Simplicity/N.O. Gears -The gears will "probably" be made of steel, so it is important to keep down its size and number |

**Pugh-Matrix Second Iteration (Reference: 1)**

| Criterias | Alternatives | | | | | | | | | | | |
|---|---|---|---|---|---|---|---|---|---|---|---|---|
| | 1 | 2 | 5 | 6 | 7 | 8 | 9 | 10 | 11 | 12 | 13 | 14 |
| Housing Simplicity | REFERENCE | - | 0 | - | - | 0 | 0 | - | - | 0 | - | - |
| Housing Axial Thickness | | 0 | 0 | 0 | 0 | 0 | - | - | - | - | - | - |
| Cylindrical and Concentric Shape | | 0 | 0 | 0 | 0 | 0 | 0 | 0 | 0 | 0 | 0 | 0 |
| Manufacturability In Chalmers Course Lab | | 0 | 0 | 0 | 0 | 0 | 0 | 0 | 0 | 0 | 0 | 0 |
| ∑ + | 0 | 0 | 0 | 0 | 0 | 0 | 0 | 0 | 0 | 0 | 0 | 0 |
| ∑ 0 | 0 | 3 | 4 | 3 | 3 | 4 | 3 | 2 | 2 | 3 | 2 | 2 |
| ∑ - | 0 | 1 | 0 | 1 | 1 | 0 | 1 | 2 | 2 | 1 | 2 | 2 |
| Netto | 0 | -1 | 0 | -1 | -1 | 0 | -1 | -2 | -2 | -1 | -2 | -2 |
| Rank | 1 | 2 | 1 | 2 | 2 | 1 | 2 | 3 | 3 | 2 | 3 | 3 |
| **Further Development** | Y | Y | Y | Y | Y | Y | Y | N | N | Y | N | N |

## E. Kesselring Matrix Transmission

# Kesselring Matrix Transmission

| Gear Simplicity | |
|---|---|
| Est. N.O Gears | Value |
| x > 9 | 1 |
| 7 < x <= 9 | 2 |
| 5 < x <= 7 | 3 |
| 2 < x <= 5 | 4 |
| x <= 2 | 5 |

| Axial Thickness | |
|---|---|
| mm | Value |
| x > 150 | 1 |
| 110 < x <= 150 | 2 |
| 80 < x <= 110 | 3 |
| 50 < x <= 80 | 4 |
| < 50 | 5 |

| Manufacturability | |
|---|---|
| Estimation | Värde |
| a | 1 |
| b | 2 |
| c | 3 |
| d | 4 |
| e | 5 |

| Housing Simplicity | |
|---|---|
| Est. (Bearings, Rotating Parts) | Value |
| Very Complex | 1 |
| Complex | 2 |
| Neutral | 3 |
| Simple | 4 |
| Very Simple | 5 |

| Space Effiency | |
|---|---|
| Shape | Value |
| Assymetrical | 1 |
| Symmetrical | 2 |
| Concentric | 3 |
| Circular | 4 |
| Circ + Conc | 5 |

| | A | B | C | D | E | SUMMA | SUMMA_REL |
|---|---|---|---|---|---|---|---|
| A (Gear Simplicity) | - | 0,5 | 1 | 1 | 1 | 3,5 | 1,17 |
| B (Housing Simplicity) | 0.5 | - | 1 | 1 | 1 | 3 | 1 |
| C (Housing Axial Thickness) | 0 | 0 | - | 1 | 0 | 1 | 0,33 |
| D (Space Efficiency) | 0 | 0 | 0 | - | 1 | 1 | 0,33 |
| E (Manufacturability at Chalmers CL) | 0 | 0 | 1 | 0 | - | 1 | 0,33 |

| Chalmers | | Kesselring-Matrix | | | | | | | | | | | | | | | | | |
|---|---|---|---|---|---|---|---|---|---|---|---|---|---|---|---|---|---|---|---|
| | | | | Created: 2021-02-17 | | | | | | | | | | | | | | | |
| Criterias | | Concepts | | | | | | | | | | | | | | | | | |
| | | Ideal | | 1 | | 2 | | 5 | | 6 | | 7 | | 8 | | 9 | | 12 | |
| | w | v | t | v | t | v | t | v | t | v | t | v | t | v | t | v | t | v | t |
| A (Gear Simplicity) | 1,17 | 5 | 5,833333333 | 4 | 4,66667 | 4 | 4,666666667 | 3 | 3,5 | 3 | 3,5 | 3 | 3,5 | 3 | 3,5 | 3 | 3,5 | 4 | 4,66667 |
| B (Housing Simplicity) | 1 | 5 | 5 | 5 | 5 | 3 | 3 | 5 | 5 | 3 | 3 | 2 | 2 | 3 | 3 | 4 | 4 | 4 | 4 |
| C (Housing Axial Thickness) | 0,33 | 5 | 1,666666667 | 4 | 1,33333 | 4 | 1,333333333 | 4 | 1,33333 | 4 | 1,33333 | 4 | 1,33333 | 4 | 1,33333 | 3 | 1 | 3 | 1 |
| D (Space Efficiency) | 0,33 | 5 | 1,666666667 | 5 | 1,66667 | 5 | 1,666666667 | 5 | 1,66667 | 5 | 1,66667 | 5 | 1,66667 | 5 | 1,66667 | 5 | 1,66667 | 5 | 1,66667 |
| E (Manufacturability at Chalmers CL) | 1 | 5 | 5 | 4 | 4 | 4 | 4 | 4 | 4 | 4 | 4 | 4 | 4 | 4 | 4 | 4 | 4 | 4 | 4 |
| *T (Total Weighted Value)* | | 19,16666667 | | 16,66666667 | | 14,66666667 | | 15,5 | | 13,5 | | 12,5 | | 13,5 | | 14,16666667 | | 15,33333333 | |
| *T / T ideal* | | 1,00 | | 0,87 | | 0,77 | | 0,81 | | 0,70 | | 0,65 | | 0,70 | | 0,74 | | 0,80 | |
| Rank | | | | 1 | | 4 | | 2 | | 6 | | 7 | | 6 | | 5 | | 3 | |
| Decision | | Further Development With Concept 1 & 12 | | | | | | | | | | | | | | | | | |

# F. Elimination Matrix Total

| Chalmers | Elimination matrix for: Transmission Assembly | | | | | | | | | | | | | | | | | | | | | | | | | | | | | | |
|---|---|---|---|---|---|---|---|---|---|---|---|---|---|---|---|---|---|---|---|---|---|---|---|---|---|---|---|---|---|---|---|
| Made by: | Emil Alexsson & Carl Lund | | | | | | | | | | | | | | | | | | | | | | | | | | | | Created: 21-02-18<br>Modifierad: | | Sid 1 |
| | | | | | | | | | | | | | | | | | | | | | | | | | | | | | + Yes<br>- No | | + Keep Solution<br>- Eliminate solution |
| Concept | Elimination criteria | | | | | | | | | | | | | | | | | | | | | | | | | | | | Comment | | DECISION |
| | Requirement 1.1 Gear Ratio 11:1 - 12:1 | Requirement 2.1 Water Proof | Requirement 2.2 Temperature Intervall | Requirement 2.3 Debris | Requirement 3.1 Radial Space | Requirement 3.2 Axial Space | Requirement 5.1 Brake Disc | Requirement 5.2 Brake Caliper | Requirement 5.3 Upright | Requirement 6.1 Rotating Assembly Protection | Requirement 6.2 Sealed Lubrication | Requirement 7.1 Housing | Requirement 8.1 Budget | Requirement 9.1 Service Interval | Requirement 10.2 Housing | Requirement 10.3 Gear Set | Requirement 10.1 Housing | | | | | | | | | | | | | |
| 1.1 | + | + | + | + | + | + | + | + | + | + | + | + | + | + | + | + | + | | | | | | | | | | | | | + |
| 1.2 | + | + | + | + | + | + | + | + | + | + | + | + | + | + | + | + | + | | | | | | | | | | | | | + |
| 1.3 | + | + | + | + | + | + | + | + | + | + | + | + | + | + | + | + | + | | | | | | | | | | | | | + |
| 1.4 | + | + | + | + | + | + | + | + | + | + | + | + | + | + | + | + | + | | | | | | | | | | | | | + |
| 12.1 | + | + | + | + | + | + | + | + | + | + | + | + | + | + | + | + | + | | | | | | | | | | | | | + |
| 12.2 | + | + | + | + | + | + | + | + | + | + | + | + | + | + | + | + | + | | | | | | | | | | | | | + |
| 12.3 | + | + | + | + | + | + | + | - | | | | | | | | | | | | | | | | | | | | | Caliper on Rotating Housing | | - |
| 12.4 | + | + | + | + | + | + | + | - | | | | | | | | | | | | | | | | | | | | | Caliper on Rotating Housing | | - |

## G. Pugh Matrix Total

**Pugh-Matrix**

| Criterias | Alternatives | | | | | | |
|---|---|---|---|---|---|---|---|
| | 1.1 | 1.2 | 1.3 | 1.4 | | 12.1 | 12.2 |
| Simplicity | REFERENS | 0 | + | 0 | | REFERENS | 0 |
| Axial Thickness | | 0 | 0 | 0 | | | 0 |
| Radial Size | | 0 | 0 | 0 | | | 0 |
| Manufacturability In Chalmers Course Lab | | - | 0 | - | | | - |
| ∑ + | 0 | 0 | 0 | 0 | | 0 | 0 |
| ∑ 0 | 3 | 3 | 0 | 3 | | 0 | 3 |
| ∑ - | 1 | 1 | 0 | 1 | | 0 | 1 |
| Netto | -1 | -1 | 0 | -1 | | 0 | -1 |
| Rank | 2 | 2 | 1 | 2 | | 1 | 2 |
| **Further Development** | N | N | Y | N | | Y | N |

## H. Data_analysis_FSAC_Autocross_2021_03_23.m

```
%% Preamble
%Processing of data from CFS 19 tests for generating loadcases ... to dimension
%a gearbox for CFS 22
%Erik Henrikson 2021-02-16
%Updated 2021-03-23

%% Load all
data = load('FSAC_Autocross_1.mat');

%% Create matrices

%Speed
RR_Speed = ... data.runs.logfile20191024143952.fullRun.PE_RR_Speed_Estimate_37;%-
RL_Speed = ... data.runs.logfile20191024143952.fullRun.PE_RL_Speed_Estimate_41;
FR_Speed = ... data.runs.logfile20191024143952.fullRun.PE_FR_Speed_Estimate_45;%-
FL_Speed = ... data.runs.logfile20191024143952.fullRun.PE_FL_Speed_Estimate_49;

%Torque
RR_Torque = ... data.runs.logfile20191024143952.fullRun.PE_RR_Torque_Estimate_37;%-
RL_Torque = ... data.runs.logfile20191024143952.fullRun.PE_RL_Torque_Estimate_41;
FR_Torque = ... data.runs.logfile20191024143952.fullRun.PE_FR_Torque_Estimate_45;%-
FL_Torque = ... data.runs.logfile20191024143952.fullRun.PE_FL_Torque_Estimate_49;

%GPS
GPSx = data.runs.logfile20191024143952.fullRun.FN_GPS_xPos_65;
GPSy = data.runs.logfile20191024143952.fullRun.FN_GPS_yPos_65;

%fixing sign errors
RR_Speed(:,1) = -RR_Speed(:,1);
FR_Speed(:,1) = -FR_Speed(:,1);
RR_Torque(:,1) = -RR_Torque(:,1);
FR_Torque(:,1) = -FR_Torque(:,1);

%% Analyse sample rates
SampleRates = zeros(8,1); %length = number of channels analysed

SampleRates(1) = mean(diff(RR_Speed(:,2)))^-1;
SampleRates(2) = mean(diff(RL_Speed(:,2)))^-1;
SampleRates(3) = mean(diff(FR_Speed(:,2)))^-1;
SampleRates(4) = mean(diff(FL_Speed(:,2)))^-1;
SampleRates(5) = mean(diff(RR_Torque(:,2)))^-1;
SampleRates(6) = mean(diff(RL_Torque(:,2)))^-1;
SampleRates(7) = mean(diff(FR_Torque(:,2)))^-1;
```

```
44 SampleRates(8) = mean(diff(FL_Torque(:,2)))^-1;
45
46 SampleRates %To manually check that sample rates are (virtually) ...
       the same
47
48 SampleRate = mean(SampleRates); %assume this sample rate for all
49
50 %% Cutoff
51
52 %Find length of shortest vector
53 newLength = min([
54     length(RR_Speed);
55     length(RL_Speed);
56     length(FR_Speed);
57     length(FL_Speed);
58     length(RR_Torque);
59     length(RL_Torque);
60     length(FR_Torque);
61     length(FL_Torque)
62     ]);
63
64 %cut vectors to match the shortest
65 RR_Speed = RR_Speed(1:newLength,:);
66 RL_Speed = RL_Speed(1:newLength,:);
67 FR_Speed = FR_Speed(1:newLength,:);
68 FL_Speed = FL_Speed(1:newLength,:);
69 RR_Torque = RR_Torque(1:newLength,:);
70 RL_Torque = RL_Torque(1:newLength,:);
71 FR_Torque = FR_Torque(1:newLength,:);
72 FL_Torque = FL_Torque(1:newLength,:);
73
74 %Write start times to CW to manually check that they start ...
       roughly at the
75 %same time
76 StartTimes = [
77     RR_Speed(1,2)
78     RL_Speed(1,2)
79     FR_Speed(1,2)
80     FL_Speed(1,2)
81     RR_Torque(1,2)
82     RL_Torque(1,2)
83     FR_Torque(1,2)
84     FL_Torque(1,2)
85 ]
86 %% Filter
87
88 Fpass = 0.05; %Pass frequency
89
90 %Speed
91 RR_Speed_Smooth = lowpass(RR_Speed(:,1),Fpass,SampleRate);
92 RL_Speed_Smooth = lowpass(RL_Speed(:,1),Fpass,SampleRate);
93 FR_Speed_Smooth = lowpass(FR_Speed(:,1),Fpass,SampleRate);
94 FL_Speed_Smooth = lowpass(FL_Speed(:,1),Fpass,SampleRate);
95
96 %Torque
97 RR_Torque_Smooth = lowpass(RR_Torque(:,1),Fpass,SampleRate);
```

```
98  RL_Torque_Smooth = lowpass(RL_Torque(:,1),Fpass,SampleRate);
99  FR_Torque_Smooth = lowpass(FR_Torque(:,1),Fpass,SampleRate);
100 FL_Torque_Smooth = lowpass(FL_Torque(:,1),Fpass,SampleRate);
101
102 %GPS
103 GPSxy = [GPSx(:,1) GPSy];
104
105 % lat = deg2rad(50.791671);
106 % long = deg2rad(6.050551);
107 % xref = 4017509; %[m]
108 % yref = 425841; %[m]
109 % fixGPS = @(xy) [-sin(lat) cos(lat); -sin(long)*cos(lat) ...
      -sin(long)*sin(lat)]...
110 %     *[xy(1)-xref; xy(2)-yref];
111 %
112 % GPSfixed = zeros(numel(GPSx(:,1)),2);
113 % for i = 1:numel(GPSx(:,1))
114 %     GPSfixed(i,:) = fixGPS(GPSxy(i,1:2));
115 % end
116
117 %move origin
118 GPSx_zero = GPSx(:,1)+12790*ones(size(GPSx(:,1)));
119 GPSy_zero = GPSy(:,1)+145*ones(size(GPSy(:,1)));
120 %plot(GPSx_zero,GPSy_zero(:,1))
121
122 GPSxy_zero = [GPSx_zero GPSy_zero GPSx(:,2)]; %x,y,time
123
124 %Remove outliers, thresholds worked well for this data but may ...
      not work for
125 %all.
126 %-70<x<70
127 %-100<y<70
128 GPSxy_clean = GPSxy_zero;
129 GPS_points = length(GPSxy_zero(:,1)) + 1;
130 for i = 1:GPS_points-1
131     if (GPSxy_zero(GPS_points-i,1) < -70) || ...
          (GPSxy_zero(GPS_points-i,1) > 70) || ...
          (GPSxy_zero(GPS_points-i,2) < -100) || ...
          (GPSxy_zero(GPS_points-i,2) > 70)
132          GPSxy_clean(GPS_points-i,:) = [];
133     end
134 end
135
136 %% Distance, speed and animated plot
137 distance5Laps = sum(sqrt(diff(GPSxy_clean(:,1)).^2 + ...
      diff(GPSxy_clean(:,2)).^2));
138
139 time = diff(GPSxy_clean(:,3)); %time in seconds betwen each data ...
      point
140
141 GPSspeed = sqrt(diff(GPSxy_clean(:,1)).^2 + ...
      diff(GPSxy_clean(:,2)).^2)./time; %average velocity between ...
      points
142
143 GPSspeed(GPSspeed>50) = 50;
144
```

```
GPSspeed_Smooth = movmean(GPSspeed,3);

speedometer = [-cos(GPSspeed_Smooth./50.*pi) ...
    sin(GPSspeed_Smooth./50.*pi)];

trackGraph = 0; % =1 to plot the movement of the car on the track

playBackSpeed = 100; %playback speed in %

%plot
if trackGraph == 1
figure()
plot(GPSxy_clean(:,1),GPSxy_clean(:,2))
axis equal
title('Track From GPS-data')
xlabel('[m]')
ylabel('[m]','Rotation',0)
xlim([-40 100])
ylim([-80 60])
hold on
car = plot(GPSxy_clean(1,1),GPSxy_clean(1,2),'or');
text(40,43,['(of ' num2str(GPSxy_clean(end,3)) ' s)'])
text(40,36,['Playback Speed: ' num2str(playBackSpeed) '%'])
timeText = text(40,50,'Time: 0s');
carSpeed = text(40,29,'Vehicle Speed: 00.0 km/h');
needle = plot([60 50],[0 0],'-r','LineWidth',3);
% text(50,0,'0')
% text(60,10,'90')
% text(70,0,'180')
text([46 60-14*cosd(10) 60-14*cosd(30) 60-14*cosd(50) ...
    60-14*cosd(70) 60 60-14*cosd(110) 74 60],[0 14*sind(10) ...
    14*sind(30) 14*sind(50) 14*sind(70) 14 14*sind(110) 0 ...
    -5],{'0','10','30','50','70','90','110','180','km/h'}, ...
'HorizontalAlignment','center')
velocityTicks = [0 10 30 50 70 90 110 180];
plot(60-11*cosd(velocityTicks),11*sind(velocityTicks),'.k')
for i = 500:length(GPSxy_clean(:,1))
    car.XData = GPSxy_clean(i,1);
    car.YData = GPSxy_clean(i,2);
    needle.XData = [60+10*speedometer(i-1,1) 60];
    needle.YData = [10*speedometer(i-1,2) 0];
    pause(time(i-1)/(playBackSpeed/100))
    timeText.String = ['Time: ' num2str(GPSxy_clean(i,3)) ' s'];
    carSpeed.String = ['Vehicle Speed: ' ...
        num2str(GPSspeed_Smooth(i-1)*3.6,'%04.1f') ' km/h'];
end
end

%Time driving
timeDriving = sum(time(find(GPSspeed≠0))); %[s]

%Scaled to 1500km
totalTimeDrivingHours = timeDriving*(1500e3/distance5Laps)/3600; ...
    %[h]

%% Plot
```

```
195
196 %plot(RR_Torque(:,2),RR_Torque(:,1),'.r')
197 % hold on
198 %plot(RR_Torque(:,2),RR_Torque_Smooth)
199 % plot(RL_Torque(:,2),RL_Torque_Smooth)
200 % plot(FR_Torque(:,2),FR_Torque_Smooth)
201 % plot(FL_Torque(:,2),FL_Torque_Smooth)
202
203 %plot(RR_Speed(:,2),RR_Speed_Smooth/max(RR_Speed_Smooth),'.b')
204 % hold on
205 % plot(RR_Torque(:,2),RR_Torque_Smooth/max(RR_Torque_Smooth),'.r')
206
207 %Plot xy
208 %plot(GPSx,GPSy,'.r')
209 % plot(GPSxy(:,1),GPSxy(:,2))
210 % axis equal
211 % GPSxy_clean = rmoutliers(GPSxy(:,1:2));
212 % figure()
213 % plot(GPSxy_clean(:,1),GPSxy_clean(:,2))
214 % axis equal
215
216
217
218
219 %% Method from Niklas Dahlstrand (not used)
220
221 n_data_points = 10; %Number of rows to be imported to KISSsoft
222
223 duration = (RR_Speed(end,2) - RR_Speed(1,2))/n_data_points;
224
225 indices = round(linspace(1,newLength,n_data_points + 1));
226
227 FreqTorqSpee = zeros(n_data_points,3);
228
229 for i = 1:n_data_points
230     FreqTorqSpee(i,1) = RR_Speed(indices(i+1),2) - ...
           RR_Speed(indices(i),2);
231     FreqTorqSpee(i,2) = max([
232         mean(RR_Torque_Smooth(indices(i):indices(i+1)));
233         mean(RL_Torque_Smooth(indices(i):indices(i+1)));
234         mean(FR_Torque_Smooth(indices(i):indices(i+1)));
235         mean(FL_Torque_Smooth(indices(i):indices(i+1)))
236         ]);
237     FreqTorqSpee(i,3) = max([
238         mean(RR_Speed_Smooth(indices(i):indices(i+1)));
239         mean(RL_Speed_Smooth(indices(i):indices(i+1)));
240         mean(FR_Speed_Smooth(indices(i):indices(i+1)));
241         mean(FL_Speed_Smooth(indices(i):indices(i+1)));
242         ]);
243 end
244
245 %Normalise
246 FreqTorqSpee(:,1) = ...
       FreqTorqSpee(:,1)/sum(FreqTorqSpee(:,1))*100; %sum=100%
247 FreqTorqSpee(:,2) = FreqTorqSpee(:,2)/max(FreqTorqSpee(:,2)); ...
       %highest value=1
```

```
248 FreqTorqSpee(:,3) = FreqTorqSpee(:,3)/max(FreqTorqSpee(:,3)); ...
        %highest value=1
249
250 %% Max values
251
252 maxTorque = zeros(numel(RR_Torque_Smooth,1));
253 maxSpeed = maxTorque;
254 for i = 1:numel(RR_Torque_Smooth)
255     [¬,maxTorque_index] = max(abs([
256     RR_Torque_Smooth(i);
257     RL_Torque_Smooth(i);
258     FR_Torque_Smooth(i);
259     FL_Torque_Smooth(i);
260     ]));
261     switch maxTorque_index
262         case 1
263             maxTorque(i) = RR_Torque_Smooth(i);
264         case 2
265             maxTorque(i) = RL_Torque_Smooth(i);
266         case 3
267             maxTorque(i) = FR_Torque_Smooth(i);
268         case 4
269             maxTorque(i) = FL_Torque_Smooth(i);
270     end
271     [¬,maxSpeed_index] = max(abs([
272     RR_Speed_Smooth(i);
273     RL_Speed_Smooth(i);
274     FR_Speed_Smooth(i);
275     FL_Speed_Smooth(i);
276     ]));
277     switch maxSpeed_index
278         case 1
279             maxSpeed(i) = RR_Speed_Smooth(i);
280         case 2
281             maxSpeed(i) = RL_Speed_Smooth(i);
282         case 3
283             maxSpeed(i) = FR_Speed_Smooth(i);
284         case 4
285             maxSpeed(i) = FL_Speed_Smooth(i);
286     end
287 end
288
289
290 %% cut out the data points from when the vehicle is stationary
291 cutoffTorque = 0.09; %[Nm]
292 cutoffSpeed = 10; %[rpm]
293 cutoffIndices = 1; %to initiate
294 negativeTorqueCount = 0;
295 negTorqueSpeed = [];
296 for i = 1:numel(maxTorque)
297     if (maxTorque(i) < cutoffTorque) || (maxSpeed(i) < cutoffSpeed)
298         cutoffIndices = [cutoffIndices i];
299         if maxTorque(i) < -0.05
300             negativeTorqueCount = negativeTorqueCount + 1;
301             negTorqueSpeed = [negTorqueSpeed maxSpeed(i)];
302         end
```

```
303     end
304 end
305 cutoffIndices(1) = []; %to remove the initial value that was ...
       needed for the expression in the loop
306 maxTorque_cut = maxTorque;
307 maxTorque_cut(cutoffIndices) = [];
308 maxSpeed_cut = maxSpeed;
309 maxSpeed_cut(cutoffIndices) = [];
310 time_cut = RR_Torque(:,2);
311 time_cut(cutoffIndices) = [];
312
313 maxTorque_non0 = [];
314 maxSpeed_non0 = [];
315 n = numel(maxTorque);
316 for i = 1:n
317     if ((maxTorque(i) > cutoffTorque) && (maxSpeed(i) > ...
          cutoffSpeed)) || ((maxTorque(i) < -0.05))
318         maxTorque_non0 = [maxTorque_non0 maxTorque(i)];
319         maxSpeed_non0 = [maxSpeed_non0 maxSpeed(i)];
320     end
321 end
322
323 %plot the cutoff thresholds
324 %figure()
325 %plot(time_cut,maxTorque_cut,'.r')
326 % figure()
327 % plot(RR_Speed(:,2),RR_Speed_Smooth)
328 % title('Speed Cutoff')
329 % xlabel('Time [s]')
330 % ylabel('Speed [rpm]')
331 % hold on
332 % plot([RR_Speed(1,2) RR_Speed(end,2)],cutoffSpeed*[1 1])
333 % figure()
334 % plot(RR_Torque(:,2),RR_Torque_Smooth)
335 % title('Torque Cutoff')
336 % xlabel('Time [s]')
337 % ylabel('Speed [rpm]')
338 % hold on
339 % plot([RR_Torque(1,2) RR_Torque(end,2)],cutoffTorque*[1 1])
340
341 %% Method recommended by contacts from Volvo
342
343 %number of loadcases in torque- and speed dimension ...
       respectively, total
344 %number of loadcases will equal: torqueBins*speedBins ...
       (+1*speedBins if
345 %negative torques are added later)
346 torqueBins = 8;
347 speedBins = 4;
348
349 %no negative torques
350 %[frequency,torqueEdges,speedEdges] = ...
       histcounts2(maxTorque_cut,maxSpeed_cut,[torqueBins speedBins]);
351
352 %one bin for all negative values, positive values divided ...
       equally into
```

```
353 %bins. Useful if data contains only a few negative data points
354 torqueEdges = [min(maxTorque_non0) ...
       linspace(0,max(maxTorque_non0),torqueBins)];
355 speedEdges = ...
       linspace(min(maxSpeed_non0),max(maxSpeed_non0),speedBins+1);
356 [frequency,torqueEdges,speedEdges] = ...
357 histcounts2(maxTorque_non0,maxSpeed_non0,torqueEdges,speedEdges);
358
359 figure() %Plot the data, not needed for final result
360 histogram2(maxTorque_non0,maxSpeed_non0,torqueEdges,speedEdges, ...
361 'Normalization','probability');
362 xlabel('Torque [Nm]')%,'FontSize',14)
363 ylabel('Speed [RPM]')
364 zlabel('Frequency')
365 ax = gca;
366 ax.FontSize = 14;
367
368 volvoFreqTorqSpee = zeros(numel(frequency),3); %uniform ...
       intervals for torque and speed, frequency changed
369 volvoFreqTorqSpee(:,1) = reshape(frequency,numel(frequency),1);
370 volvoFreqTorqSpee(:,2) = repmat(torqueEdges(1:end-1) + ...
       diff(torqueEdges)./2,1,speedBins);
371 volvoFreqTorqSpee(:,3) = repelem(speedEdges(1:end-1) + ...
       diff(speedEdges)./2,1,torqueBins);
372
373 %Remove loadcases with frequency = 0
374 for i = 1:length(volvoFreqTorqSpee(:,1))
375     if volvoFreqTorqSpee(speedBins*torqueBins - i + 1,1) == 0
376         volvoFreqTorqSpee(speedBins*torqueBins - i + 1,:) = [];
377     end
378 end
379
380
381 %Normalise
382 volvoFreqTorqSpee(:,1) = ...
       volvoFreqTorqSpee(:,1)/sum(volvoFreqTorqSpee(:,1))*100; ...
       %sum=100%
383 volvoFreqTorqSpee(:,2) = ...
       volvoFreqTorqSpee(:,2)/max(volvoFreqTorqSpee(:,2)); %max = 1
384 volvoFreqTorqSpee(:,3) = ...
       volvoFreqTorqSpee(:,3)/max(volvoFreqTorqSpee(:,3)); %max = 1
385
386 % figure()
387 % subplot(1,2,1)
388 % %uncut
389 % histogram2(maxTorque,maxSpeed,[torqueBins speedBins])
390 % title('Uncut')
391 %
392 % subplot(1,2,2)
393 % %cut
394 % histogram2(maxTorque_cut,maxSpeed_cut,[torqueBins speedBins])
395 % title('Cut')
396
397 %% Write to CSV/xlsx
398
399 %writematrix(FreqTorqSpee,'loadcase_FSAC_Autocross.txt')
```

```
400 %csvwrite('loadcase_FSAC_Autocross.csv',FreqTorqSpee)
401
402 %might have to check decimal separator (,.) and file extension, ...
       appears to
403 %best be done in Microsoft Excel
404 loadCase_FSAC_Autocross = table(volvoFreqTorqSpee(:,1), ...
405 volvoFreqTorqSpee(:,2),volvoFreqTorqSpee(:,3),'VariableNames', ...
406 {'Frequency','Torque','Speed'});
407 writetable(loadCase_FSAC_Autocross, ...
408 'loadCase_FSAC_Autocross.xlsx','FileType','spreadsheet', ...
409 'WriteMode','replace','WriteVariableNames',0)
```

# I. Load spectrum For Transmission

| Frequency in % | Normated Torque | Normated Speed |
|---|---|---|
| 0,522755228 | -0,02323262 | 0,141897451 |
| 20,75645756 | 0,076923077 | 0,141897451 |
| 0,809758098 | 0,230769231 | 0,141897451 |
| 1,711767118 | 0,384615385 | 0,141897451 |
| 1,117261173 | 0,538461538 | 0,141897451 |
| 0,215252153 | 0,692307692 | 0,141897451 |
| 0,092250923 | 0,846153846 | 0,141897451 |
| 1,96801968 | -0,02323262 | 0,427931634 |
| 20,87945879 | 0,076923077 | 0,427931634 |
| 7,861828618 | 0,230769231 | 0,427931634 |
| 5,412054121 | 0,384615385 | 0,427931634 |
| 3,93603936 | 0,538461538 | 0,427931634 |
| 2,449774498 | 0,692307692 | 0,427931634 |
| 0,215252153 | 0,846153846 | 0,427931634 |
| 0,143501435 | 1 | 0,427931634 |
| 2,593275933 | -0,02323262 | 0,713965817 |
| 8,999589996 | 0,076923077 | 0,713965817 |
| 4,274292743 | 0,230769231 | 0,713965817 |
| 4,325543255 | 0,384615385 | 0,713965817 |
| 4,63304633 | 0,538461538 | 0,713965817 |
| 4,581795818 | 0,692307692 | 0,713965817 |
| 1,035260353 | 0,846153846 | 0,713965817 |
| 0,112751128 | 1 | 0,713965817 |
| 0,061500615 | 0,384615385 | 1 |
| 0,215252153 | 0,538461538 | 1 |
| 0,471504715 | 0,692307692 | 1 |
| 0,563755638 | 0,846153846 | 1 |
| 0,04100041 | 1 | 1 |

## J. Tooth root stress for the sun in KISSsoft

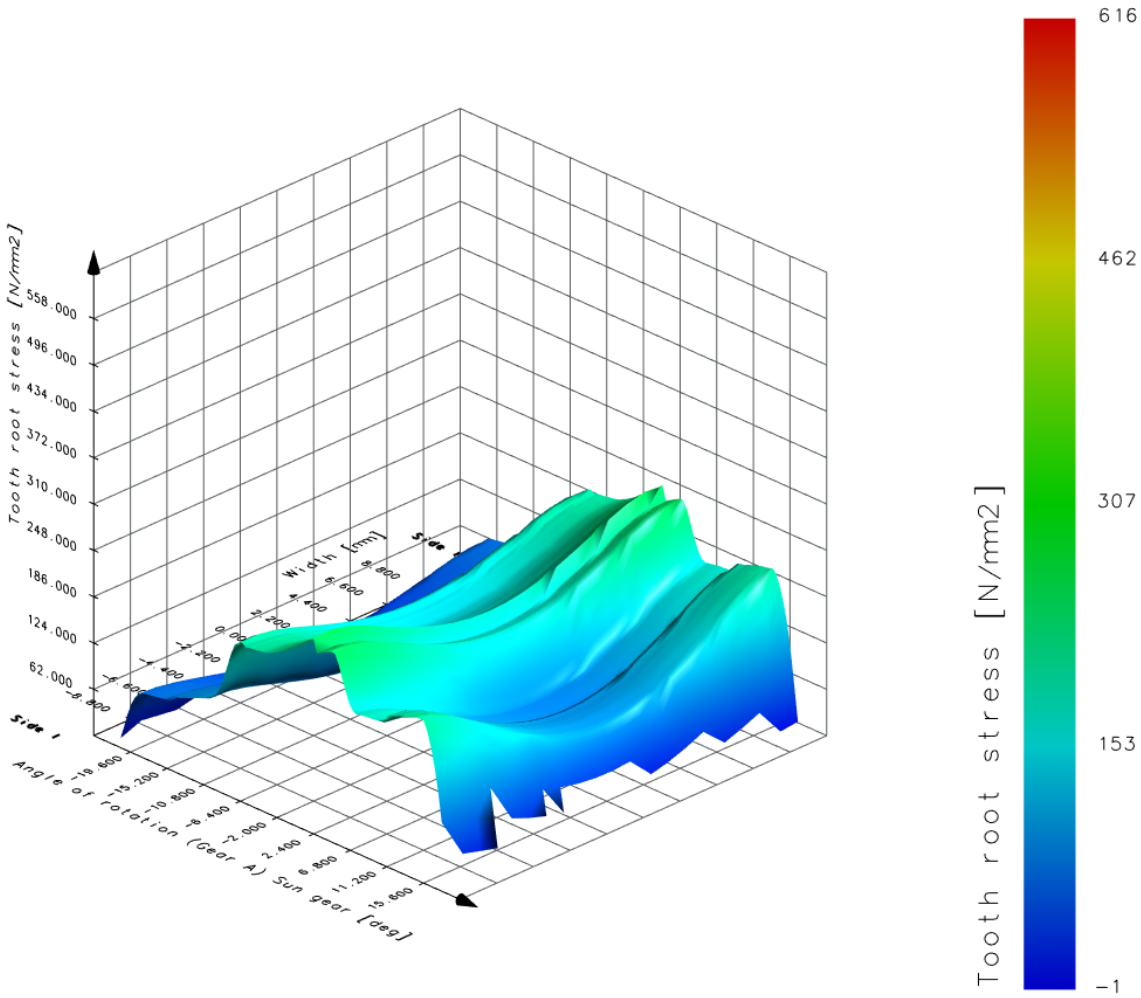

## K. Hertzian stress between the sun and planets in KISSsoft

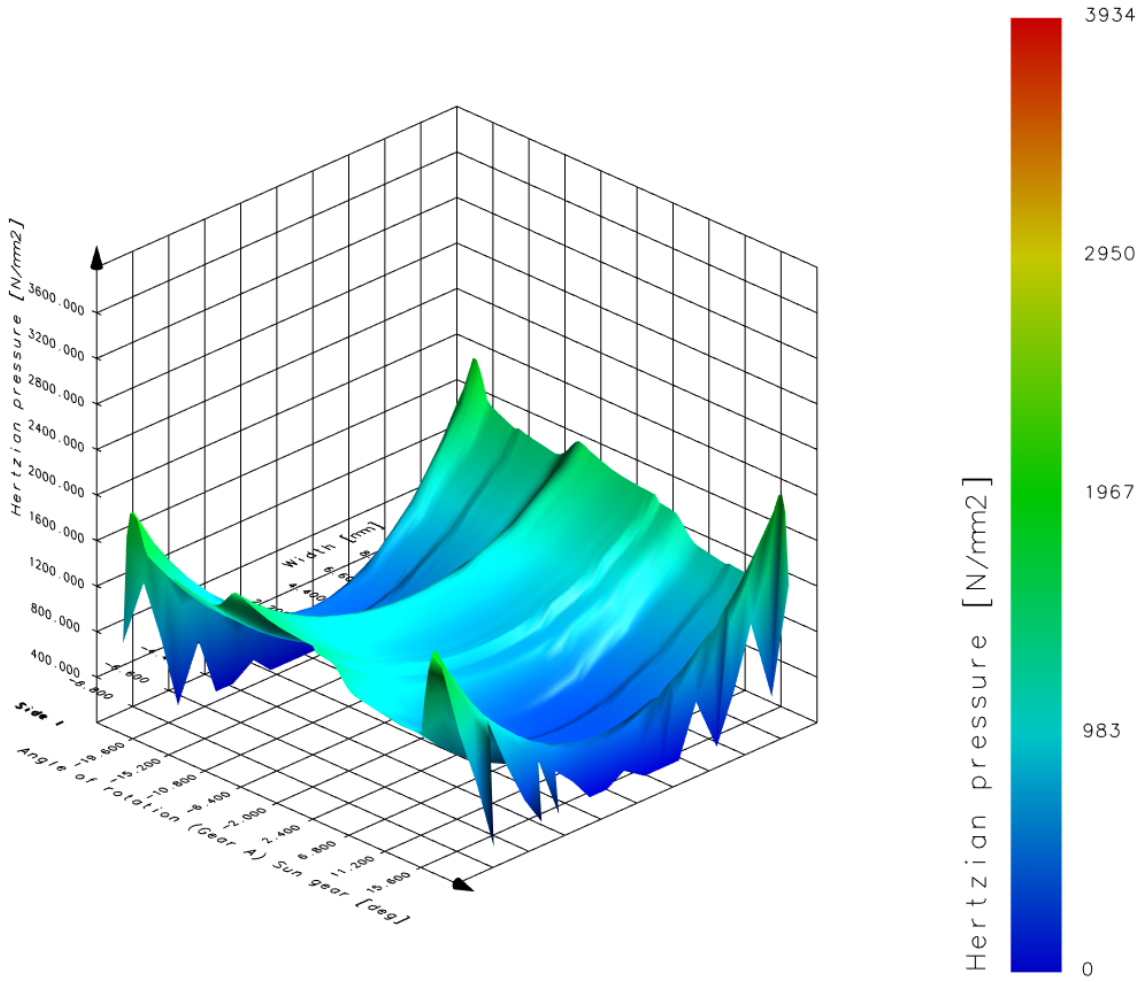

## L. Calibration of Angle Sensor Data

In order to define load cases for the gearbox housing and bearings, sensor data needed to be calibrated. This methodology deviated from the project purpose but was considered necessary.

## L.1 Interpretation of Angle Sensor Data

The data is logged in a .mdf format which was loaded with MATLAB-tools from CFS into a new script. When plotting the data from the angle sensors it is discovered that the data for the front left (FL) wheel is not continuous while the data from the front right (FR) wheel seems to be continuous, see Figure L.1. When compared with the video tape from the competition, the behaviour of the FR data log seems to correlate with the motion of the car. The data for the rear wheels behaves in a similar sense but with continuous data for the rear left (RL) wheel and non continuous data for the rear right (RR) wheel.

In order to understand what the data from the angle sensors represents, former CFS member Erik Lund is contacted. He worked in a group responsible for the low voltage-system in CFS19 that installed the sensors on Victoria. Erik Lund provided information about the specification of the angle sensor and explained what the amplitude of the logged data corresponded to.

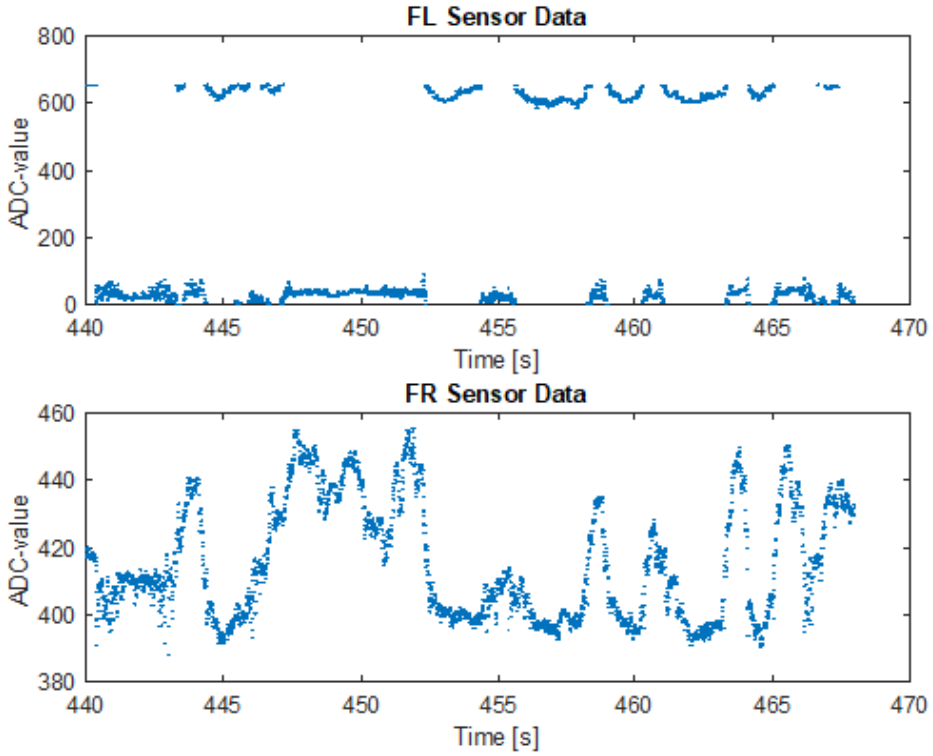


**Figure L.1:** ADC-values for both front pushrod pivot shaft angles

The angle sensors for all four wheels are of the model Novotechnik SP2831 308

000 001 which is a linear potentiometer measuring 308°of rotation. The sensor can rotate continuously 360°, which means that the sensor have 52°where it is out of range transmitting an unreliable signal. The output voltage of the sensor is between $\approx$ 0 - 5V and the internal resistance is $\approx$ 0-5k$\Omega$. The sensor have three terminals; terminal 1 (brown), terminal 2 (red) and terminal 3 (orange). Terminal 1 and 3 are reference terminals and terminal 2 is connected to the wiper which based on its position changes the resistance between it and the two reference terminals [22].

The y-axis on the plot with data from the angle sensors seen in Figure L.1 shows data that is processed by an Analog-to-Digital-Converter (ADC). The ADC converts the analog voltage signal from the angle sensor to a digital signal that can be processed by microcontrollers [11]. The ADC in Victoria modifies the values according to the following equation:

$$ADC\,reading = \frac{ADC\,resolution}{System\,voltage} \cdot Analog\,value \tag{11.1}$$

The system voltage, which is the voltage in the microcontroller circuits, is 3.3V in Victoria according to Erik Lund. The ADC interprets 12 bits which gives it a resolution of 4095 steps.

With these values, the corresponding analog signal would be possible to compute since the gain, the quotient between ADC resolution and system voltage, is known. The problem in this case is that the ADC-values is multiplicated with a factor of 100 in order to get two significant digits when converted to binary numbers and the onboard CANBUS[1] system can handle a maximum number of 16 bits which translates into a maximum number of 65535 in base 10. When the input binary signal is higher than this threshold, the CANBUS system interprets the signal as the value subtracted by 65535.

This CANBUS threshold is therefore the reason that the logged data from the FL angle sensor is non continuous. Since the angle sensors can be clocked differently, the voltage signal can be higher from one angle sensor than the other. The FL angle sensor is therefore, unfortunately, clocked in a position which sends signals under and above the threshold which results in a non continuous logged CANBUS-data.

[1]Controller Area Network bus, a computer communication system commonly used in the automotive industry for data communication between control units in vehicles [21]

## L.2 Data Formating

After interpreting what the data describes the next step is to calibrate the data so that it can be converted into wheel motion which in turn can be used to calculate forces on the wheels with a transfer function. Erik Lund provided a SIMULINK model that simulates Victoria's CANBUS signal based on possible voltage signals from the angle sensors, see Figure L.2.

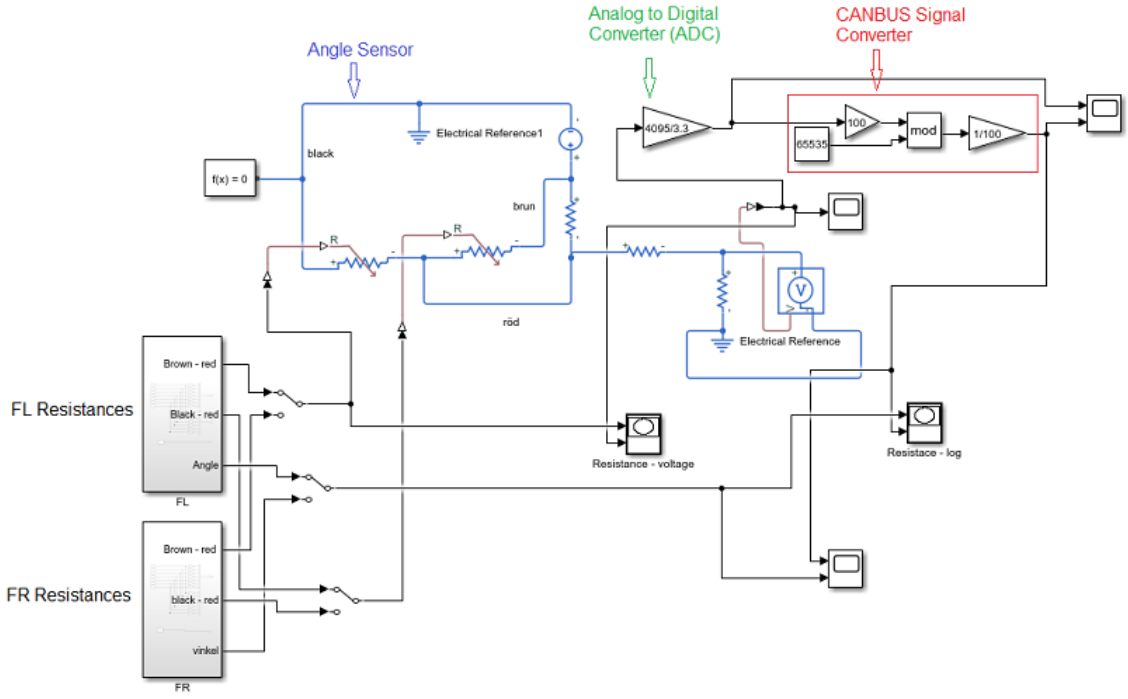


**Figure L.2:** SIMULINK model for simulating CANBUS signals from resistances

The Figure shows how the signal from the angle sensor is processed and howthe ADC and CANBUS interact. The resistances from the angle sensors is storedin the blocks in the bottom left corner. These resistances are found by measuringthe resistance from the angle sensors at each wheel on the car.

First, the car is raised on jack stands and the shock absorbers are removed. Then a spirit level with angle adjustability was placed on one of the pushrod actuator shafts on a steady surface, see Figure L.3. The wheel was dropped down to its lowest position and the spirit level was reset. In this reference point, the resistances from the angle sensor was measured with a multimeter. Then the wheel was raised until the spirit level indicated that the pushrod actuator shaft was rotated 5°and a new resistance was measured. This was repeated until the wheel was in its highest position.

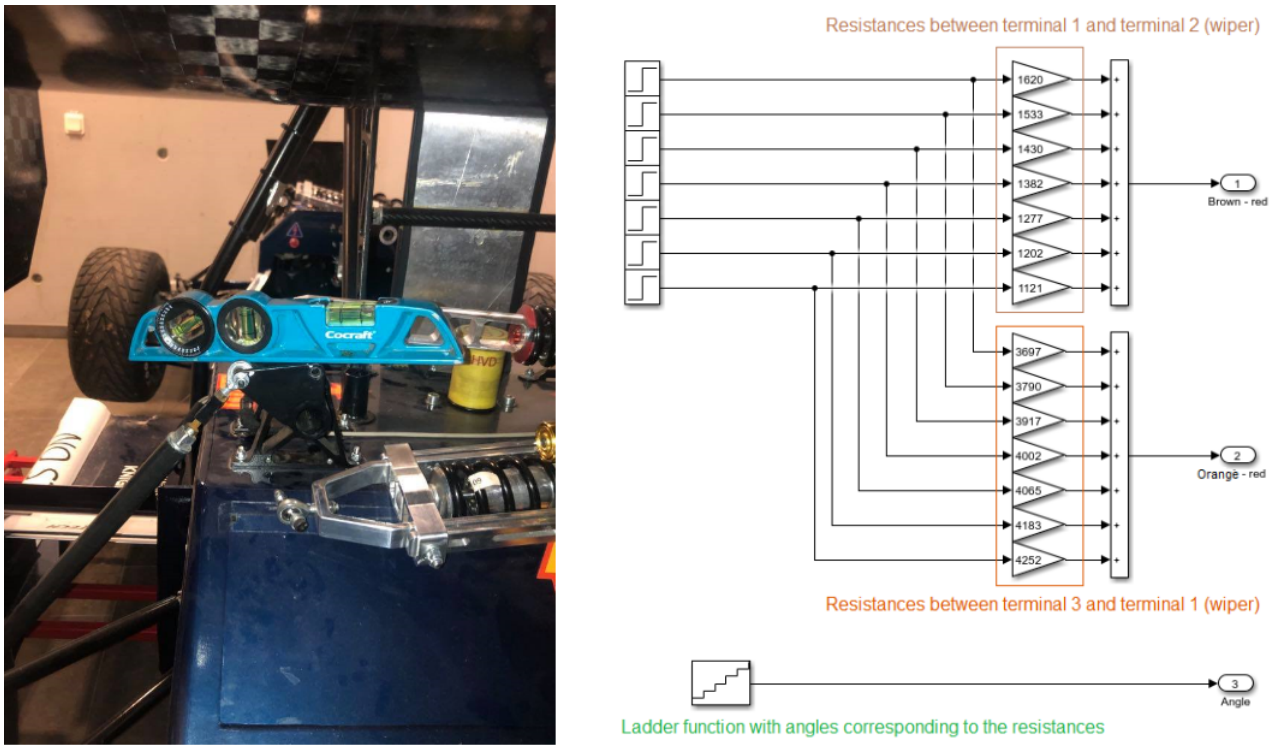


**Figure L.3:** Angle measuring point on pushrod pivot shaft and measured resistances inside SIMULINK block

When measuring the resistance of the RL angle sensor it was noticed that when the wheel was in the position approximately corresponding to stand still, its idle position, the resistance was almost 5kΩ. According to the sensor data sheet, 5kΩ is the maximum resistance for the sensor [22]. When the wheel was raised above its idle position the resistance remained unchanged and then became infinite, indicating that the sensor was clocked out of its 308 °range. This means that the logged data from the RL wheel is unreliable. Therefore it is decided that only the data from the front wheels will be used.

The measured resistances from each front wheel are loaded into the blocks in the SIMULINK model, see Figure L.3. The angles are loaded into a ladder function that emits angle-values in steps of 5°corresponding to the measured angles. These signals are simulated in the SIMULINK model resulting in graphs with resistances on the x-axis and CANBUS-values on the y-axis, see Figure L.4.

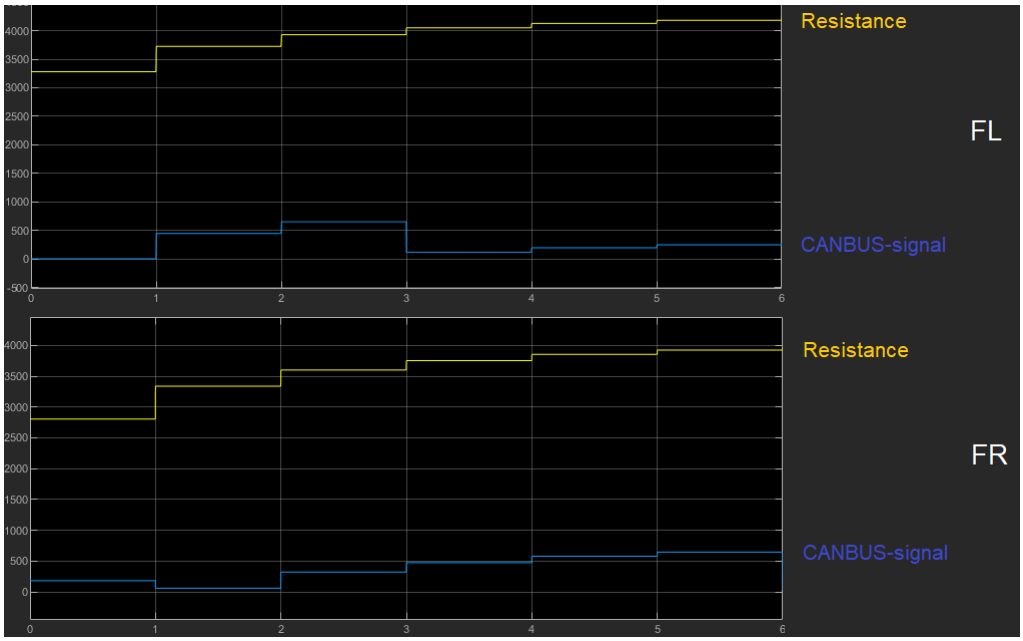


**Figure L.4:** Graphs from SIMULINK showing sensor resistance and its corresponding CANBUS-signal

The data points from the simulated relationship between resistance/angle and CANBUS-signal is loaded into MATLAB and polynomial curves are computed to fit the data points, see Figure L.5. These curves thereby corresponds to the transfer functions between any CANBUS-signal to the respective angle for each front wheel angle sensor.

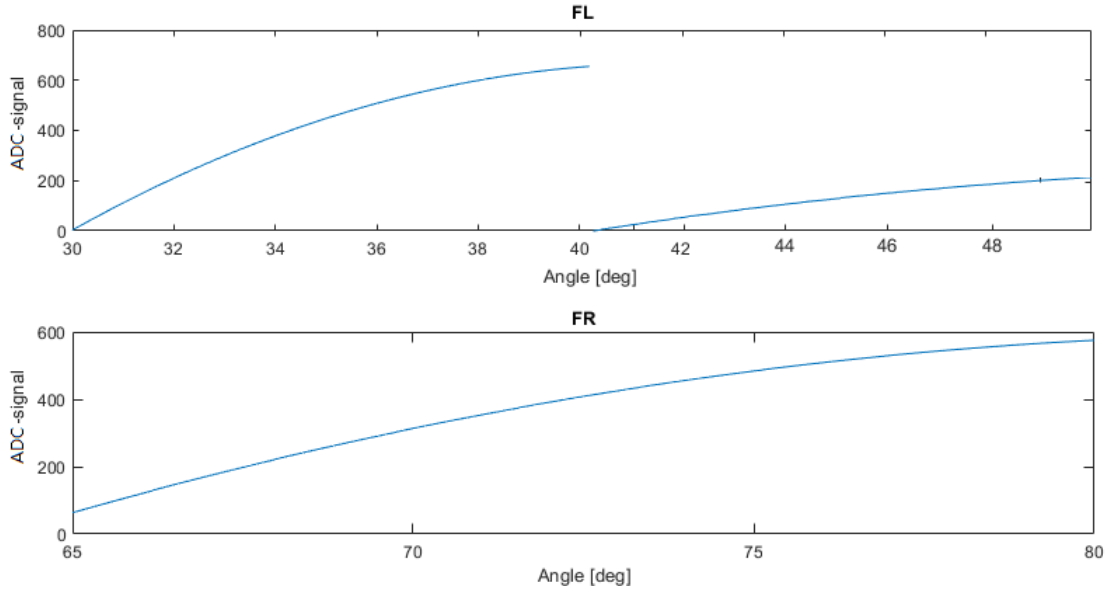


**Figure L.5:** Transfer function between CANBUS-signal and angle for each front wheel

## L.3 Translating Sensor Angles to Resulting Forces

Since the transfer function between the logged CANBUS-signal and the angle sensor for each front wheel is defined, the next step is to convert all data points from the CANBUS-signal into their corresponding angle. This is done in MATLAB and results in the graphs in Figure L.6.

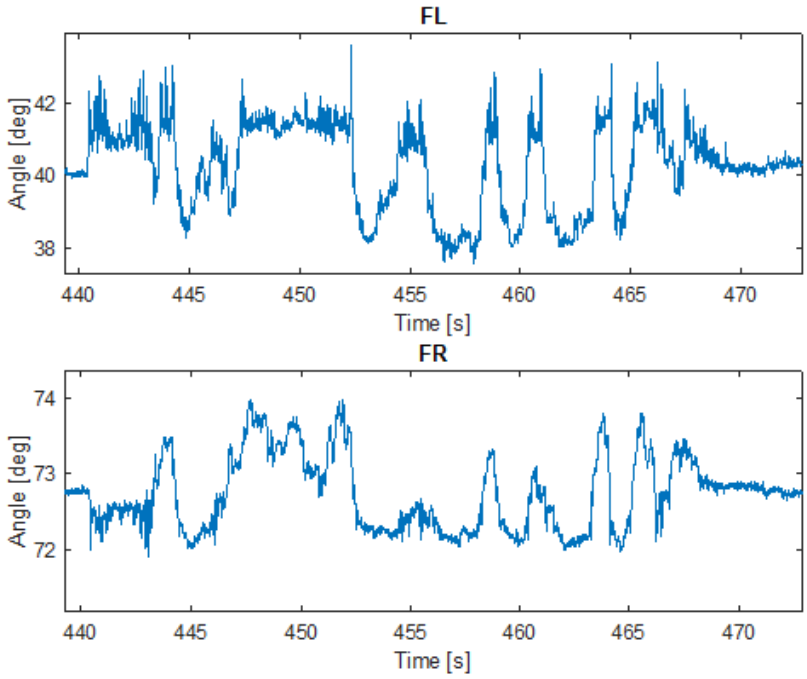


**Figure L.6:** Victorias CANBUS-signal converted into sensor angles for one lap in Achen 2019

As seen in the Figure, the amplitude of the angles from the FL sensor is about twice the amplitude of the angles from the FR sensor. After inspection of Victoria's suspension system and the shape of the autocross track it is concluded that this is not realistic. Victoria is equipped with a combined heave and roll suspension, a suspension technology refered to as a HeRo-system, see Figure L.7. Since the pushrod actuators are directly connected to the upright and the pivot shaft where the angle is measured on both sides, there should be no significant difference in amplitude between the FL and FR angles. In addition, the autocross layout have got many sharp right turns which in theory should result in similar amptitudes between the FL and FR measured angles.

The SIMULINK model is reviewed and many adjusted versions is created in order to find the reason for the scaling error in the transfer function, but without any progress. The initial idea was to calculate the kinematic relationships between the pivot shaft angles and the shock absorbers to calculate the resulting forces from the ground on the wheels. Because of the scaling error in the transfer function the method is revised and the approach is instead to normalize the angle data and scale the movement of the pivot shaft against normal forces with hand calculations instead.


**Figure L.7:** Victoria's HeRo-system on front axle

Normal forces on the wheels from the ground during acceleration, retardation and cornering is the force most related to the pivot shaft angle since these are the forces the suspension systems shock absorbers are mainly designed to handle. In order to convert the angles into approximate normal forces, the video recording as well as the accelerometer- and angle data from Achen are studied.

The time stamp used as a reference situation for hand calculations is when the car accelerates from stand still in a straight line, which is at 440.90s in the data log. The values are compared to when the car is idling right before it takes off. At these time stamps, the following data are found from the respective sensors, see Figure L.8

| Data from Achen, Germany 2019 | | | |
|---|---|---|---|
| **Timestamp [s]** | **FL Pivot Shaft Angle [deg]** | **FR Pivot Shaft Angle [deg]** | **Longitudinal Acceleration [m/s^2]** |
| Idle @440,40s | 40,665 | 72,627 | -0,28478 |
| Acceleration @440,90s | 41,706 | 72,261 | 9,41738 |

**Figure L.8:** Data at reference idle and acceleration times

Using this information, all pivot shaft angle data points from the lap is normalized against the angles at idle. Then the theoretical normal forces on the front wheels is hand calculated with the recorded longitudinal acceleration.

## M. Bearings.m

```
%Bearings
%clear all

%% Input paramaters

%geometrical data
r = 16/2*25.4e-3; %[m] wheel radius
ow = -0.049; %[m] distance from hub mounting posistion to centre ...
    of wheel
L1 = 0.0465; %[m] distance from hub mounting position to centre ...
    of outer bearing
L2 = 0.0465; %[m] distance between centres of bearings

bearing_inner = 'SKF61810';
bearing_outer = 'SKF61817';

type = 1;
%1 = Deep groove ball bearing
%2 = angle contact ball bearing

nu = 90; %[mm^2/s] actual operating vescosity of oil
eta_c = [0.4 0.5]; %[-] "slight contamination"

speedBins = 10; %number of bins to split the speed into for the ...
    load spectrum
loadBins = 20; %number of bins to split the load into for the ...
    load spectrum

%% load data

%Normal force (z)
FL_FN = load('FL_FN.mat').FL_FN;
FR_FN = load('FR_FN.mat').FR_FN;

%Lateral force (y)
FL_FL = load('FL_FL.mat').FL_FL;
FR_FL = load('FR_FL.mat').FR_FL;

latestStart = max([FL_FN(1,2) FR_FN(1,2) FL_FL(1,2) FR_FL(1,2)]);
firstEnd = min([FL_FN(end,2) FR_FN(end,2) FL_FL(end,2) ...
    FR_FL(end,2)]);

FL_FN = FL_FN(FL_FN(:,2)≥latestStart,:);
FR_FN = FR_FN(FR_FN(:,2)≥latestStart,:);
FL_FL = FL_FL(FL_FL(:,2)≥latestStart,:);
FR_FL = FR_FL(FR_FL(:,2)≥latestStart,:);

FL_FN = FL_FN(FL_FN(:,2)≤firstEnd,:);
FR_FN = FR_FN(FR_FN(:,2)≤firstEnd,:);
FL_FL = FL_FL(FL_FL(:,2)≤firstEnd,:);
FR_FL = FR_FL(FR_FL(:,2)≤firstEnd,:);

```

```
48
49 %Tangential force (x)
50 FT_tot = load('FT_tot.mat').FT_tot;
51 FT = FT_tot/4; %Assume equally distributed
52
53 data = load('FSAC_Autocross_1.mat');
54 FR_Speed = ...
       data.runs.logfile20191024143952.fullRun.PE_FR_Speed_Estimate_45;
55 FL_Speed = ...
       data.runs.logfile20191024143952.fullRun.PE_FL_Speed_Estimate_49;
56
57 FR_Speed(:,1) = -FR_Speed(:,1); %fix sign error
58
59 FR_Speed = FR_Speed(FR_Speed(:,2)≥FL_FN(1,2),:);
60 FR_Speed = FR_Speed(FR_Speed(:,2)≤FL_FN(end,2),:);
61 FL_Speed = FL_Speed(FL_Speed(:,2)≥FL_FN(1,2),:);
62 FL_Speed = FL_Speed(FL_Speed(:,2)≤FL_FN(end,2),:);
63
64 FR_Speed(:,1) = FR_Speed(:,1)/11.5;
65 FL_Speed(:,1) = FL_Speed(:,1)/11.5;
66
67 FR_Speed_long = interp1(FR_Speed(:,2),FR_Speed(:,1),FR_FL(:,2));
68 FL_Speed_long = interp1(FL_Speed(:,2),FL_Speed(:,1),FR_FL(:,2));
69 %% Free body diagram
70
71 % Front left
72 R_riz_FL = (FL_FN(:,1)*(L1-ow)-FL_FL(:,1)*r)/L2;
73
74 R_roz_FL = -FL_FN(:,1) - R_riz_FL;
75
76 R_ao_FL = abs([-FL_FL(:,1) FL_FN(:,2)]); %always positive for ...
       later calculations
77
78 R_rix_FL = FT(:,1)*((L1-ow)/L2);
79
80 R_rox_FL = -FT(:,1) - R_rix_FL;
81
82 R_ri_FL = [sqrt(R_rix_FL(:,1).^2 + R_riz_FL(:,1).^2) FL_FN(:,2)];
83
84 R_ro_FL = [sqrt(R_rox_FL(:,1).^2 + R_roz_FL(:,1).^2) FL_FN(:,2)];
85
86 %Front right
87 R_riz_FR = (FR_FN(:,1)*(L1-ow)-FR_FL(:,1)*r)/L2;
88
89 R_roz_FR = -FR_FN(:,1) - R_riz_FR;
90
91 R_ao_FR = abs([-FR_FL(:,1) FL_FN(:,2)]); %always positive for ...
       later calculations
92
93 R_rix_FR = FT(:,1)*((L1-ow)/L2);
94
95 R_rox_FR = -FT(:,1) - R_rix_FR;
96
97 R_ri_FR = [sqrt(R_rix_FR(:,1).^2 + R_riz_FR(:,1).^2) FL_FN(:,2)];
98
99 R_ro_FR = [sqrt(R_rox_FR(:,1).^2 + R_roz_FR(:,1).^2) FL_FN(:,2)];
```

```
100
101
102 %% load spectrum
103
104 %% Defines a set of selected bearings
105 %Data format: (d,D,B,C,C0,Pu,Nref,Nlim,m,f0)
106 % Add on more bearings if relevant
107 %       1   2   3     4     5      6    7      8      9    10
108 %       d   D   B     C     C0    P_U Nref   Nlim    m    f0
109 DGBB =[50,80,10,16800,11400,560,18000,11000,0.18,14;
110     60,78,10,11900,11400,490,17000,11000,0.11,17;
111     65,85,10,12400,12700,540,16000,10000,0.13,17;
112     80,100,10,13000,15000,640,13000,8000,0.15,17;
113     80,110,16,25100,20400,1020,12000,7500,0.38,14;
114     50,65,7,6760,6800,285,20000,13000,0.052,17;
115     50,72,12,14600,11800,500,19000,12000,0.14,16;
116     40,62,12,13800,10000,425,24000,14000,0.12,16;
117     40,68,9,13800,10200,440,22000,14000,0.13,16;
118     85,110,13,19500,20800,880,1200,7500,0.27,17;
119     90,115,13,19.5e3,22e3,915,11e3,7e3,0.28,17;
120     70,90,10,12.4e3,13.2e3,560,15e3,9e3,0.14,17;
121     65,95,11,20.8e3,15e3,0.735e3,15e3,9.5e3,0.29,14;
122     75 , 95 , 10 , 12.7e3 , 14.3e3 , 0.61e3 , 14e3 , 8.5e3 , ...
            0.15 , 17];
123
124 DGBB_names=['SKF16010';'SKF61812';'SKF61813';'SKF61816'; ...
125     'SKF61916';'SKF61810';'SKF61910';'SKF61908'; ...
126     'SKF16008';'SKF61817';...
127     'SKF61818';'SKF61814';'SKF16012';'SKF61815';];
128
129 % ACBB = [
130 %     40, 80, 18, 37.7, 26, 1.1, 11000, 11000, 0.37,
131 %     ];
132
133 % ACBB_names = [
134 %     'SKF7208BEP',
135 %     ];
136
137 %Table 8 in SKF catalogue
138 DGBB_eXY = [
139     0.172 0.19 0.56 2.3 %f0*F_a/C_0 SKF page 315 2014
140     .345 .22 .56 1.99
141     .689 .26 .56 1.71
142     1.03 .28 .56 1.55
143     1.38 .3 .56 1.45
144     2.07 .34 .56 1.31
145     3.45 0.38 .56 1.15
146     5.17 .42 .56 1.04
147     6.89 0.44 .56 1.00
148     ];
149
150 %% Life of bearings
151 %idx_i = strcomp(bearing_inner,)
152
153
154 switch type
```

```
155     case 1 %Deep groove ball bearing
156         P_i_FL = R_ri_FL;
157         P_i_FR = R_ri_FR;
158         idx_i = strmatch(bearing_inner,DGBB_names);
159         idx_o = strmatch(bearing_outer,DGBB_names);
160         p = 3; %exponent from SKF bearing calculation
161         %Only the outer bearing is loaded axially
162         factor_FL = DGBB(idx_o,10)*R_ao_FL(:,1)/DGBB(idx_o,5); ...
                %make work for both left and right!!!
163         factor_FR = DGBB(idx_o,10)*R_ao_FR(:,1)/DGBB(idx_o,5);
164         e_FL = zeros(size(factor_FL));
165         X_FL = zeros(size(factor_FL));
166         Y_FL = zeros(size(factor_FL));
167         for i = 1:length(factor_FL)
168             for j = 1:length(DGBB_eXY(:,1))-1
169                 if factor_FL(i) < DGBB_eXY(1,1)
170                     e_FL(i) = DGBB_eXY(1,2);
171                     X_FL(i) = DGBB_eXY(1,3);
172                     Y_FL(i) = DGBB_eXY(1,4);
173                     %fprintf('Too low\n')
174                 elseif (factor_FL(i) < DGBB_eXY(j+1,1)) && ...
                        (factor_FL(i) > DGBB_eXY(j,1))
175                     %fprintf('Just right!\n')
176                     e_FL(i) = DGBB_eXY(j,2) + ...
                            (DGBB_eXY(j+1,2)-DGBB_eXY(j,2))/ ...
177                         (DGBB_eXY(j+1,1)-DGBB_eXY(j,1))...
178                             *(factor_FL(i)-DGBB_eXY(j,1));
179                     X_FL(i) = DGBB_eXY(j,3) + ...
                            (DGBB_eXY(j+1,3)-DGBB_eXY(j,3))/ ...
180                         (DGBB_eXY(j+1,1)-DGBB_eXY(j,1))...
181                             *(factor_FL(i)-DGBB_eXY(j,1));
182                     Y_FL(i) = DGBB_eXY(j,4) + ...
                            (DGBB_eXY(j+1,4)-DGBB_eXY(j,4))/ ...
183                         (DGBB_eXY(j+1,1)-DGBB_eXY(j,1))*...
184                             (factor_FL(i)-DGBB_eXY(j,1));
185                 elseif factor_FL(i) > DGBB_eXY(end,1)
186                     e_FL(i) = DGBB_eXY(end,2);
187                     X_FL(i) = DGBB_eXY(end,3);
188                     Y_FL(i) = DGBB_eXY(end,4);
189                     %fprintf('Too High\n')
190                 end
191             end
192         end
193         e_FR = zeros(size(factor_FR));
194         X_FR = zeros(size(factor_FR));
195         Y_FR = zeros(size(factor_FR));
196         for i = 1:length(factor_FR)
197             for j = 1:length(DGBB_eXY(:,1))-1
198                 if factor_FR(i) < DGBB_eXY(1,1)
199                     e_FR(i) = DGBB_eXY(1,2);
200                     X_FR(i) = DGBB_eXY(1,3);
201                     Y_FR(i) = DGBB_eXY(1,4);
202                     %fprintf('Too low\n')
203                 elseif (factor_FR(i) < DGBB_eXY(j+1,1)) && ...
                        (factor_FR(i) > DGBB_eXY(j,1))
204                     %fprintf('Just right!\n')
```

```
205                     e_FR(i) = DGBB_eXY(j,2) + ...
                            (DGBB_eXY(j+1,2)-DGBB_eXY(j,2))/ ...
206                     (DGBB_eXY(j+1,1)-DGBB_eXY(j,1))...
207                         *(factor_FR(i)-DGBB_eXY(j,1));
208                     X_FR(i) = DGBB_eXY(j,3) + ...
                            (DGBB_eXY(j+1,3)-DGBB_eXY(j,3))/ ...
209                     (DGBB_eXY(j+1,1)-DGBB_eXY(j,1))...
210                         *(factor_FR(i)-DGBB_eXY(j,1));
211                     Y_FR(i) = DGBB_eXY(j,4) + ...
                            (DGBB_eXY(j+1,4)-DGBB_eXY(j,4))/ ...
212                     (DGBB_eXY(j+1,1)-DGBB_eXY(j,1))...
213                         *(factor_FR(i)-DGBB_eXY(j,1));
214                 elseif factor_FR(i) > DGBB_eXY(end,1)
215                     e_FR(i) = DGBB_eXY(end,2);
216                     X_FR(i) = DGBB_eXY(end,3);
217                     Y_FR(i) = DGBB_eXY(end,4);
218                     %fprintf('Too High\n')
219                 end
220             end
221         end
222
223         %Equivalent load
224         P_o_FL = R_ao_FL; %Predefine
225         for i = 1:length(factor_FL)
226             if R_ao_FL(i)/R_ro_FL(i) ≤ e_FL(i)
227                 P_o_FL(i,1) = R_ro_FL(i);
228             elseif R_ao_FL(i)/R_ro_FL(i) > e_FL(i)
229                 P_o_FL(i,1) = X_FL(i)*R_ro_FL(i) + ...
                        Y_FL(i)*R_ao_FL(i);
230             else
231                 fprintf('Well, FUCK!\n')
232             end
233         end
234         P_o_FR = R_ao_FR; %Predefine
235         for i = 1:length(factor_FR)
236             if R_ao_FR(i)/R_ro_FR(i) ≤ e_FR(i)
237                 P_o_FR(i,1) = R_ro_FR(i);
238             elseif R_ao_FR(i)/R_ro_FR(i) > e_FR(i)
239                 P_o_FR(i,1) = X_FR(i)*R_ro_FR(i) + ...
                        Y_FR(i)*R_ao_FL(i);
240             else
241                 fprintf('Well, FUCK!\n')
242             end
243         end
244
245         %L_10m = a_SKF*(C/P)^p;
246 %         histogram2(FL_Speed_long(:,1),P_o_FL(:,1),[speedBins ...
    loadBins])
247 %         figure
248 %         histogram2(FR_Speed_long(:,1),P_o_FR(:,1),[speedBins ...
    loadBins])
249
250         [freq_o_FL,speedEdges_FL,loadEdges_o_FL] = ...
            histcounts2(FL_Speed_long(:,1),P_o_FL(:,1),[speedBins ...
            loadBins]);
```

```
251         [freq_o_FR,speedEdges_FR,loadEdges_o_FR] = ...
               histcounts2(FR_Speed_long(:,1),P_o_FR(:,1),[speedBins ...
               loadBins]);
252         [freq_i_FL,¬,loadEdges_i_FL] = ...
               histcounts2(FL_Speed_long(:,1),P_i_FL(:,1),[speedBins ...
               loadBins]);
253         [freq_i_FR,¬,loadEdges_i_FR] = ...
               histcounts2(FR_Speed_long(:,1),P_i_FR(:,1),[speedBins ...
               loadBins]);
254         speedMids_FL = zeros(numel(speedEdges_FL)-1,1); %predefine
255         speedMids_FR = speedMids_FL;
256         loadMids_o_FL = speedMids_FL; %predefine
257         loadMids_o_FR = speedMids_FL;
258         loadMids_i_FL = speedMids_FL;
259         loadMids_i_FR = speedMids_FL;
260         for i = 1:speedBins
261             speedMids_FL(i) = ...
                   (speedEdges_FL(i)+speedEdges_FL(i+1))/2;
262             speedMids_FR(i) = ...
                   (speedEdges_FR(i)+speedEdges_FR(i+1))/2;
263         end
264         for i = 1:loadBins
265             loadMids_o_FL(i) = ...
                   (loadEdges_o_FL(i)+loadEdges_o_FL(i+1))/2;
266             loadMids_o_FR(i) = ...
                   (loadEdges_o_FR(i)+loadEdges_o_FR(i+1))/2;
267             loadMids_i_FL(i) = ...
                   (loadEdges_i_FL(i)+loadEdges_i_FL(i+1))/2;
268             loadMids_i_FR(i) = ...
                   (loadEdges_i_FR(i)+loadEdges_i_FR(i+1))/2;
269         end
270         %dimension: speedBins x loadBins
271         a_SKF_o_FL = ...
               a_SKF_calculation(loadMids_o_FL',speedMids_FL', ...
272         DGBB(idx_o,6),(DGBB(idx_o,1)+DGBB(idx_o,2))/2,eta_c,nu,1);
273         a_SKF_o_FR = ...
               a_SKF_calculation(loadMids_o_FR',speedMids_FR', ...
274         DGBB(idx_o,6),(DGBB(idx_o,1)+DGBB(idx_o,2))/2,eta_c,nu,1);
275         a_SKF_i_FL = ...
               a_SKF_calculation(loadMids_i_FL',speedMids_FL', ...
276         DGBB(idx_i,6), (DGBB(idx_i,1)+DGBB(idx_i,2))/2,eta_c,nu,1);
277         a_SKF_i_FR = ...
               a_SKF_calculation(loadMids_i_FR',speedMids_FR', ...
278         DGBB(idx_i,6),...
279              (DGBB(idx_i,1)+DGBB(idx_i,2))/2,eta_c,nu,1);
280
281         L10_o_FL = (DGBB(idx_o,4)./loadMids_o_FL).^p;
282         L10_o_FR = (DGBB(idx_o,4)./loadMids_o_FR).^p;
283         L10_i_FL = (DGBB(idx_i,4)./loadMids_i_FL).^p;
284         L10_i_FR = (DGBB(idx_i,4)./loadMids_i_FR).^p;
285
286         L10m_o_FL = a_SKF_o_FL.*L10_o_FL;
287         L10m_o_FR = a_SKF_o_FR.*L10_o_FR;
288         L10m_i_FL = a_SKF_i_FL.*L10_i_FL;
289         L10m_i_FR = a_SKF_i_FR.*L10_i_FR;
290
```

```
291         U_o_FL = (freq_o_FL.*speedMids_FL)';
292         U_o_FR = (freq_o_FR.*speedMids_FR)';
293         U_i_FL = (freq_i_FL.*speedMids_FL)';
294         U_i_FR = (freq_i_FR.*speedMids_FR)';
295 
296         U_o_FL = U_o_FL./sum(U_o_FL,'all');
297         U_o_FR = U_o_FR./sum(U_o_FR,'all');
298         U_i_FL = U_i_FL./sum(U_i_FL,'all');
299         U_i_FR = U_i_FR./sum(U_i_FR,'all');
300 
301         L10m_o_FL_tot = 1/sum((U_o_FL./L10m_o_FL),'all');
302         L10m_o_FR_tot = 1/sum((U_o_FR./L10m_o_FR),'all');
303         L10m_i_FL_tot = 1/sum((U_i_FL./L10m_i_FL),'all');
304         L10m_i_FR_tot = 1/sum((U_i_FR./L10m_i_FR),'all');
305 
306         fprintf...
307             ('\nOuter Left bearing: %s\n%.2f million ...
                   revolutions\n%.2f km\nSafety ...
                   factor:%.2f\nWeight: %.3f kg\n\n',...
308             bearing_outer,L10m_o_FL_tot,L10m_o_FL_tot*2*r*1e3, ...
309             L10m_o_FL_tot*2*r*1e3/1500,DGBB(idx_o,9))
310         fprintf...
311             ('Outer Right bearing: %s\n%.2f million ...
                   revolutions\n%.2f km\nSafety factor: ...
                   %.2f\nWeight: %.3f kg\n\n',...
312             bearing_outer,L10m_o_FR_tot,L10m_o_FR_tot*2*r*1e3, ...
313             L10m_o_FR_tot*2*r*1e3/1500,DGBB(idx_o,9))
314         fprintf...
315             ('Inner Left bearing: %s\n%.2f million ...
                   revolutions\n%.2f km\nSafety factor: ...
                   %.2f\nWeight: %.3f kg\n\n',...
316             bearing_inner,L10m_i_FL_tot,L10m_i_FL_tot*2*r*1e3, ...
317             L10m_i_FL_tot*2*r*1e3/1500,DGBB(idx_i,9))
318         fprintf...
319             ('Inner Right bearing: %s\n%.2f million ...
                   revolutions\n%.2f km\nSafety factor: ...
                   %.2f\nWeight: %.3f kg\n',...
320             bearing_inner,L10m_i_FR_tot,L10m_i_FR_tot*2*r*1e3, ...
321             L10m_i_FR_tot*2*r*1e3/1500,DGBB(idx_i,9))
322     case 2
323         p = 10/3;
324         %Here a similar calculation would be done as for case 1 ...
              ( deep groove ball
325         %bearings) but for another type of bearing i.e. angular ...
              contact
326         %bearings. This part is not done yet but the skeleton ...
              structure is
327         %there if the need arises to expand the analysis to ...
              other types of
328         %bearings.
329 
330 end
```

## N. a_SKF_calculation.m

```
function a_SKF = a_SKF_calculation(P,n,P_U,dm,eta_c,nu,type)
%P = equivalent load [N] vector
%n = speed [rpm] vector
%P_U = fatigue load limit [N] scalar
%dm = [mm] scalar
%eta_c = contamination factor [-] scalar
%nu = viscosity of lubricant [mm^2/s] scalar
%type = indicator of rolling bearing type (1=ball bearing, ...
    2=roller bearing)

%Erik Henrikson, Carl Lund 2021-04

%debug parameters
% n = speedMids_FL;%1500*ones(10,1);%[200 500 300]; %[rpm]
% dm = 120; %[mm]
% nu = 50; %[mm^2/s]
% type = 1;
% eta_c = [0.4 0.5];
% P_U = 560; %[N]
% P = loadMids_o_FL;%[1578.428 1612.861]; %[N]

if dm < 100
    eta_c = eta_c(1);
else
    eta_c = eta_c(2);
end

slope = (log10(21) - log10(50))/(log10(100) - log10(20)); ...
    %assume this slope for all relevant curves

%[n (nu1 at dm=100)]
rpm = [
    10000 4;
    5000 6;
    3000 7.2;
    2000 8.4;
    1500 9.4;
    1000 11.8;
    500 20.5;
    200 48;
    100 84;
    50 160;
    ];

nu1_100 = spline(rpm(:,1),rpm(:,2),n);

nu1_log = log10(nu1_100) + slope*(log10(dm)-log10(100));
nu1 = (ones(size(nu1_log))*10).^nu1_log;

kappa = nu./nu1;

kappa(kappa>4) = 4;
```

```
kappa(kappa<0.1) = 0.1;

%Loading data from graph
switch type
    case 1
        aSKFgraph = load('a_SKF_radial_ball_bearings.csv');
        kappalines = [0.1 0.2 0.3 0.4 0.6 1 2 4];
    case 2
        aSKFgraph = load('a_SKF_radial_roller_bearings.csv');
        kappalines = [0.1 0.2 0.3 0.4 0.5 0.8 1 2 4];
end

kappaLine = zeros(length(aSKFgraph(:,1)),2,numel(n));

etacPuP = eta_c*P_U./P;

a_SKF = zeros(numel(P),numel(n)); %predefine
for j = 1:numel(n)
for i = 1:length(aSKFgraph(:,1))
    kappaLine(i,1,j) = ...
       interp1(kappalines,aSKFgraph(i,1:2:end),kappa(j)); %x
    kappaLine(i,2,j) = ...
       interp1(kappalines,aSKFgraph(i,2:2:end),kappa(j)); %y
end
etacPuP(etacPuP>max(kappaLine(:,1,j))) = max(kappaLine(:,1,j));
a_SKF(:,j) = interp1(kappaLine(:,1,j),kappaLine(:,2,j),etacPuP);
end

% figure
% loglog(aSKFgraph(:,1:2:end),aSKFgraph(:,2:2:end),'.r')
% xlim([0.005 5])
% ylim([0 50])
% xlabel('\eta_c P_U/P')
% ylabel('a_{SKF}')
% xticks([0.005 0.01 0.02 0.1 0.2 0.5 1 2 5])
% yticks([0 0.1 0.2 0.5 1 2 5 10 20 50])
% grid on
% hold on
% for i = 1:5:length(aSKFgraph(:,1))
%     loglog(aSKFgraph(i,1:2:end),aSKFgraph(i,2:2:end),':k')
% end
%loglog(kappaIDX5x,kappaIDX5y,'*b')
% loglog(kappaLine(:,1,2),kappaLine(:,2,2),'-ob');
%loglog([eta_c*P_U/P(1) eta_c*P_U/P(1) 0],[0 a_SKF(1,1) a_SKF(1,1)])

end
```

**DEPARTMENT OF MECHANICS AND MARITIME SCIENCES**
**CHALMERS UNIVERSITY OF TECHNOLOGY**
Gothenburg, Sweden
www.chalmers.se


CHALMERS